MEDICAL UNIVERSITY
OF VIENNA

Diploma Thesis

DEVELOPMENT OF A COMPUTER CONTROLLED STIMULATION AND RECORDING SYSTEM FOR TRANS-SPINAL ELECTRICAL STIMULATION

Carried out for the purpose of obtaining the degree of Master of Science

Submitted at Vienna University of Technology,

Faculty of Mechanical and Industrial Engineering, by

Steffen EICKHOFF

Mat.Nr.: 1429714

Under the supervision of

Ao. Univ.-Prof. Dipl.-Ing. Dr. h.c. Dr. Winfried Mayr

Institute of Mechanics and Mechatronics (E325), Vienna University of Technology

Center for Medical Physics and Biomedical Engineering, Medical University of Vienna

and

Dipl.-Ing. Dr. Matthias Krenn

Center for Medical Physics and Biomedical Engineering, Medical University of Vienna

Vienna, September 2017

ABSTRACT

Spinal cord injury (SCI) causes impairment of the neuronal connection of the brain with the spinal cord as well as with the peripheral nervous system. This impairment can lead to partial (incomplete) or complete loss of motoric and / or sensory functions of anatomical structures, innervated below the spinal lesion. Electrical spinal cord stimulation (SCS) is able to elicit posterior root muscle (PRM) reflexes in subjects with SCI classified as motoric complete. While this was originally observed using epidurally implanted electrodes, numerous studies find non-invasive transcutaneous spinal cord stimulation (tSCS) capable of evoking similar spinal reflexes. Recent studies in this field are approach selective stimulation and modulation of spinal excitability, which often employs the use of sub-threshold conditioning pulses prior to the stimulation. In this thesis a two-channel stimulation system, also capable of recording muscle reflexes, is developed and technically evaluated. This evaluation under laboratory conditions verified that the system fulfills the specific requirements of research investigations in the area of neuromodulation in SCS and is safe to be applied in a preliminary clinical study. The initial results of this study suggest that spinal cord excitability can be modified incorporating peripheral nerve stimulation prior to eliciting PRM reflexes.

The recording system for electromyographic (EMG) signals has 16 channels of which eight are used to measure the PRM reflexes bilaterally in the four big synergistic muscle groups of the lower limb. These EMG signals are amplified with a gain of 590 V/V and filtered at a bandwidth of 30 – 590 Hz. Furthermore, the system has 4 digital markers, which allow to manually mark specific events during the stimulation procedure. Marker and EMG amplifier are connected to a National Instruments™ data acquisition card (NI USB 6221 OEM) to visualize and store the measurement data.

The stimulation system is composed of two BIOPAC® STMISOLA linear isolated stimulators, which are connected to the NI USB 6221 OEM. As a protective measure against DC currents being applied to the subject, high pass filters with cut-off frequencies of 2.2 Hz are placed between NI-card and stimulators. The output is generated via a LabVIEW™ program in which stimulation modes, specifically designed for the relevant type of SCS

studies, are contained. The system is capable of emitting rectangular single or double pulses, as well as different types of stimulation patterns in a range of +/- 100mA. Phase durations of up to 1 ms have been evaluated and verified as being free from distorting effects of the filter circuitry.

The system is further tested in the course of a preliminary study in a clinical environment with one spinal cord injured subject. The first channel applies stimulation impulses to the posterior roots of the subject, which elicit PRM reflexes that serve as a probe. The second stimulation channel delivers different patterns of stimulation to the sural nerve, a purely afferent peripheral nerve, at the subjects left ankle. A comparison of the PRM reflex peak-to-peak response magnitudes, with and without stimulation of the sural nerve prior to spinal cord stimulation, shows a strong suppressive conditioning effect in the ipsilateral leg. These preliminary results are in good accordance to recent literature.

ACKNOWLEDGEMENTS

Contents

LIST OF ABBREVIATIONS AND ACRONYMS

ADC	analog-digital conversion
ADP	adenosine diphosphate
AO	analog output
ATP	adenosine triphosphate
CH	channel
CMAP	compound muscle action potential
CNS	central nervous system
DAC	digital-analog conversion
DAQ	data aquisition
DC	direct current
ECM	extracellular matrix
EEG	electroencephalography
EMG	electromyography
EOG	electrooculography
eSCS	epidural spinal cord stimulation
G	gain
Ham, H	hamstrings
HE	haematoxylin and eosin
I/O	input/output
L	left
MUAP	motor unit action potential
NI	National Instruments™

PNS	peripheral nervous system
PPS	pulses per second
PRM	posterior root muscle reflex
PRR	posterior roots reflex
Q	quadriceps
R	right
SA	sinoatrial
SCI	spinal cord injury
SCS	spinal cord stimulation
SCSI	small computer system interface
SR	sarcoplasmic reticulum
TA	tibialis anterior
TDMS	technical data management solution
TNC	troponin C
TNI	troponin I
TNT	troponin T
TS	triceps surae
tSCS	transcutaneous spinal cord stimulation
VI	virtual instrument

1 INTRODUCTION

Spinal cord stimulation (SCS) is a neuromodulation technique, that has been used in the past decades for a variety of medical purposes. The fundamental principle of SCS, that all applications have in common, is the modulation of the activity within the neuronal structures of the spinal cord using electrical signals generated by technical devices. These electrical impulses can either be applied via implanted (e.g., epidural stimulation) or non-invasive surface electrodes (transcutaneous = through intact skin). The stimulation can be used to suppress undesired nerve activities, e.g., pain or spasticity, that are common after effects of spinal cord injuries (SCI), stroke or other diseases. Treatment of chronic pain with SCS was first successfully practised by Shealy et al. in the mid-sixties at Case Western Reverse University (Shealy, Mortimer, & Reswick, 1965). This and other theoretical and experimental works lead to the development of the first wearable SCS devices for pain treatment in the 1970s. After these first applications showed the safety and effectiveness of pain reduction, a continual development and refinement of this technology is documented (Compton, Shah, & Hayek, 2012).

Besides suppressing undesired neuronal activity, spinal cord stimulation is also used to evoke or augment motor functions. This is of special interest in diseased individuals with limited or no ability to move, such as paraplegic subjects, with the aim of reconstruction of lost or restricted movement. In 1998 Dr. M.R. Dimitrijevic and his colleagues found evidence for the existence of a spinal central pattern generator, that can be activated even when isolated from brain control. Their study showed that non-patterned SCS is able to produce rhythmical, step-like motor output in complete spinal cord injured subjects

(Dimitrijevic, Gerasimenko, & Pinter, 1998). Besides this landmark study, there is a multitude of promising scientific investigations, for the application of SCS in these populations (Dy et al., 2010; Gerasimenko, Roy, & Edgerton, 2008).

Due to anatomical and electro-physiological properties of the neuronal structures of the spine, the electric field induced via conventional SCS interacts with different populations of nerve fibres to different extents. The selective stimulation of specific nerve fibres is one of the main future perspectives of functional electrical stimulation and a lot of research is done in this field. Most approaches of selective stimulation include sub-threshold pulses, that act as conditioning and inhibit or augment excitability of certain nerve fibre populations prior to the stimulation pulses.

1.1 Research Aim

Often, these sub-threshold conditioning pulses can be applied to the subject via the same electrode set as the stimulation pulses. However, when conditioning pulses have to be applied spatially separated from the stimulation pulses, two sets of electrodes are required. The use of two separately controlled single channel stimulators can cause a variety of problems such as inaccurate timing of the channels to each other, the possible induction of more noise to the measurements and increased setup time, due to more hardware. Commercially available stimulation devices with multiple output channels often lack the high degree of free programmability, that is required for scientific studies, where conditioning and stimulation pulses have to be timed very accurately.

Therefore, the aim of this thesis is the development and evaluation of a computer controlled two-channel stimulation system for scientific studies, that require very precisely timed stimulation at two spatially different sites. To further simplify the hardware setup, the system shall combine both functions, EMG measurements and the two-channel stimulation.

1.2 Requirements of the system

To reduce the influence of noise to the recorded signals and to simplify the instrumentational setup procedure prior to measurements, the system should consist of as few single devices as possible. In order to record the electrical muscle signals of the four big synergistic muscle groups of the lower extremities, the knee and ankle flexors and extensors, for both legs, the system requires at least eight recording channels. Also, to indicate specific events during the stimulation / recording procedure, a marker system has to be implemented. To enable

synchronized stimulation at different areas of the spinal cord, and also with different amplitudes, frequencies and pulse shapes, the stimulation system has to have two output channels. These outputs should be independent from one another and freely programmable to enable the generation of various stimulation patterns and pulse shapes, with the least possible restrictions.

1.3 Overview of chapters

The remainder of this thesis is divided into four chapters. First, in Chapter 2, the theoretical background of this work is laid out, beginning with a detailed explanation of the anatomy and physiology of muscle tissue. On this foundation, the principles of measuring myoelectrical (electrical muscle activity) signals, using electromyography (EMG). Now the basics of electrical nerve stimulation in general, as well as in the specific case of stimulation of posterior root nerve fibres, is explained. This includes a brief presentation of the functional structure of the human nervous system.

After providing this theoretical background knowledge, the next two chapters describe the development of the technical system for stimulation posterior root nerves and recording resulting muscle activity. First the implementation of hardware and software, necessary for the recording system is shown in Chapter 3. This part of the system is then technically evaluated under laboratory conditions to ensure quality and meaningfulness of the recorded data. Then, in Chapter 4, the development of the stimulation system is described, followed by an evaluation to guarantee precise stimulation output and more importantly, subjects safety.

Chapter 5 shows an example of the application of the recording and stimulation system developed in the present work. After describing the methodology of the presented case study, results are shown and interpreted.

2 BACKGROUND

Due to the interdisciplinary nature of the field of biomedical engineering, it is always necessary to understand form and function of the biological system, as well as the basic working principles of the technical devices. Therefore, this chapter will first provide a brief introduction to the anatomy and physiology of the different types of muscle tissue. Afterwards, the electrodiagnostic technique of electromyography (EMG) is explained in general and specific examples of its application are shown. Lastly, the principles of electrical nerve stimulation are presented, also first in general terms, followed by the specific application in the field of posterior root stimulation.

2.1 The Muscle

The information provided in this chapter is structurally based on the textbooks of McComas (1996) and Schmidt et al. (2003). For the sake of legibility, these are only referred to, when directly cited.

With up to 50% of the body mass, muscle tissue is the most abundant type of tissue in the human body. It is required for very different tasks such as locomotion, maintaining posture and for movement of internal organs. Due to these strongly varying tasks, there are different types of muscle fibres, matching the various specific requirements and powered by different molecular mechanisms.

The working principle of skeletal muscle tissue, responsible for movements of the skeleton, is relative sliding motion of the contractile protein filaments actin and myosin. This contraction process is controlled by the intracellular concentration of the neurotransmitter ion Ca^{2+}, which is released in consequence of neuronal activities.

2.1.1 Anatomy and histology of muscle

General classification

The general classification of muscle tissue follows differences in histological structure and mechanisms of contraction. The broadest distinction is made between striated and smooth

muscles (Figure 2.1); striated muscle tissue is further divided into cardiac and skeletal muscles.
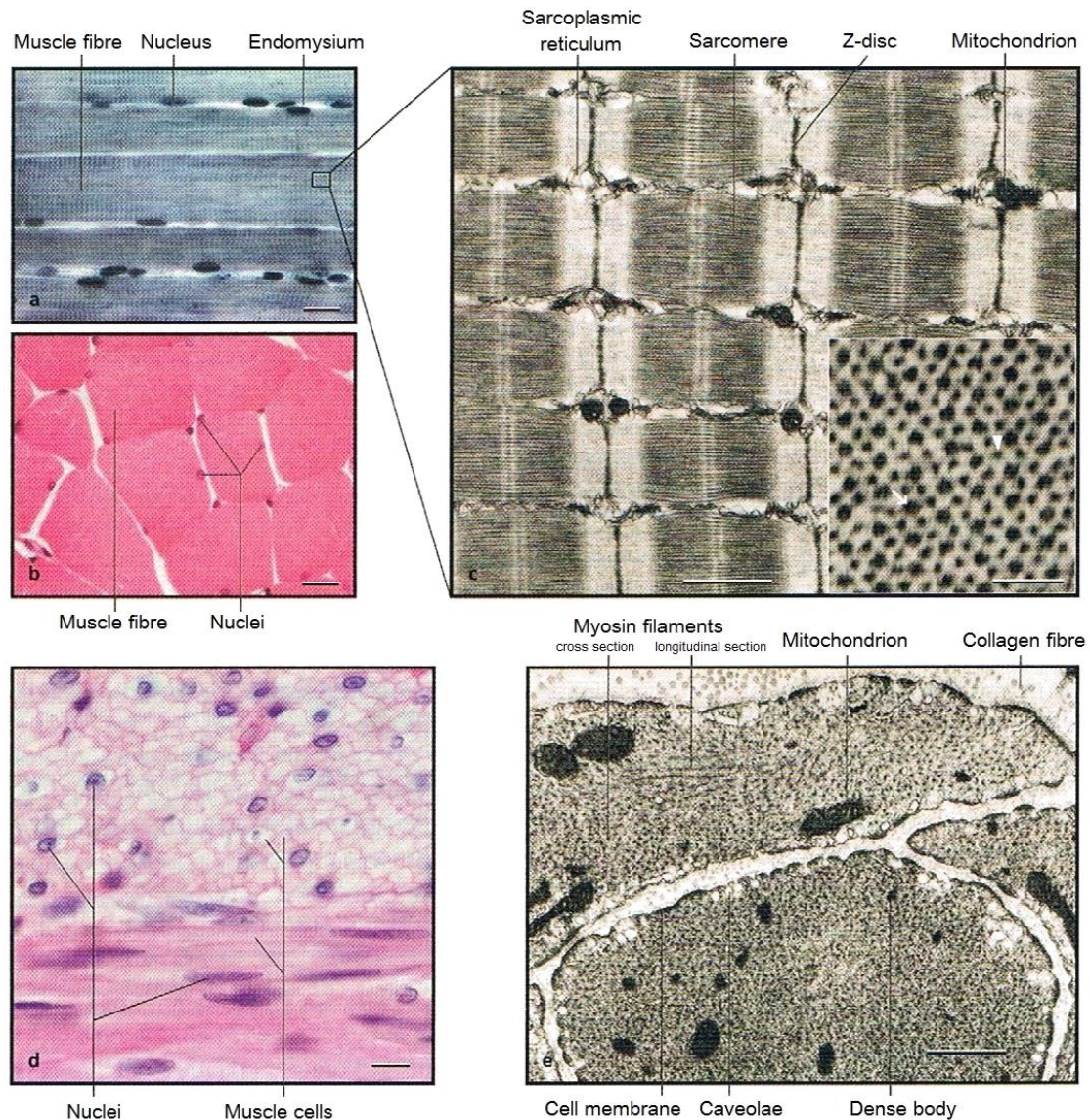
Figure 2.1: Histology of striated (skeletal) and smooth muscle tissue. (**a**) Longitudinal section (EH-staining), (**b**) cross section (HE-staining) of a skeletal muscle. Scale bar = 20 µm. (**c**) Electron microscope image of a longitudinal section of a skeletal muscle (M. triceps). Scale bar = 1 µm. Insert: cross sectional image of the overlap zone of thin (arrowhead) and thick (arrow) filaments. Scale bar = 0.1 µm. (**d**) Tissue sample of smooth muscle of the human Jejunum (PAS-staining for good visibility of the cell borders). Smooth muscle cells are recognizable in the cross section (upper part) and in the longitudinal section (lower part). Scale bar = 20 µm. (**e**) Electron microscope image of smooth muscle cells of the vas deferens. Scale bar = 0.5 µm. (Robert F. Schmidt, 2003)

Striated muscles are characterized by the regular arrangement of actin and myosin filaments within their cells (muscle fibres). These protein filaments are forming repeating contractile units, so-called sarcomeres. In HE stained histological samples, one can easily observe these sarcomeres, resulting in a periodic sequence of dark and light stripes. In polarized light, the

dark stripes are birefringent (anisotropic) and are therefore referred to as the A-band. The light stripes are called the I-band because of their isotropic behaviour in polarized light.

Skeletal muscles are connected by tendons or fasciae to the skeleton and can be consciously controlled to effect movement or to maintain posture. Their cells, the myocytes, have multiple flattened nuclei at their outer edges are cylindrically arranged and up to several centimetres long. These voluntarily controllable muscles can be further divided in two main types of fibre based on different numbers of mitochondria, aerobic enzymes and myoglobin content. This varying anatomical structure results in different contractile and metabolic behaviour of type I and type II muscle fibres. Slow twitch (type I) muscle fibres are also called "red fibres" because of the high myoglobin concentration. They are highly vascularized by small capillaries to be sufficiently supplied with high amounts of oxygen needed for aerobic power generation. This way of generation of mechanical power takes comparatively long time, therefore the name "slow twitch", but can be performed over an extended period of time due to the continuous supply of oxygen. The second type of skeletal muscle fibre is generating mechanical energy by glycolytic metabolic processes and is called fast twitch (type II) or "white" fibre. It contains less myoglobin and mitochondria, which leads to a light red to white colour. In humans, there are two subtypes of type II muscle fibre, which can be distinguished by their ratio of oxidative/glycolytic metabolism. Type IIA fibres are still containing a relatively high number of mitochondria and are therefore both, fast oxidative and glycolytic. In contrast, Type IIX fibres exhibit a low number of mitochondria and work almost exclusively glycolytically.

Cardiac muscle tissue can anatomically be differentiated from the skeletal muscle due to the branched arrangement of its much shorter fibres of 50-100µm length. Its cells only have one nucleus, which is positioned centrally. Cardiac muscles are working rhythmically, controlled by neuronal structures like the SA (sinoatrial) node, and cannot be consciously controlled.

The second broad category of muscle tissue are the smooth muscles, found in the walls of most hollow organs like blood vessels or the digestive and respiratory systems. Unlike the striated muscle, they contain no sarcomere structures and therefore histologically exhibit no striation patterns. It is a highly heterogenous type of tissue, with strongly variable organ and region-specific anatomical structures. Their control mechanisms vary from vegetative innervation to control by hormones or other neurotransmitters, having in common, that they are not consciously controllable.

The skeletal muscle – hierarchical structure

Like most biological tissues, muscle exhibits a highly hierarchical structure (Figure 2.2).
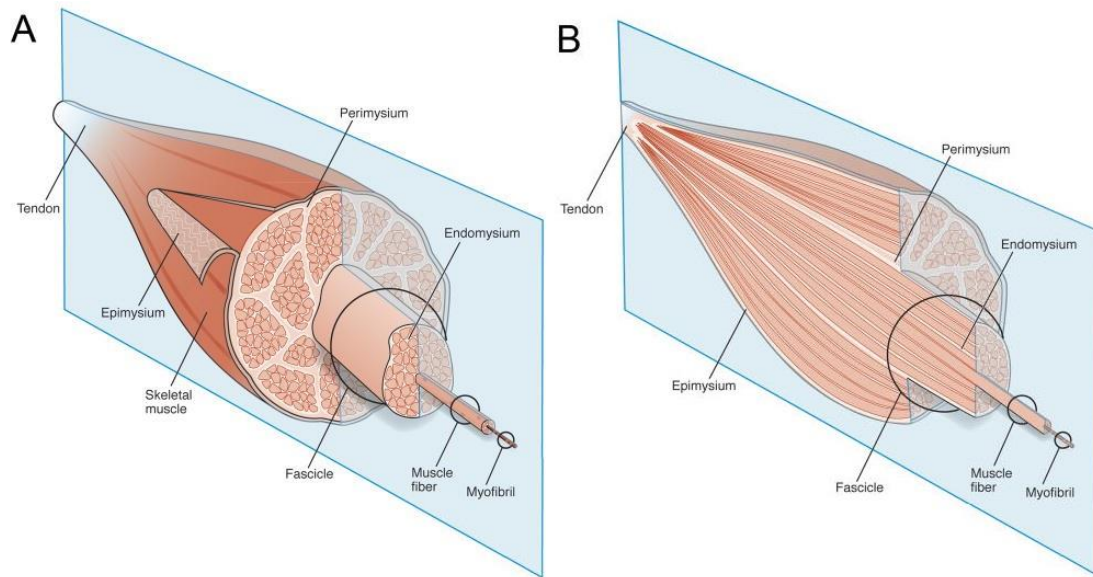
Figure 2.2: Schematic diagram of the gross organization of muscle tissue and muscle ECM-tendon organization.(A) Muscle ECM can be categorized as epimysium (surrounding the muscle), perimysium (surrounding muscle fascicles), and endomysium (surrounding muscle fibers). **(B)** Cross-section of muscle tissue indicating that the perimysium may be continuous with the tendon, whereas endomysium is contained within muscle fascicles. (Gillies & Lieber, 2012)

A skeletal muscle is connected to bones via tendons or fasciae and is entirely surrounded by a layer of connective tissue, called epimysium. The muscle is made up of multiple fascicles, which are surrounded by the perimysium layer. Every fascicle is again a bundle of smaller fibre structures, the myocytes or muscle fibres, separated by the endomysium. At the level of each of these connective tissue layers, there are blood vessels and nerve fibres permeating the muscle.

Microanatomy of a skeletal myocyte

Myocytes are the multinucleate, spindle-shaped cellular basic units of skeletal muscles. They are bundles of several hundreds of myofibrils, surrounded by the cell membrane, the so-called sarcolemma. These thin fibrils are parallelly aligned and draw through the whole length of the muscle cell. Myofibrils are principally composed of repeating sarcomeres, the basic contractile units of the striated muscle.

At the neuromuscular (or myoneural) junction, the muscle fibre connects with the axon of a motor neuron (Figure 2.3). The processes that are necessary to transmit the action potential from the axon to the muscle cell, are explained in the subsection "Contraction activation" of Chapter 2.1.2.
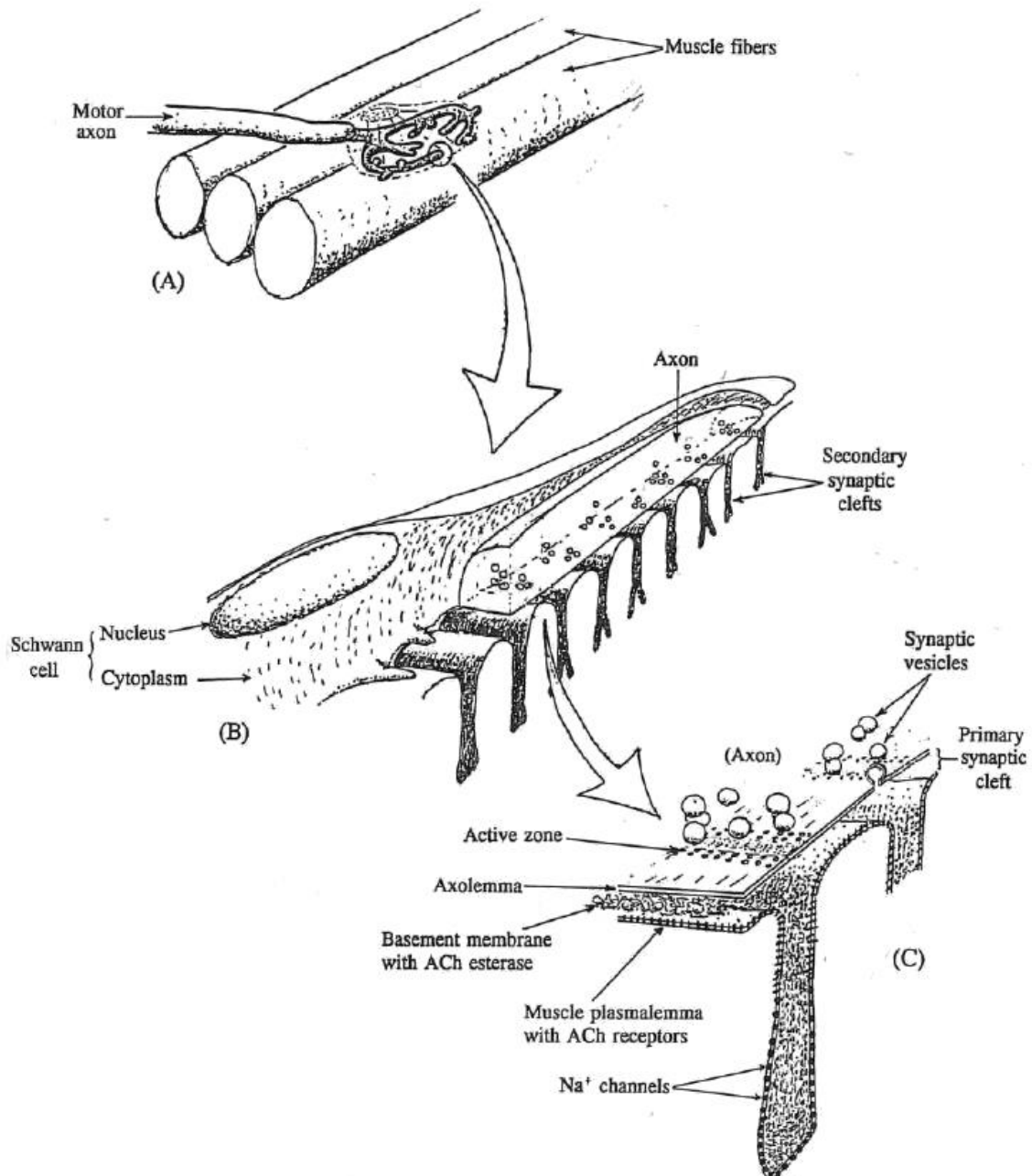
Figure 2.3: Mammalian neuromuscular junction, shown at progressively higher magnification. The different structures in the junction have not been drawn to scale. Note the synaptic vesicle emptying in C. (McComas, 1996)

In many places, the sarcolemma creases internally, forming a system of tubular folds. These tubules are running perpendicular to the surface and transverse to the longitudinal axis of the muscle cell and are therefore called T-tubules (transversal tubules).
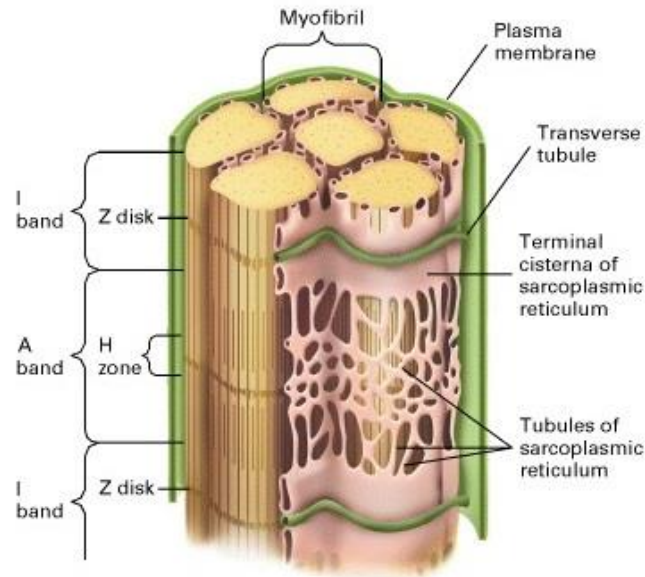
Figure 2.4: Transversal and longitudinal tubules in a myocyte. Three-dimensional drawing of a portion of a muscle cell (myofiber) composed of six myofibrils. The transverse (T) tubules, which are invaginations of the plasma membrane, enter myofibers at the Z disks, where they come in close contact with the terminal cisternae of the SR, forming triads. The terminal cisternae store Ca^{2+} ions and connect with the lace-like network of SR tubules that overlie the A band. (Lodish et al., 2000)

Besides the invaginations of the T-tubules, there is a second system of cavities, formed by extensions of the (smooth) endoplasmic reticulum (sarcoplasmic reticulum SR). These tubules are aligned parallel to the myofibrils, in the longitudinal axis of the muscle, and are called L-tubules. They act as a reservoir of calcium ions and are in close contact with the transversal membrane folds, forming functional structures called triads. Each triad includes one T-tubule and two Ca^{2+} chambers of the L-tubules system, one on each side. Within the triad, voltage-dependent calcium channels of both tubules systems are in contact (Figure 2.4).

The sarcomere

Sarcomeres are the repeating contractile base unit of the myofibrils, out of which the muscle cells are composed. The sarcomeres are made of three filament systems: the thin filaments which primarily contain actin and other regulatory proteins, the thick filament system which is mainly built from myosin and the titin polypeptide filaments.

The Z-discs (from German *Z-Scheibe, Zwischenscheibe* "disc in between") delimit a sarcomere on both sides. The thin actin filament system, as well as the titin filaments are permeating the Z-discs, connecting two neighbouring sarcomeres (Figure 2.5). This region,

which does not include the thick myosin filament, is named I-Band. The area where the myosin filament is located, is called A-band. Therefore every sarcomere, defined as the filament system in between two Z-discs, includes one A-band and two half I-bands.
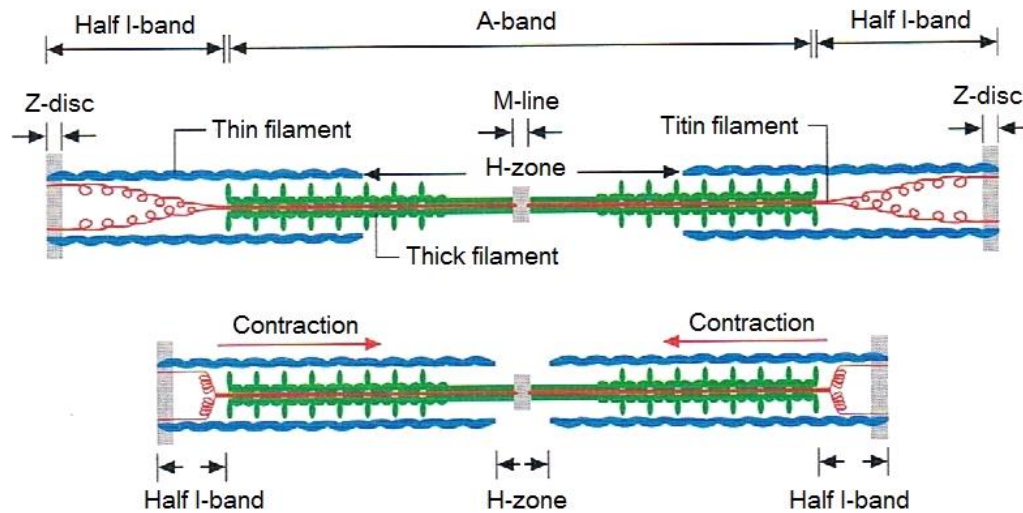
Figure 2.5: Detailed structure of a sarcomere in relaxed (upper part) and contracted state (lower part). (Robert F. Schmidt, 2003)

The region in the middle of the sarcomere, occupied only by myosin and not by actin or titin filaments, is named H-zone (from German *heller* "brighter") due to its brighter appearance under polarized light. The H-zone lies within the A-band and contains the central structure, the so-called M-line (from German *Mittel* "middle"). Here the myosin and the elastic titin filaments are anchored.

2.1.2 Physiology of skeletal muscle contraction

Molecular mechanisms – the sliding filament theory

The shortening of a skeletal muscle occurs by relative sliding movements of actin and myosin filaments. Both filaments themselves keep their length during contraction, but the relative movement of the actin filaments towards the M-line results in shortening of the I-bands, while the A-bands maintain a length of 1.6 µm. The shortening of the I-bands leads to the shortening of the whole sarcomere (Figure 2.5). The common action of many sarcomeres connected in series and parallel leads to the macroscopically observable contraction of the muscle. Stretching of sarcomeres means elongation of I-bands, which goes with an elongation of the titin filaments. In the relaxed muscle, these spring-like

filaments are responsible for most of the stretching resistance, they hold the sarcomere together and keep the A-band centred.

The molecular base mechanism behind the sliding filament theory is the cyclic interaction between myosin and actin under consumption of high-energetic ATP, the so-called cross-bridge cycling. To understand this fundamental mechanism, one must take a closer look at the molecular structure of myosin and actin. Myosin belongs to the group of mechanoenzymes, which convert the energy of chemical bonds into mechanical energy. Its complex structure exhibits six polypeptide chains, two identical heavy chains and two pairs of light chains (Figure 2.6).
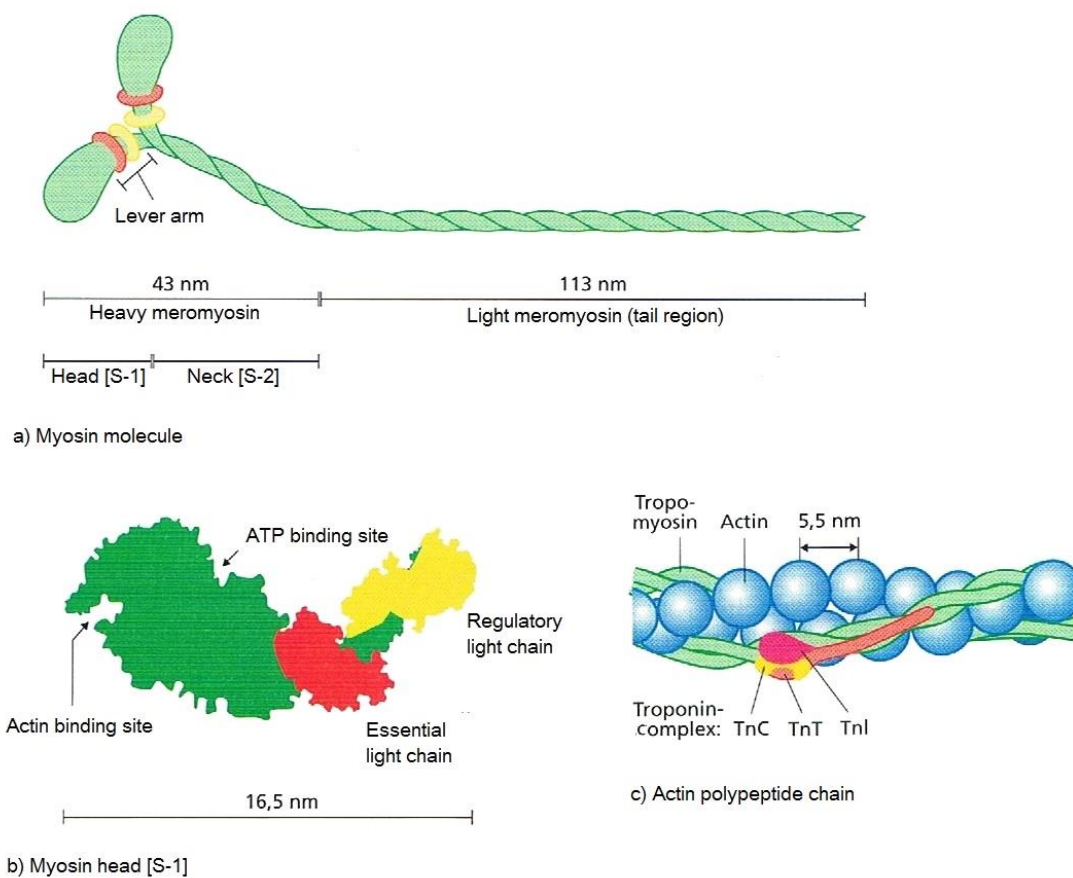
Figure 2.6: Molecular structure of myosin and actin a) Division of the molecule in three domains. b) Nuclear structure of the myosin head. c) Part of an actin polypeptide chain with the regulatory troponin complex. (Robert F. Schmidt, 2003)

The molecule can either be divided into heavy and light meromyosin or into the three domains: head, neck (which are both subunits of the heavy meromyosin) and tail region (which corresponds to the light meromyosin). The latter aggregates with the tails of other molecules to form the myosin filament, out of which myosin heads arise in a regular arrangement.

The polymerized contractile protein actin exists in form of a double-stranded helix (F-actin), built out of the globular monomer (G-actin), which has a diameter of 5.5nm. Every winding of the polymer consists of 14 monomer units. Along the actin chain extends the thread-like tropomyosin, which also consists of two helical arranged peptide chains. In the regular distance of seven actin monomer units round troponin complexes bind to the actin, partially hidden in the groove between the two actin helices. These complexes consist of three subunits: The tropomyosin binding TnT, the inhibitory (actin binding) TnI and the Ca^{2+} binding TnC (Figure 2.6.c). Due to different concentrations of Ca^{2+} ions, different subunits of the troponin complex are exposed or hidden in the actin groove.
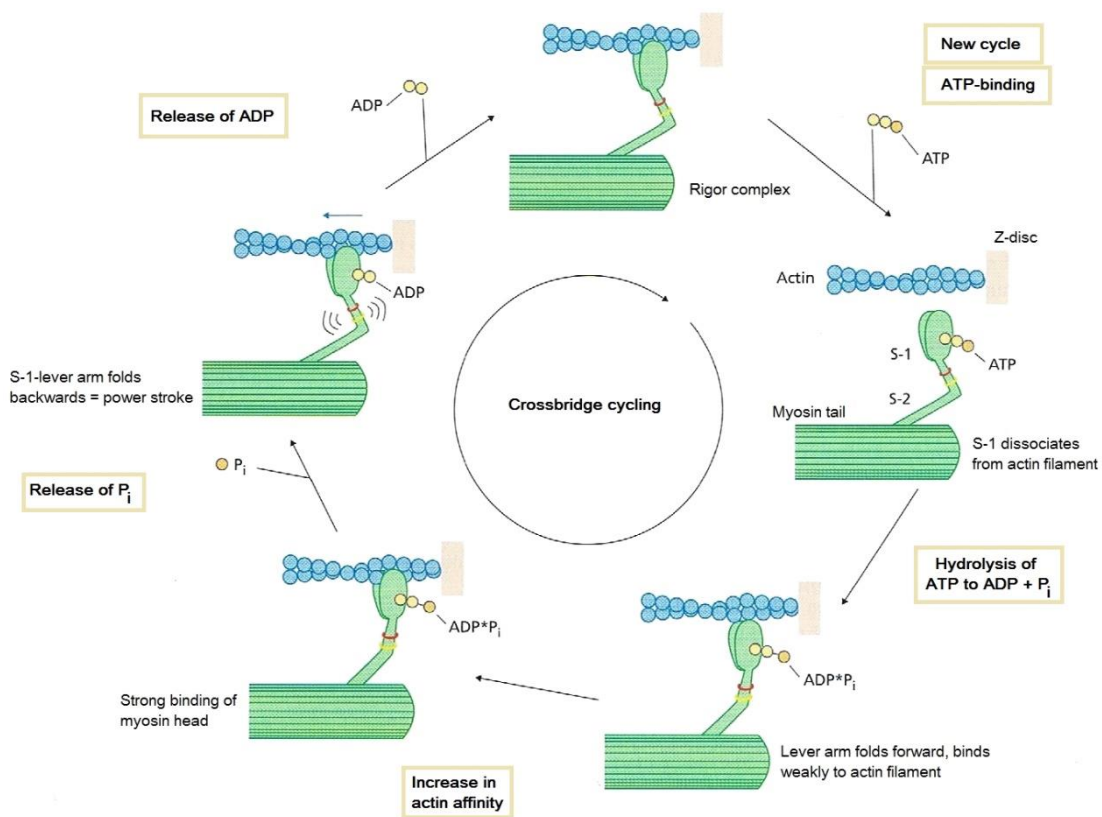
Figure 2.7: Cross-bridge cycling Step-wise process of cross-bridge cycling under cleavage of ATP. Most of the movement of the myosin molecule is probably occurring in the lever arm region, where the light chains are located. (Robert F. Schmidt, 2003)

It is assumed that within the contraction process, in both sarcomere halves, cross-bridges interact with the actin filaments such that a uniform tensile force is acting on them towards the sarcomere center. The myosin head binds and unbinds 10-100-times per second to actin, which is presumably accompanied by the hydrolysis of one ATP molecule for each binding cycle (Figure 2.7). It is functionally remarkable, that, when bound, the myosin head exhibits

a hundredfold increase of ATPase activity. According to current understanding, in every cross-bridge cycle, the following five steps are completed:

1. An ATP molecule binds to the myosin head, so that it detaches from the actin filament.

2. ATP is cleaved into ADP, an inorganic phosphate (P_i). Both reaction products remain at the myosin head. According to a low affinity, myosin-S-1 binds weakly to the actin filament.

3. The increase in actin affinity leads to a stronger binding of the myosin head.

4. The consecutive release of the hydrolysis products P_i and ADP leads to a conformation change of the myosin head, which is followed by a backwards folding of the lever arm, the so-called power stroke.

5. Before a new cycle starts, the myosin head is firmly connected to the actin (rigor complex). This state corresponds to the rigor mortis, the stiffening of a dead body due to ATP-deficiency.

Spatially and temporally the forces of millions of cross-bridge cycles are summing up and are translated over the Z-discs and cell ends to the skeleton.

Contraction activation

The cross-bridge process is regulated by the cytosolic Ca^{2+} ion concentration. An increase in the ion concentration is initiated with the arrival of an action potential (explained in more detail in Chapter 2.2.1) at the neuromuscular junction (see also Figure 2.8.c). The action potential is conducted via an α-motoneuron from the spinal column, more precisely from the anterior gray horn, to the neuromuscular junction of one or more muscle fibers. The motoneuron and all muscle fibers innervated by its axonal terminals are called a motor unit (Figure 2.8.a). At the neuromuscular junction, the action potential is transmitted to the muscle cell surface via the release of neurotransmitters into the synaptic cleft. Once arrived at the muscle surface, the contraction signal is conducted over the sarcolemma into the T-tubules system and to the voltage-dependent dihydropyridine receptors. These channel proteins undergo a conformation change, which is recognized by the ryanodine receptors on the terminal cisternae of the sarcoplasmic reticulum (L-tubules system). The ryanodine receptors now become permeable for Ca2+ ions. Following the concentration gradient, calcium ions are dispersing from their reservoir into the cytoplasm. When the cytoplasmic concentration reaches a threshold of approximately 10^{-7} mol L^{-1}, a conformation change

occurs in the troponin complex, which leads to an exposing of the myosin binding sites. Now cross-bridges with increased affinity can be formed, the myosin head binds firmly to the actin filaments.
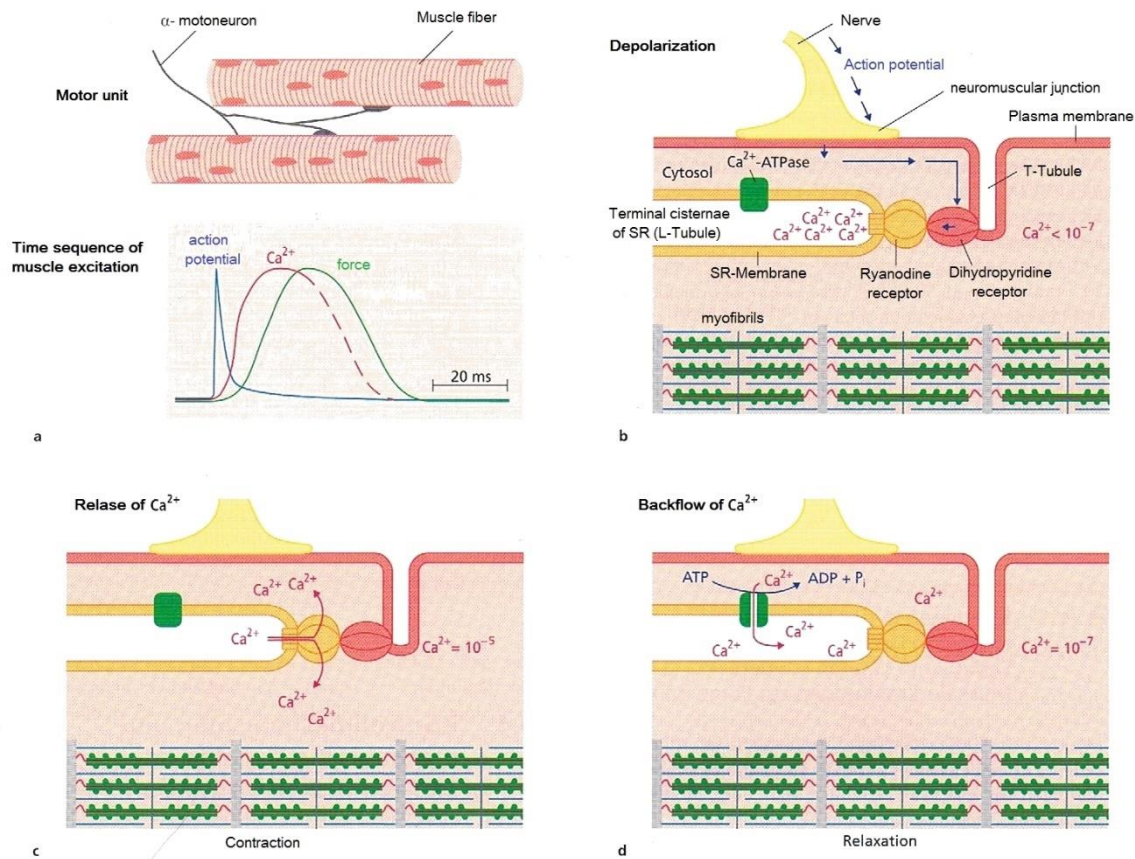
Figure 2.8: Neuromuscular junction of skeletal muscle (**a**) Schematic representation of a motor unit (here with only two muscle fibres) and typical time sequence of action potential, Ca^{2+} release and force production of a muscle fibre. (**b**) Relaxed muscle with incoming action potential. (**c**) Release of Ca^{2+}-ions from the SR leads to an increased calcium concentration – the muscle contracts. (**d**) The backflow of Ca^{2+} ions into the SR, driven by an ATP powered pump, leads to muscle relaxation. (Robert F. Schmidt, 2003)

When the muscle fiber is no longer activated with action potentials, the calcium channels close again and reverse processes take place to lower the cytoplasmic Ca^{2+} concentration again, which is mainly realized under ATP consumption via calcium pumps. When the Ca^{2+} ion concentration falls below the threshold, the regulatory troponin complex regains its inhibitory function, the myosin binding sites are no longer exposed and therefore no cross-bridges can be formed - the muscle relaxes again.

Control mechanisms of muscle contraction force

Skeletal muscles have to be able to produce different amounts of force, due to specific physiological requirements. In vivo there are two mechanisms to control the muscle contraction force. On the one hand, the contractile force can be increased by increasing the

frequency of action potentials in the α-motoneuron. On the other hand, recruiting more motor units leads to an increased muscle force production.

a Single twitches and tetanic contractions

b Derivation of action potentials of motor units in EMG
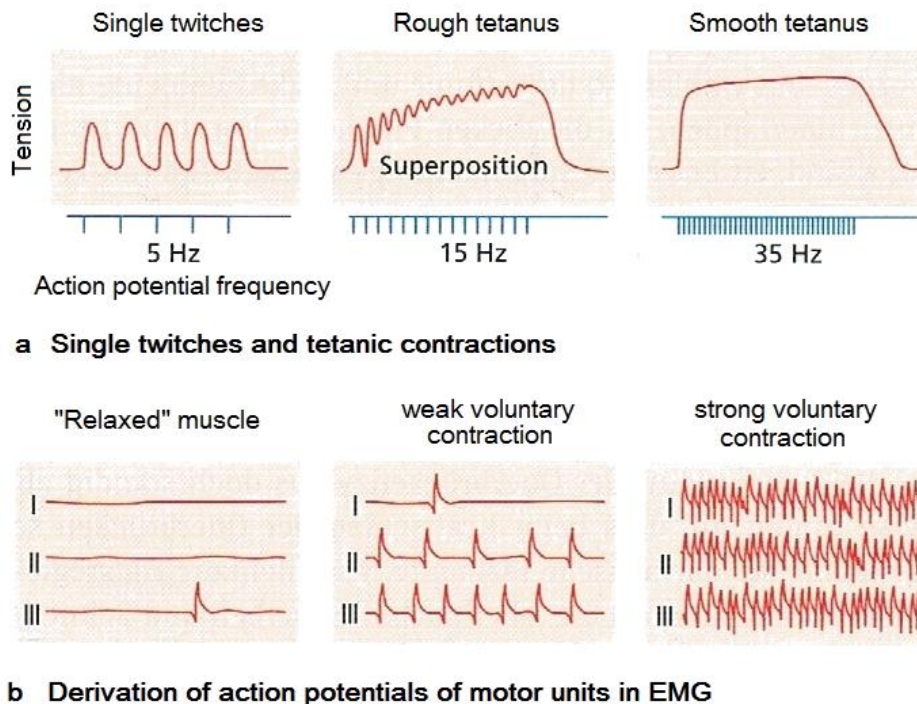
Figure 2.9: Central nervous mechanism to control skeletal muscle contraction (a) Increasing the action potential frequency leads to fusion of single twitches to tetanic contractions with higher muscle tension. (b) Principle of recruiting more motor units to increase muscle force production, shown in an example with three functional groups (I, II and III). (Robert F. Schmidt, 2003)

- Action potential pattern and state of contraction

  A single action potential arriving at the neuromuscular junction only results in a very short increase of the intracellular calcium concentration above the threshold value, directly followed by repolarization of the Ca^{2+} channel proteins. There is not enough time for the contractile apparatus to exert the maximum force, and only a single twitch can be observed.

  With higher action potential frequency of 5-15 Hz (depending on type of muscle fibre) the single twitches start to fuse to a rough tetanus, meaning that the force maxima of the twitches are summing up to a greater total force (Figure 2.9.a).

  When the frequency of action potentials arriving at the muscle cell is even higher (30-50 Hz), the cytosolic calcium concentration stays constantly above the threshold value, necessary for the cross-bridge cycle. Now the maximum force can be exerted and smooth tetanus is formed.

- Motor unit recruitment

Skeletal muscles are composed out of multiple motor units, which are innervated separately. Muscle contraction force and velocity can be controlled by the amount of motor units fired with action potentials, this phenomenon can be easily observed using electromyography (Chapter 2.2). In a relaxed muscle, almost no action potentials can be measured. In a voluntary weak contracted muscle, some motor units will show relatively high frequency action potential patterns, while in others hardly any signals can be observed. In case of a strong voluntary muscle contraction, all motor units are fired highly frequently (Figure 2.9.b).

2.2 Electromyography

"Electromyography (EMG) is an experimental technique concerned with the development, recording and analysis of myoelectric signals. Myoelectric signals are formed by physiological variations in the state of muscle fiber membranes." (Basmajian & De Luca, 1985)

After giving a general explanation of what EMG is and how volitional myoelectric signals are generated, the basic types of EMG applications, invasive and non-invasive are introduced in this chapter. Lastly, two examples for evoked EMG signals, the H-reflex and the M-wave are presented.

2.2.1 What is EMG?

Signal origin: The action potential

As described in Chapter 2.1.2, skeletal muscle contraction is controlled by the number, distribution and frequency of action potentials arriving at the sarcolemma. The electrical properties of the sarcolemma can be explained using the model of a semi-permeable membrane. The intracellular concentration of Na+ ions is much smaller than the concentration outside the cell. This difference in ionic concentrations is actively maintained by channel proteins, so-called ion pumps. The chemical gradient across the cell membrane forms an electrostatic resting potential of the sarcolemma of approximately -70 to -80 mV (Rattay, 1990).
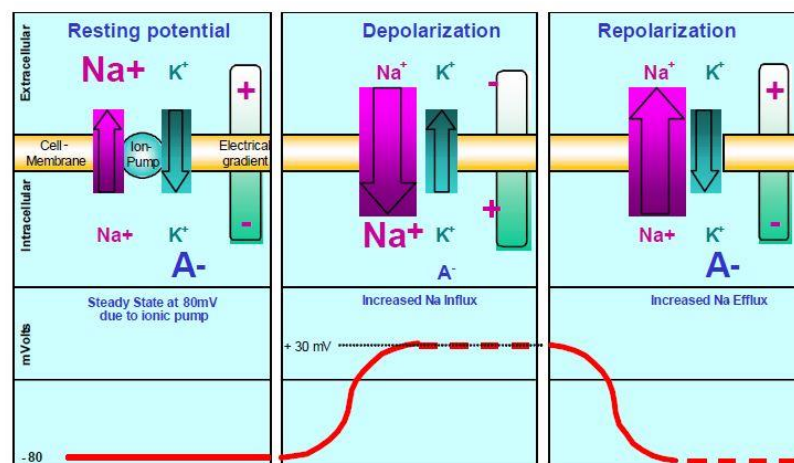
Figure 2.10: Schematic illustration of depolarization / repolarization cycle within excitable membranes (Konrad, 2005)

When, due to central nervous control or reflex, an action potential is conducted from an alpha motor neuron at the anterior horn to the motor endplates of the corresponding muscle fibers of this motor unit, a neurotransmitter is released at these endplates. This release results in an endplate potential, which leads to a very short change in the ion diffusion characteristics across the cell membrane. Channel proteins for Na+ ions open, and following the chemical gradient, Na+ ions are flowing into the cell, resulting in a rapid increase of the membrane potential, the so-called depolarization. This process is then reversed by active ion pump mechanisms, which restore the resting state of the cell by pumping Na+ ions out of the cell (Figure 2.10). These processes of depolarization and repolarization are running spatially like a chain reaction across the muscle fibers of the activated motor unit. This characteristic shift of potential across the cell membrane is called Action potential (Figure 2.11).
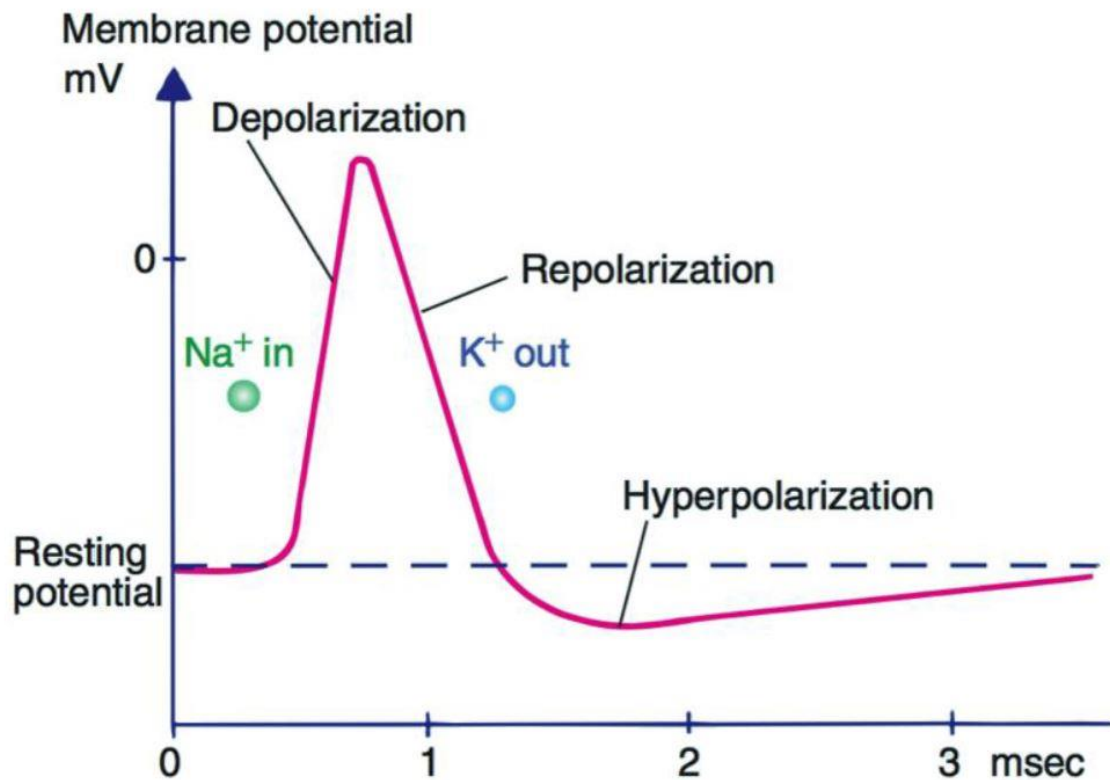
Figure 2.11: The action potential can be divided into periods of depolarization, repolarization and hyperpolarization. Simplified, the main mechanism responsible for the depolarization is the Na^+ ion influx, whereas the K^+ ion flow out of the cell leads to re- and hyperpolarization. Reprinted from (Brodal, 2010).

Signal Propagation and detection

After repolarization the cell membrane is in a refractory period, where it cannot be excited again. This causes the zone of depolarization, which is described in literature to be an area of 1-3mm² (Winter, 1990), to propagate as a front of excitation across the muscle fiber in one direction (Figure 2.12).
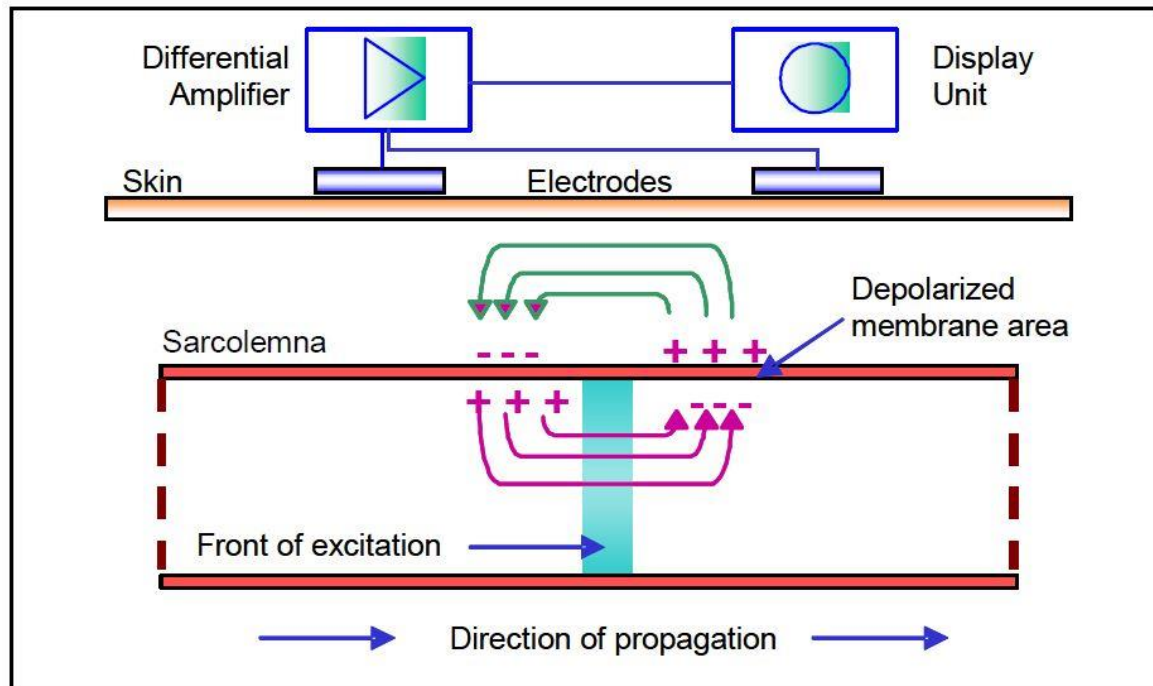
Figure 2.12: The depolarization zone propagates on muscle fiber membranes. Adopted and modified from (Kumar & Mital, 1996).

Now this front of excitation, which can also be seen as an electrical dipole (Winter, 1990), propagating across the muscle cell, also passes by the EMG detection site. The following model assumes a bipolar EMG measurement on a single muscle fiber. An electrode pair and a differential amplifier are used to measure the potential difference between two points on the muscle. The electrical dipole moving past the measuring sites leads to a time-dependent change in the measured potential-difference between the electrodes. This results in the characteristic biphasic waveform, which represents a single action potential at one muscle fiber (Figure 2.13).
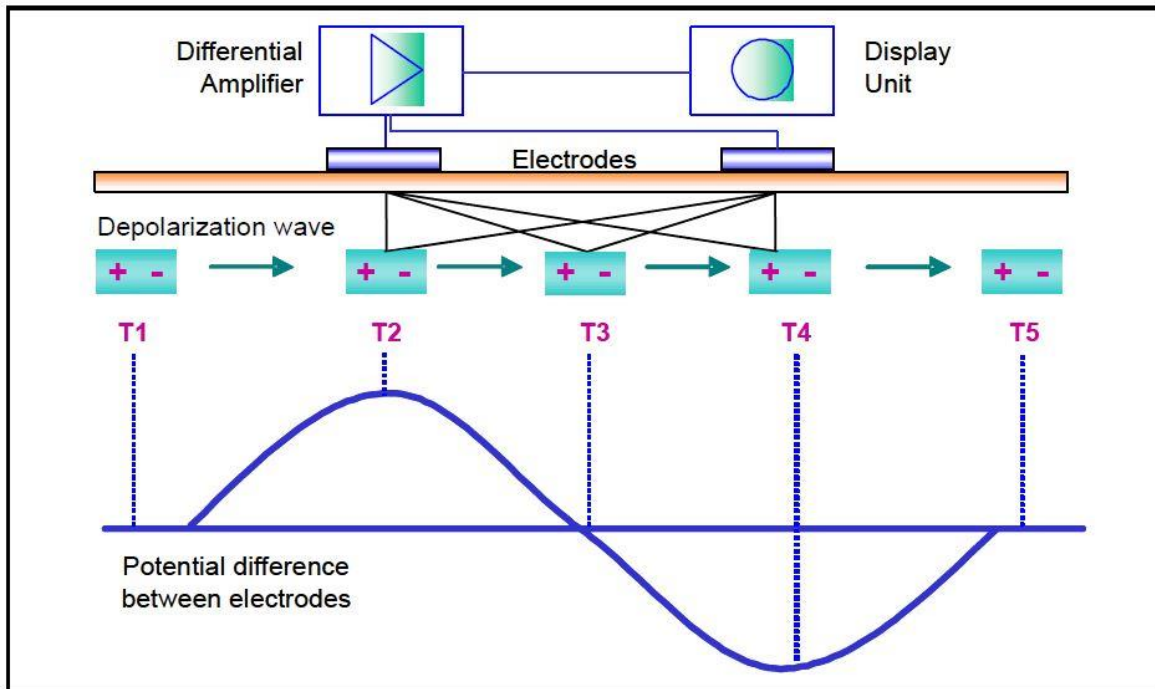
Figure 2.13: The model of a wandering electrical dipole on muscle fiber membranes
Adopted and modified from (Kumar & Mital, 1996).

Recalling the clustered innervation of muscle fibres in motor units, this model can be extended. We assume a spatially even distribution of motor endplates, which relate to the point of excitation initiation of the clustered muscle fibres around the measuring sites. Now the electrical dipoles of the single muscle fibres are travelling along the electrodes time-shifted and from different directions. The sum of these shifted and mirrored biphasic waveforms will typically result in a measured triphasic motor unit action potential (MUAP) (Figure 2.14).
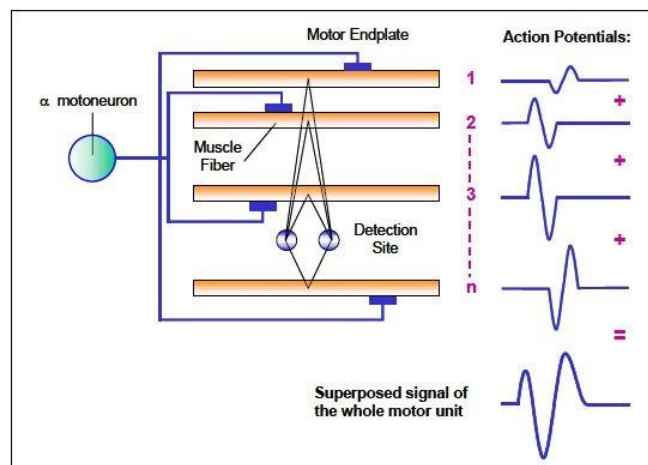
Figure 2.14: Generation of the triphasic motor unit action potential (MUAP) Adopted and modified from (Basmajian & De Luca, 1985).

Composition of EMG signal

In case of strong volitional muscle contractions, deviating from the models introduced before, multiple motor units are actively fired with action potentials. These triphasic MUAPs with different frequencies are summing up to a superposed signal measured at the muscle surface. Figure 2.15.b gives an example of EMG measurements of volitional contraction of the musculus biceps brachii with rest periods of relaxation.
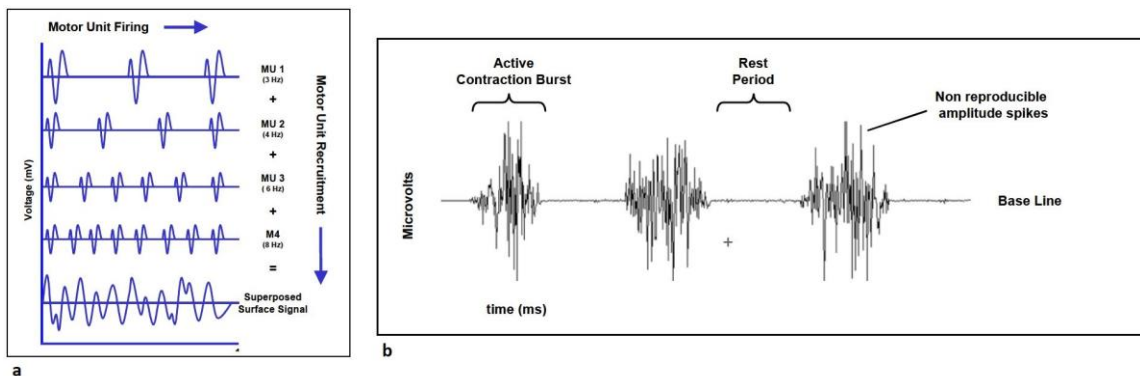
Figure 2.15: Superposed surface signal of multiple motor unit action potentials. (a) Extended model with four motor units, fired with different frequencies. **(b)** EMG measurements of volitional contraction of the M. biceps br. Adopted and modified from (Kumar & Mital, 1996) and (Konrad, 2005).

2.2.2 Types of EMG

There is a wide range of EMG applications in the fields of rehabilitation, medical research, ergonomics and sports science. To meet the specific requirements of the respective field of application, different EMG electrodes are chosen. The electrode systems can be categorized in non-invasive skin surface electrodes and invasive intramuscular electrodes.

Skin surface EMG

In most applications, surface electrodes are used because of their non-invasive character. They are placed on the belly of the muscle that is to be measured. The most common form of skin surface electrodes are pre-gelled silver / silver chloride electrodes (Figure 2.16). There are wet gel electrodes, these are typically characterized by very good conductivity, and adhesive gel electrodes, which have the advantage of easy repositioning in case of error.
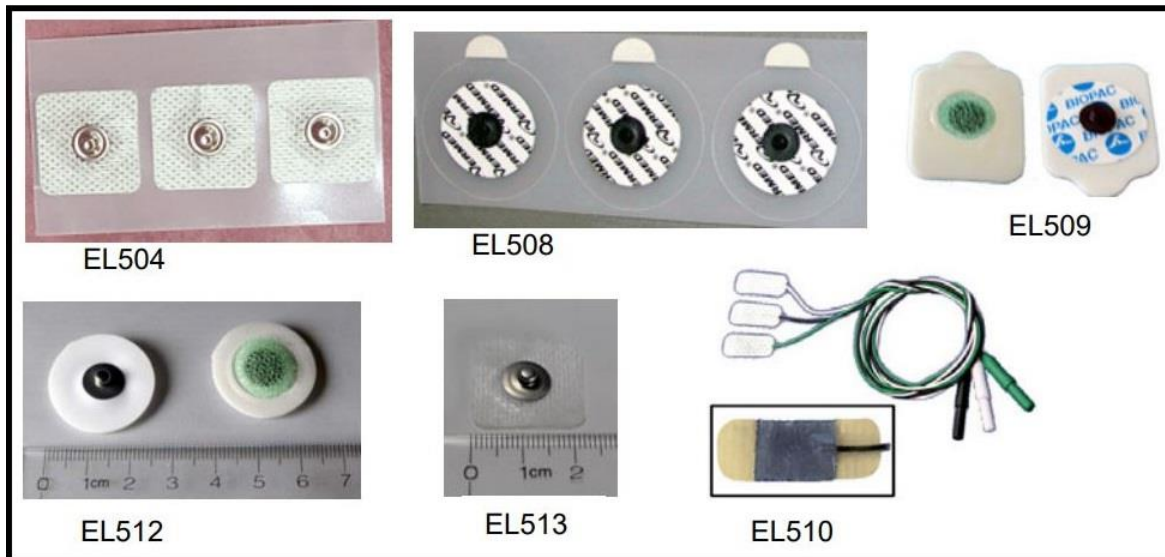
Figure 2.16: Skin surface EMG electrodes. Some examples out of BIOPAC® EL500 Series of disposable Ag/AgCl snap electrodes (BIOPAC® Systems Inc, 2016a).

Despite their ease of use, surface electrodes are only suitable for recording EMG signals on superficial muscles, whereas deeper muscles cannot be adequately measured. Further application quality limiting factors are:

- Tissue characteristics

  Although the human body, which consists to a large part of ionic liquid, is a good conductor, the conductivity strongly varies with different types of tissue. In adipose subjects for example, the thicker layer of subcutaneous fat tissue has a dampening effect on the EMG signal (Figure 2.17). This results in a smaller signal amplitude, and is accompanied with a worse signal to noise ration and thus less meaningful measurement data.
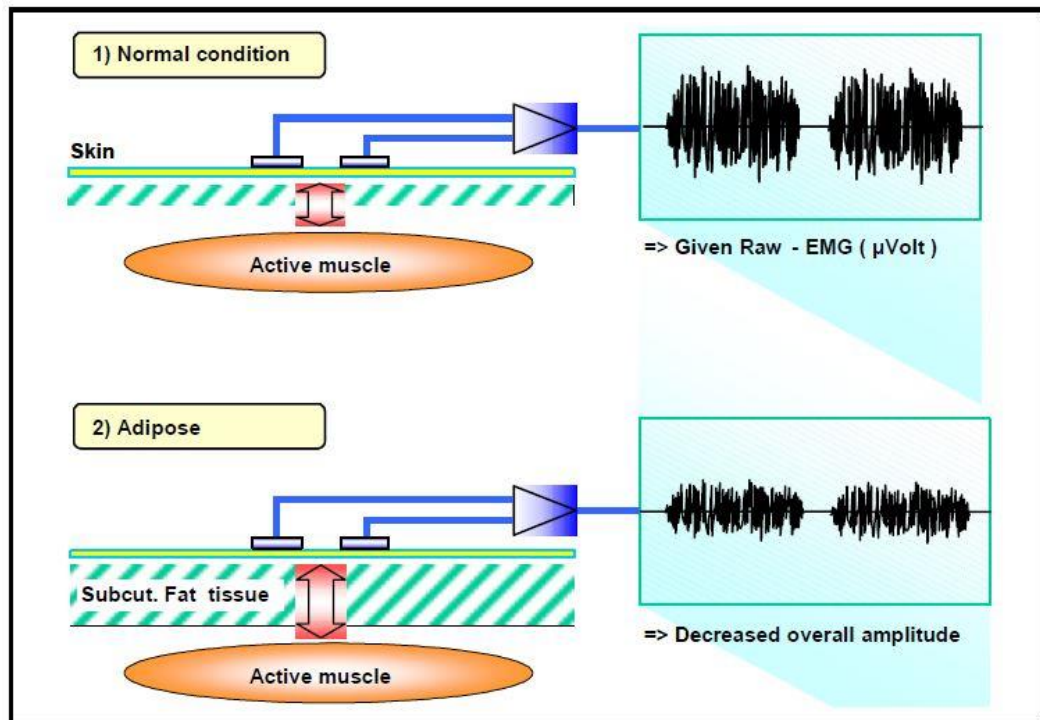
Figure 2.17: Influence of thickness of subcutaneous fat layer on surface EMG measurements. Given the same amount of muscle electricity, condition 1 produces more EMG magnitude due to smaller distance between muscle and electrodes (Konrad, 2005).

- Physiological cross talk

  The activity of neighbouring muscle groups can influence the EMG signal of the muscle that is to be examined. The phenomenon of physiological cross talk can easily be observed in measurements on the shoulder, chest or upper trunk muscles. Here, due to the short distance from the heart, the rhythmical activity of the heart muscle strongly influences the EMG recording.

- Geometrical changes during the measurement

  If the EMG measurement involves movements of the subject, geometrical changes of the muscle belly may also influence the data. During contraction, the muscle belly shortens, which may cause the electrodes to be in a sub-optimal position, not centred on the muscle anymore.

Intramuscular EMG

In kinesiological studies, that involve extensive movements of the subject during the EMG measurement, especially when non-superficial muscles are examined, invasive intramuscular EMG electrodes are preferably used. Figure 2.18 schematically depicts a widely used electrode type for this application is the fine wire electrode.
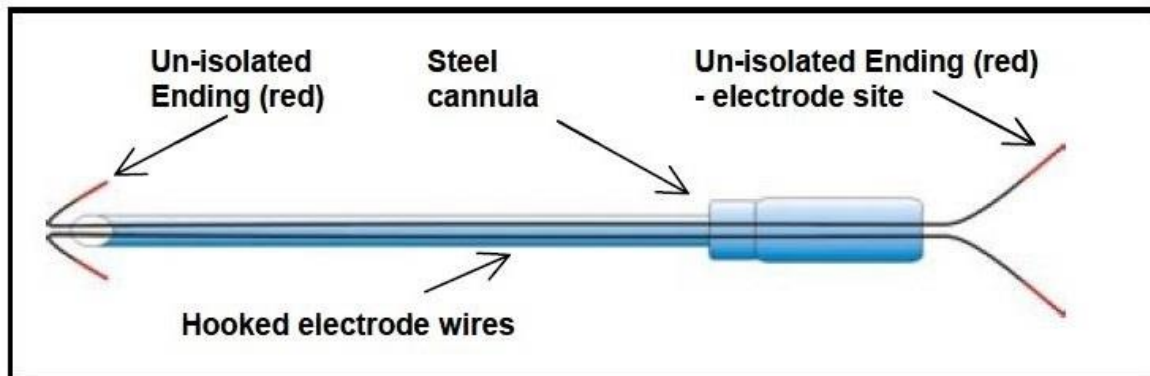
Figure 2.18: Schematics of a fine wire electrode: two fine wires with un-isolated endings are located with a steel cannula. System MEDELEC® (Konrad, 2005).

These electrodes are pairs of thin isolated wires with un-isolated ends. The hooked end is inserted via a hollow steel needle into to muscle belly (Figure 2.19). After removing the needle, the distal wire endings are connected to a pair of springs, which act as a connector for the regular pre-amplifier electrode leads.
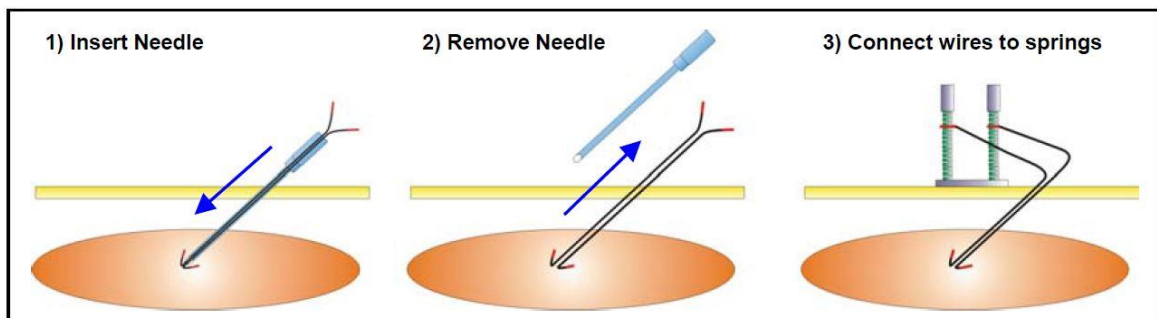
Figure 2.19: Procedure to insert the fine wires into the muscle tissue.(Konrad, 2005).

2.2.3 Evoked signals: H-reflex and M-wave

In addition to the EMG signals, obtained by measuring volitional muscle activity, as presented in Chapter 2.2.1, there are also signals due to non-volitional muscle activities. These include reflexes, like the tendon tap and the withdrawal reflex, as well as electrically evoked signals. Two types of evoked EMG signals, which are of relevance in the field of electrical stimulation, are the H reflex and the M wave.

To study the physiology of the monosynaptic connections of Ia sensory fibres to spinal motor neurons, eliciting H-reflexes can be used as an important technique. The H-reflex is named after the physiologist Paul Hoffmann (1884-1962). It is elicited, when a peripheral nerve, more precisely the Ia sensory fibres of a muscle spindle, is electrically stimulated (Hoffmann, 1922). The H-reflex is a monosynaptic spinal reflex: The afferent sensory fibre conducts this electric impulse to the soma of a motoneuron in the spinal column, using monosynaptic pathways. This motoneuron in response sends an action potential to the muscle cells it innervates (motor unit), which can be measured using EMG (Figure 2.20.a).

In humans, the H-reflex can easily be measured in the soleus muscle at the calf. Therefore, the Ia sensory fibres of the soleus muscle are stimulated via electrodes at the inside of the knee, where the tibia nerve is located. The reflex response, which is dependent on the stimulation strength, is measured at the soleus muscle using EMG skin surface electrodes. If the stimulation intensity is further increased a second EMG signal is evoked, the so-called M-wave. This signal is the result of direct stimulation of the motor axons, which innervate the soleus muscle. Due to the higher stimulation threshold of the motor axon compared to the sensory nerve tissue, the M-wave is only evoked when using strong stimulation impulses (Figure 2.20.c).
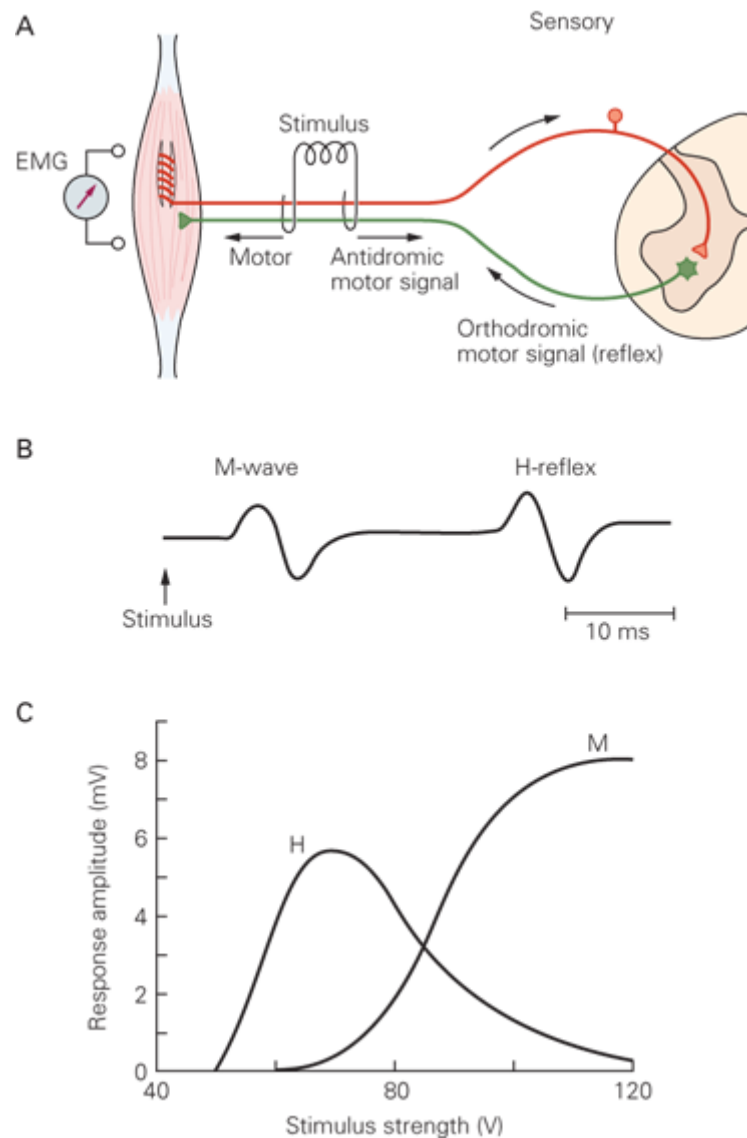
Figure 2.20: The Hoffmann reflex. A) The Hoffmann reflex (H-reflex) is evoked by electrically stimulating Ia fibers from muscle spindles in mixed nerves. The sensory fibers excite alpha moto neurons, which in turn activate the muscle. Muscle activation is detected by the electromyogram (EMG). **B)** At intermediate stimulus strengths motor axons in the mixed nerve are excited in addition to the spindle afferents. Excitation of the motor neurons produces an M-wave that precedes the H-wave (H-reflex) in the EMG. C) At low stimulus strengths only an H-wave is produced because only the spindle afferents are excited. As the stimulus strength increases, the magnitude of the H-reflex also increases, then declines, because the orthodromic motor signals generated reflexively by the spindle afferents are cancelled by antidromic signals initiated by the electrical stimulus in the same motor axons. At very high stimulus strengths only an M-wave is evoked. (Adapted, with permission, from Schieppati 1987) (Kandel, Schwartz, & Jessell, 2013).

Timing-wise, the H-reflex is measured later than the M-wave, which can be explained by considering the respective pathway length, that signals need to travel until they are recorded (Figure 2.20.b). The M-wave is evoked directly in the innervating motor axon and has therefore a much shorter pathway than the H-reflex, which has to travel to the spinal cord, across a synapse and along the whole motor axon (Kandel et al., 2013).

2.3 Electrical stimulation of nervous tissue

The application of electrical currents to the human body for medical purposes is practiced for over 2000 years (D.R. McNeal, 1977). Over the course of this long time, methodology as well as instrumentation developed from treating headache using shocks from torpedo fish to the vast field of biomedical devices, that are in use today. These include cardiac / phrenic pacemakers, visual and auditory prostheses as well as devices for neuromuscular stimulation. This subchapter will provide a brief, theoretical introduction into the principles of electrical nerve stimulation. Therefore, first the functional structure of the nervous system will be explained. Then general principles of electrical nerve stimulation will be given followed by an introduction of the application of this technique to stimulate posterior roots.

2.3.1 The nervous system

The nervous system is concerned with rapid transmission of information within an organism. In contrast to some primitive organism, the human nervous system exhibits a complex network of highly differentiated neurons (see Figure 2.21). In humans, the majority of nerve cells are located at the central nervous system (CNS), which consists of the brain and the spinal cord. Besides the central nervous system, there is the peripheral nervous system (PNS). The nerves of the peripheral system can be divided into autonomic and somatic nervous system. The somatic system is concerned with sending sensory input via afferent nerve fibres towards the CNS and transmitting voluntary movement signals via efferent fibres to the skeletal muscle system.
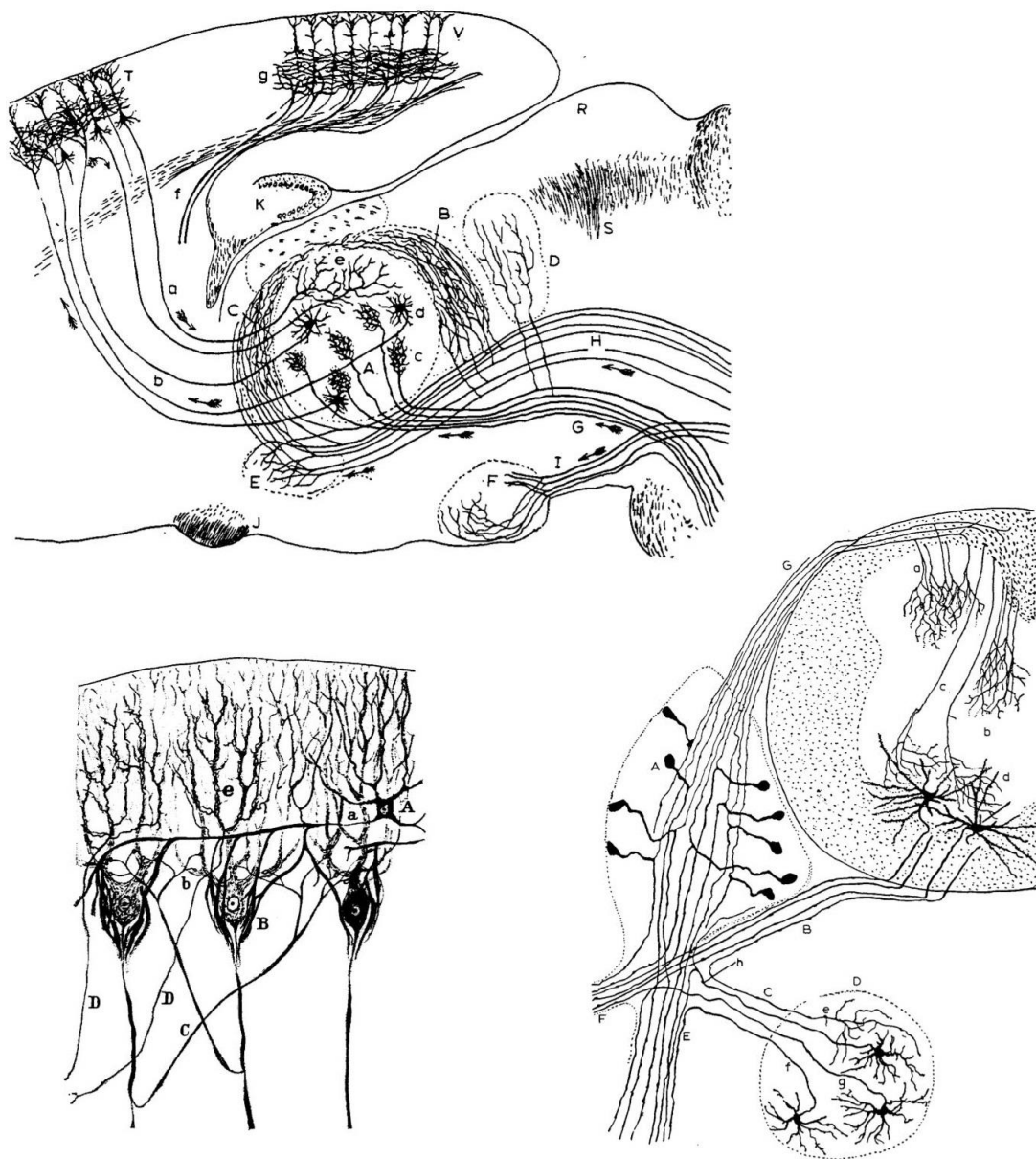
Figure 2.21: Histological samples of neurons with silver staining, made by Santiago Ramon y Cajal. The staining visualizes a complex network of highly differentiated neuronal cells.(Ramon y Cajal, 1906)

The basic build of a neuron can be simplified as the input region, consisting of the cell body (soma) and a branched network of dendrites, the conductile region of the axon and the output region with the axonal processes (Figure 2.22). The dendritic input branches as well as the cell soma are covered with up to 200.000 synapses, to receive information from other neurons and conduct them to be processed at the soma. These synapses can be either excitatory or inhibitory, meaning that they either promote or restrain excitation of the soma when they are activated. At the membrane of the soma, all potentials of these synaptic signals are summed up. If the overall potential is below a certain threshold, the cell soma

stays in its resting state and no action potential is sent. If the excitatory synaptic input is strong enough to reach the threshold, the cell membrane at the soma is depolarized and an action potential is sent to the axon.

The basics of the generation of action potentials and their propagation along the membrane of excitable tissue are explained in Chapter 2.2.1.
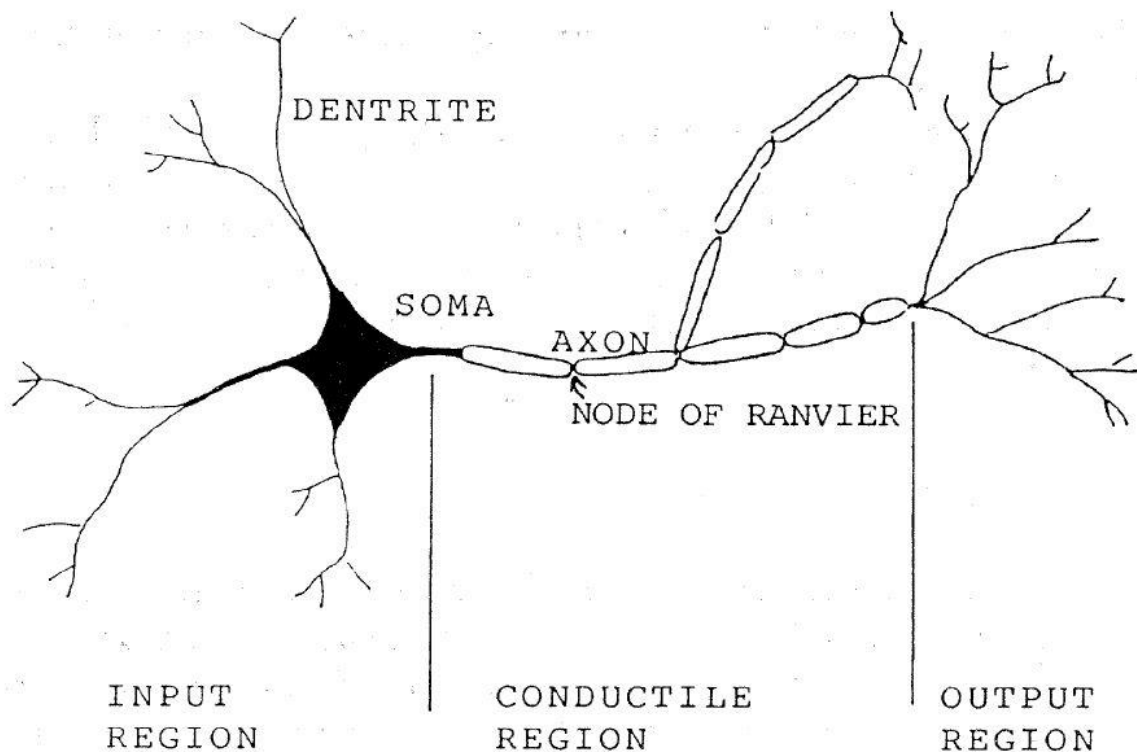
Figure 2.22: The basic build of a neuron can be divided into input, conductile and output region. (Rattay, 1990)

The axon is a long cylinder, surrounded by an excitable cell membrane and can either be myelinated or non-myelinated. Myelin is an electrically insulating fatty substance that shields some nerve fibres. It is made of Schwann cells, that are wrapped around the nerve fibre 10 to 160 times, forming an insulating sheath of up to 321 layers of cell membrane (two for each wrapping plus the axonal cell membrane itself) (Arbuthnott, Boyd, & Kalu, 1980).

Invertebrate species almost exclusively have nerve fibres without this myelin sheath. Experiments found, that the conduction velocity of these non-myelinated fibres is proportional to the square root of the fibre diameter (Hodgkin & Huxley, 1952). This lead to the development of relative large diameter nerve fibres in some invertebrates, where rapid conduction of information is required. The giant squid for example has nerve fibres with

diameter of up to 1mm, which made them very interesting specimen for the experimental work of Hodgkin and Huxley. Also in vertebrate species, non-myelinated nerve fibres are found, where slow signal conductance is sufficient, e.g., in peripheral pain and temperature sensory nerves.

Most of the nerve fibres in vertebrate species are myelinated. The myelin sheaths are periodically interrupted by the so-called nodes of Ranvier (see Figure 2.22), which are small regions where the cell membrane of the axon is exposed. This periodic distance between two nodes is typically about 100 times the outer fibre diameter. Unlike the non-myelinated fibres, where the relationship between diameter and conductance velocity is quadratic, it becomes linear in case of myelinated nerves. "In practice, this means that for warm blooded myelinated fibers having diameters less than 11 µm, the conduction velocity in meters per second can be assumed to be 4.5 times the diameter in µm, and for thicker fibers this constant of proportionality becomes about 6." (Rattay, 1990)

2.3.2 General stimulation of a nerve

Besides the natural physiological ways of eliciting action potentials within a nerve cell, as explained above, neuronal tissue can be excited by extracellular potentials. In electrical nerve stimulation, these potentials are generated as a result of an electrical field, which is induced through the skin via surface electrodes, or directly to the nerve fibre via implanted electrodes. Since excitation is initiated at the voltage-dependent ion channels of the nerve membrane in myelinated fibres, this process can only occur at the nodes of Ranvier. Here the membrane and its channel proteins are exposed to the extracellular space and, in case of electrical stimulation, they are also exposed to the extracellular potential. Since the rest of the axon is electrically insulated by the myelin sheath, the excitability of a neuron is positive proportional to the length of the exposed membrane area between two nodes, called the inter-nodal distance (Donald R. McNeal, 1976; Rattay, 1986). Also, the nerve fibre diameter has been found to positively relate to its inter-nodal distance (Nilsson & Berthold, 1988). Both dependencies support the early experimental works of Blair and Erlanger, that states that large diameter nerve fibres are excited via extracellular potentials before smaller fibres (Blair & Erlanger, 1933). This is known as the inverse recruitment order of electrical stimulation (see Figure 2.23); "inverse" due to the fact, that in natural muscle activation processes, small motor units are recruited first, followed by larger ones (Henneman, 1981).
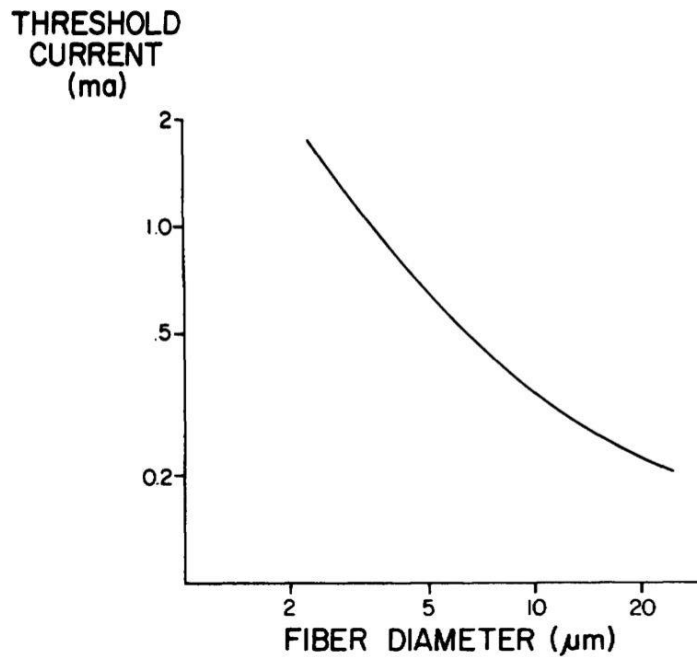
Figure 2.23: Threshold current as a function of fiber diameter with a monopolar electrode located 1mm above one of the nodes (Donald R. McNeal, 1976).

Besides these dependencies of neuronal excitability of the anatomical geometries, the stimulation intensity and pulse duration strongly influence the probability of excitation. Strong electrical impulses can elicit action potentials with shorter pulse durations than weaker impulses (Figure 2.24).
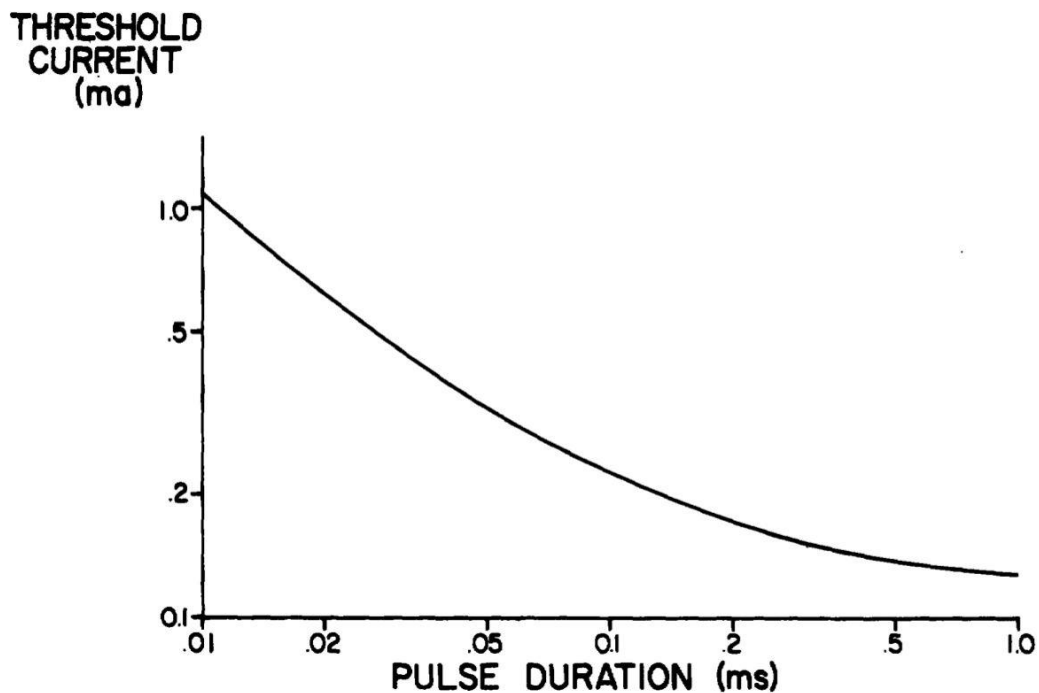
Figure 2.24: Strength-duration curve for a 20 µm fiber (internodal spacing, 2mm) with a monopolar electrode located 1mm above one of the nodes (Donald R. McNeal, 1976).

2.3.3 Posterior root stimulation

The special application of electrical stimulation to the posterior root nerve fibres (Figure 2.25) in the spinal cord has the aim to elicit so-called posterior root reflexes. In contrast to the peripheral mixed nerves (as described before, compare Figure 2.25.B), that contain both, afferent and efferent fibres, the posterior roots are only composed of afferent, sensory nerve fibres. Therefore, using posterior root stimulation, no M-waves can be evoked (Figure 2.25.A). Although functionally equivalent, the reflexes evoked with this stimulation setup are not referred to as H-reflexes, but as posterior root reflex (PRR) or sometimes as posterior root muscle (PRM) reflex (Minassian et al., 2007). Both reflexes are monosynaptic, but due to the shorter conduction pathway, the posterior root reflex exhibits a shorter onset latency.
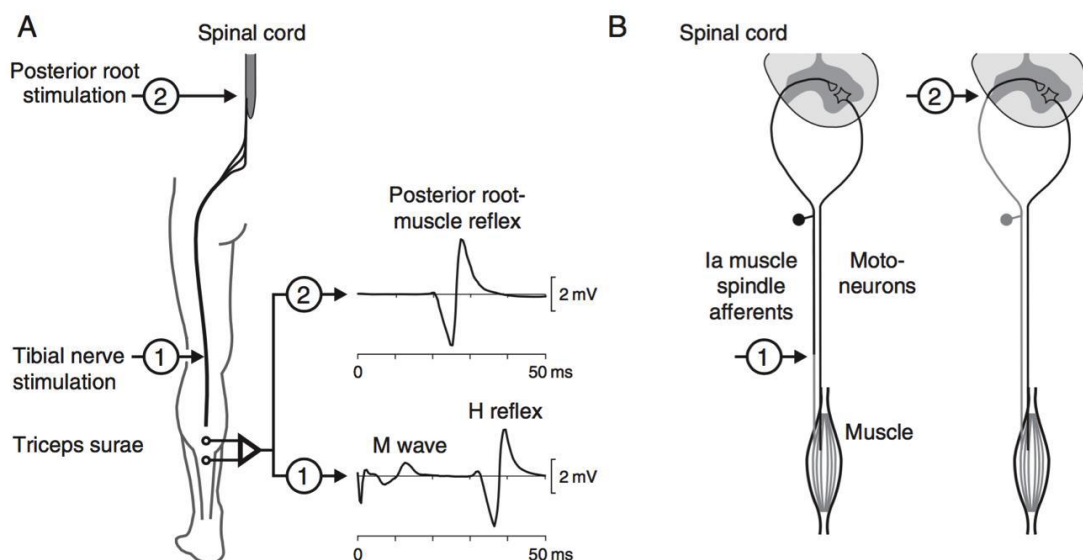
Figure 2.25: Comparison of stimulation of the tibial nerve (1) and posterior roots (2).
A) Tibial nerve stimulation evokes the H-reflex via stimulation of Ia afferents and the M-wave due to direct stimulation of motoneurons (here only to a preliminary extent). Posterior root stimulation only evokes posterior root reflexes (PRR) because of the anatomical differences in the nerve population **B)** compared to the mixed peripheral nerve (Minassian, Hofstoetter, & Rattay, 2012).

Elicitation of these posterior root reflexes can be achieved with different stimulation setups. The two fundamental approaches are the invasive epidural SCS (eSCS) and the non-invasive transcutaneous SCS (tSCS). In the case of eSCS, an electrode array is surgically placed into the epidural space, whereas in case of tSCS, the stimulation electrode is placed on the skin over the vertebrates T11-T12 and a large counter electrode is placed on the abdomen (Figure 2.26). Both methodologies have proven able to evoke PRRs in the four main muscle groups of the lower limb: (Q) Quadriceps – knee extensor, (Ham) hamstrings – knee flexor, (TS) triceps surae – ankle extensor and (TA) tibialis anterior – ankle flexor.
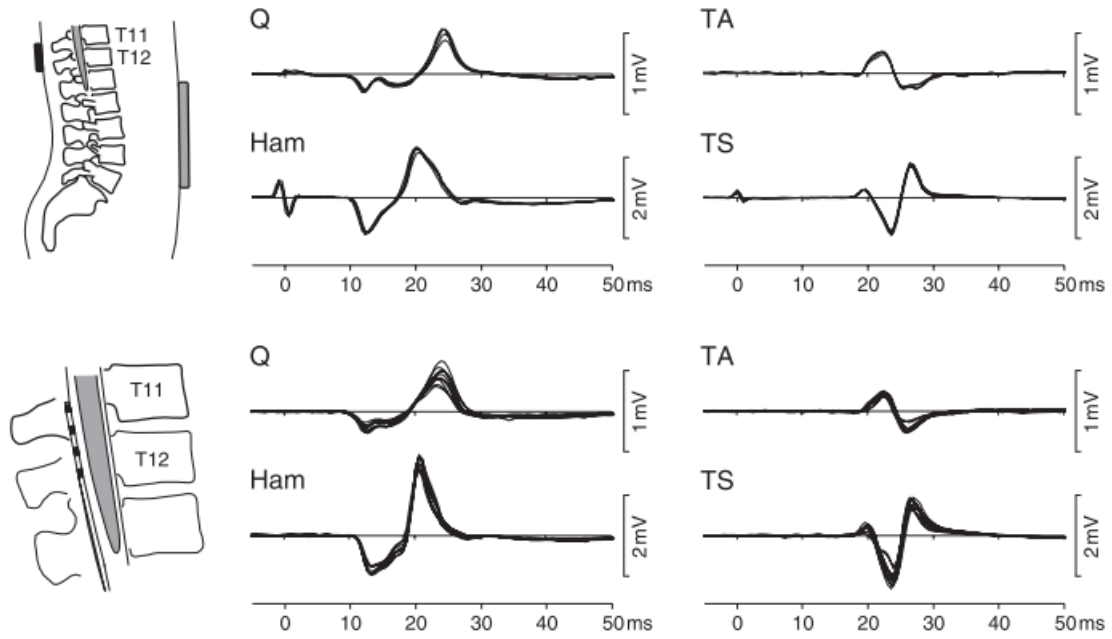
Figure 2.26: Posterior root reflexes evoked with epidural (eSCS) and transcutaneous (tSCS) spinal cord stimulation in the quadriceps (Q), hamstrings (Ham), tibialis anterior (TA) and triceps surae (TS) (Minassian et al., 2012).

3 RECORDING SYSTEM OF BIOELECTRICAL SIGNALS AND SYSTEM MARKERS

A recording system for bioelectrical signals has to fulfil a variety of functions, starting with the signal acquisition on the subject up to the storage of the processed data. For some of these functions, standard hardware components were purchased, for others own solutions have been developed (Subchapter 3.1). Furthermore, a recording software was written (Subchapter 3.2) for live visualization and data logging. The schematic below shows all technical components of the recording system, developed within this work, with the relevant chapter numbers:
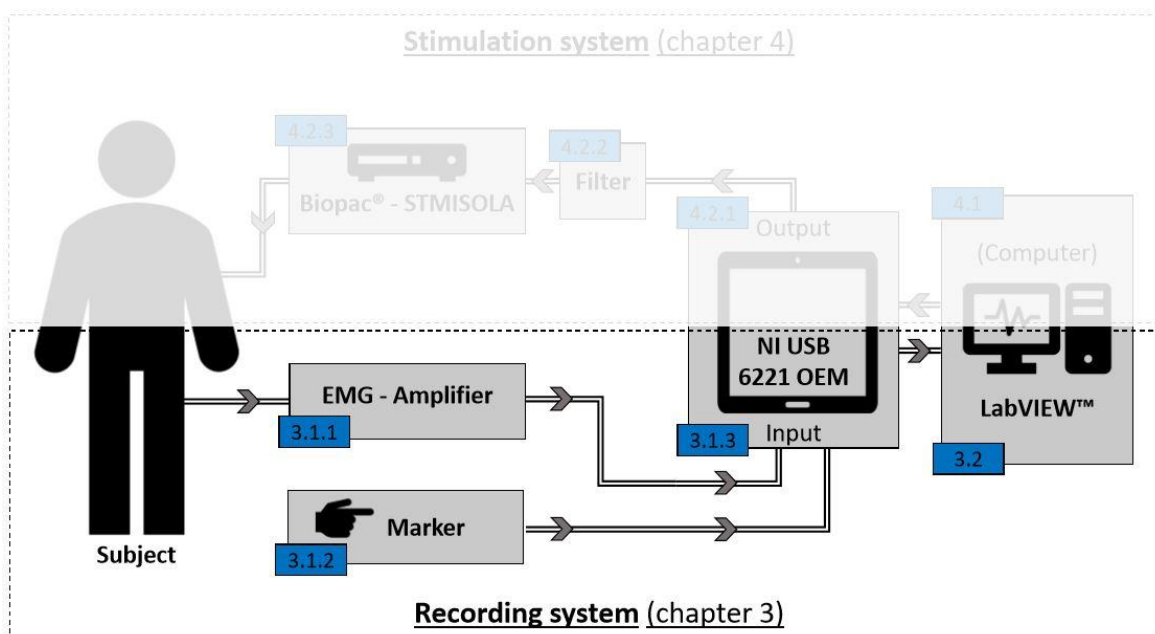
Figure 3.1: Schematic drawing of the EMG recording system with numbers of relevant subsections.

3.1 Implementation of recording hardware

The hardware part of the recording system consists of three main parts. First, the EMG amplifier, developed at the Medical University of Vienna, enlarges the biosignal amplitude. These amplified signals are then digitized and recorded by a multifunctional I/O device

connected to a computer. Finally, optional marker hardware can be attached to the system to manually mark specific events during the recording procedure.

3.1.1 EMG amplifier

The development of the EMG amplifier itself (Figure 3.2), was not part of this thesis. It was developed in 2008 by Ewald Unger and his colleagues at the Center for Medical Physics and Biomedical Engineering at the Medical University of Vienna. The device was designed in a modular build: four identical modules (Figure 3.3.B) are mounted on the mainboard (Figure 3.3.A).
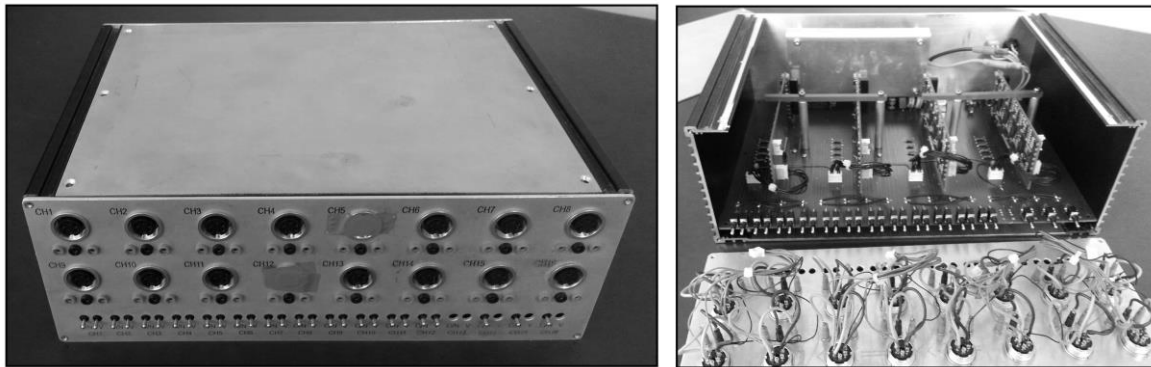
Figure 3.2: EMG amplifier in its un-refurbished state.

Since each module contains the circuitry of four EMG amplifiers, there are 16 EMG channels overall. The system was designed to amplify signals of 100Hz with a gain of 600, which are typical values for surface EMG amplification devices (Prutchi & Norris, 2005).
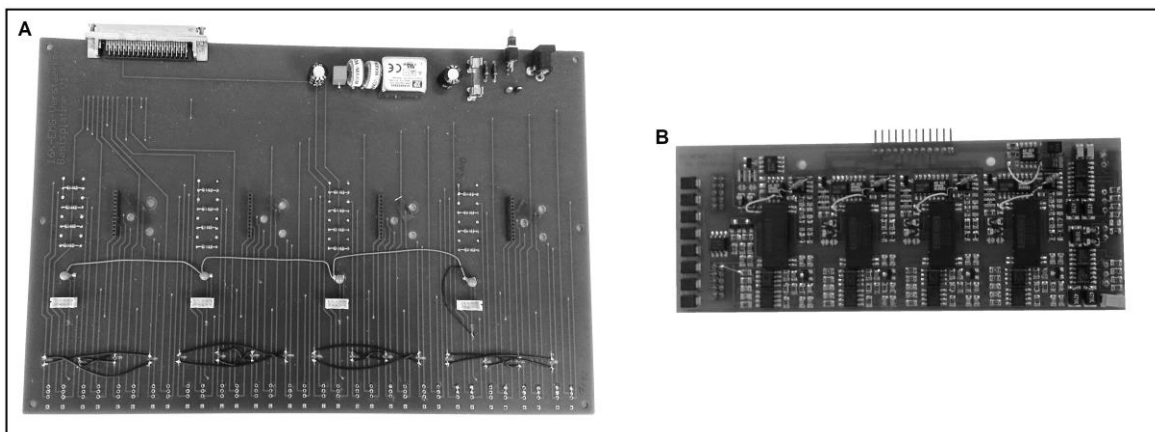
Figure 3.3: Hardware modules of EMG amplifier. (A) Mainboard with the connections for four EMG modules and a 68-pin SCSI interface. **(B)** EMG module with circuitry of four separate channels.

Due to its intensive use over the course of the last years, the EMG system needed a general refurbishment. This refurbishment, as well as some minor adjustments are part

of this diploma work. These include e.g., renewing of broken cables and old connectors, removing of unused components like the battery and switches and the manufacturing of a new front panel (Figure 3.4).
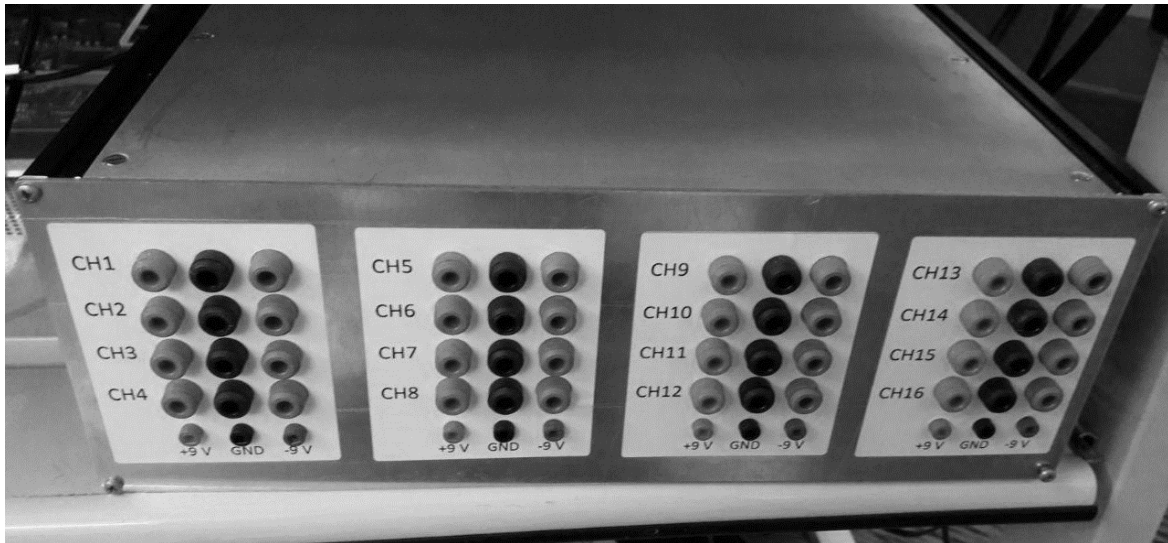
Figure 3.4: Refurbished EMG amplifier. Each block of four channels represents one EMG module. In case of future use of additional hardware, such as goniometers, a +/- 9V DC power supply is provided at each block.

3.1.2 Recording and digitization

To digitize and save the amplified bioelectrical signals, a National Instruments USB-6221 OEM device is connected via a 68-pin SCSI cable with the EMG amplifier. The USB-6221 OEM is a multifunctional DAQ (Data acquisition) device with analog and digital input and output channels. There are 16 analog input channels with sample rates of 250k samples per second and ADC (analog-digital-converter) resolution of 16 bits. In addition, the device has two analog output channels with sample rates of 833k samples per second and an ADC resolution of 16 bits. The device has 24 digital I/O channels, of which eight are clocked.
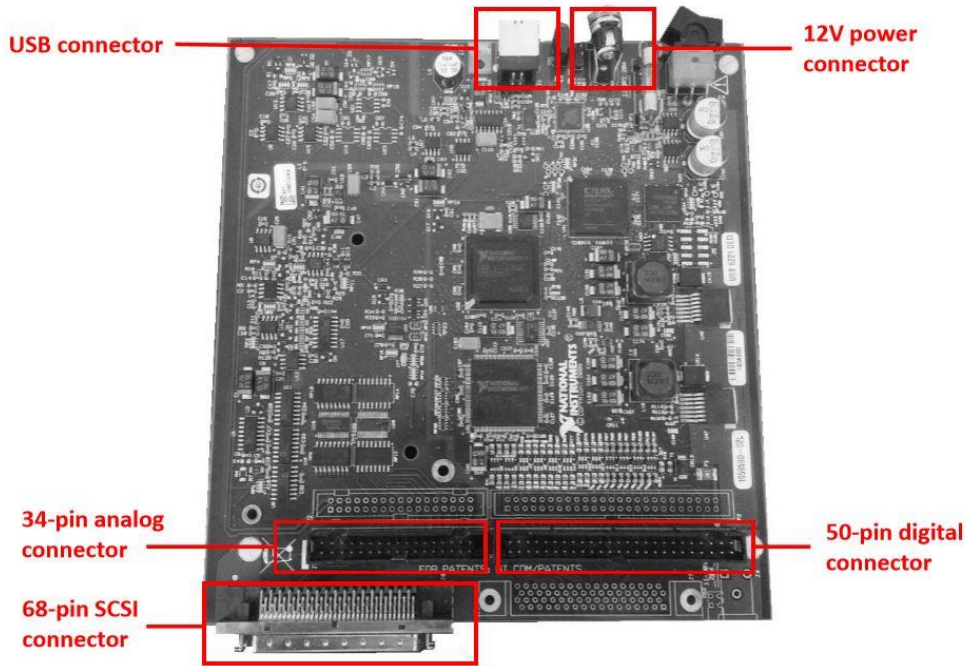
Figure 3.5: NI USB-6221 OEM with all connectors indicated.

The analog and digital I/O channels of the device are connected to the 68-pin SCSI interface as well as to both of the connector rows on top of the board (Figure 3.5). Theoretically all input and output data could be sent via the SCSI connector. However, to be able to use a standard NI 68-pin cable between amplifier and NI USB-6221 OEM, only the 16 channels of the amplifier are connected to the analog inputs via this interface.
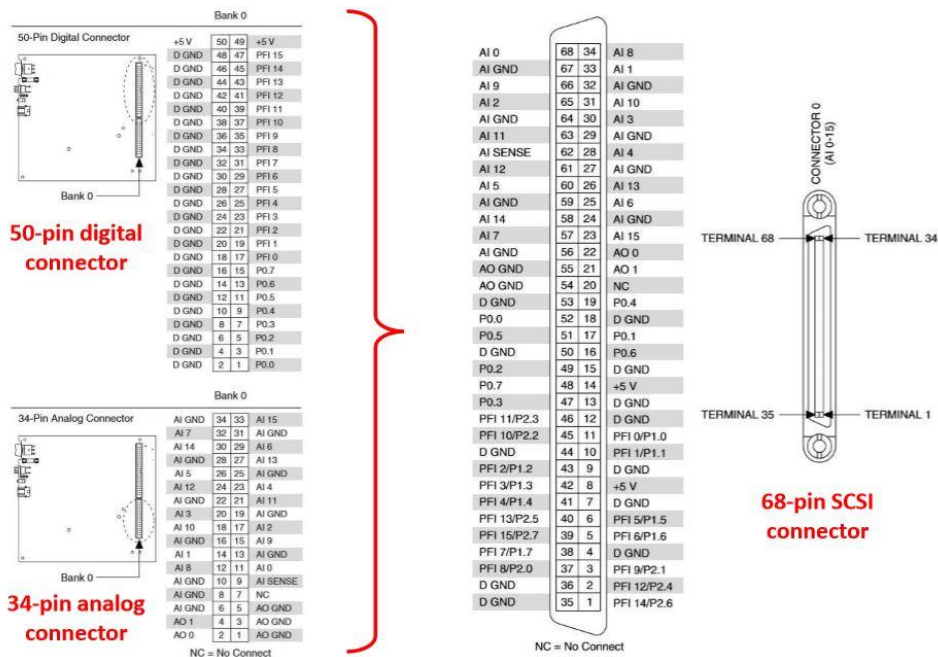
Figure 3.6: Digital and analog pinout of NI USB-6221 OEM. All channels can be either accessed via the SCSI connector or via the two row connectors. Adapted from (National Instruments™, 2008, 2016)

To access the other channels; the analog output for the stimulator control data and the digital input channels for the marker, a connector head was designed and placed on top of the two row connectors (Figure 3.7). On the connector head, the circuitry of the marker hardware (see Chapter 3.1.3) and the components of the protective high pass filters (see Chapter 4.2.2) are placed and wired.
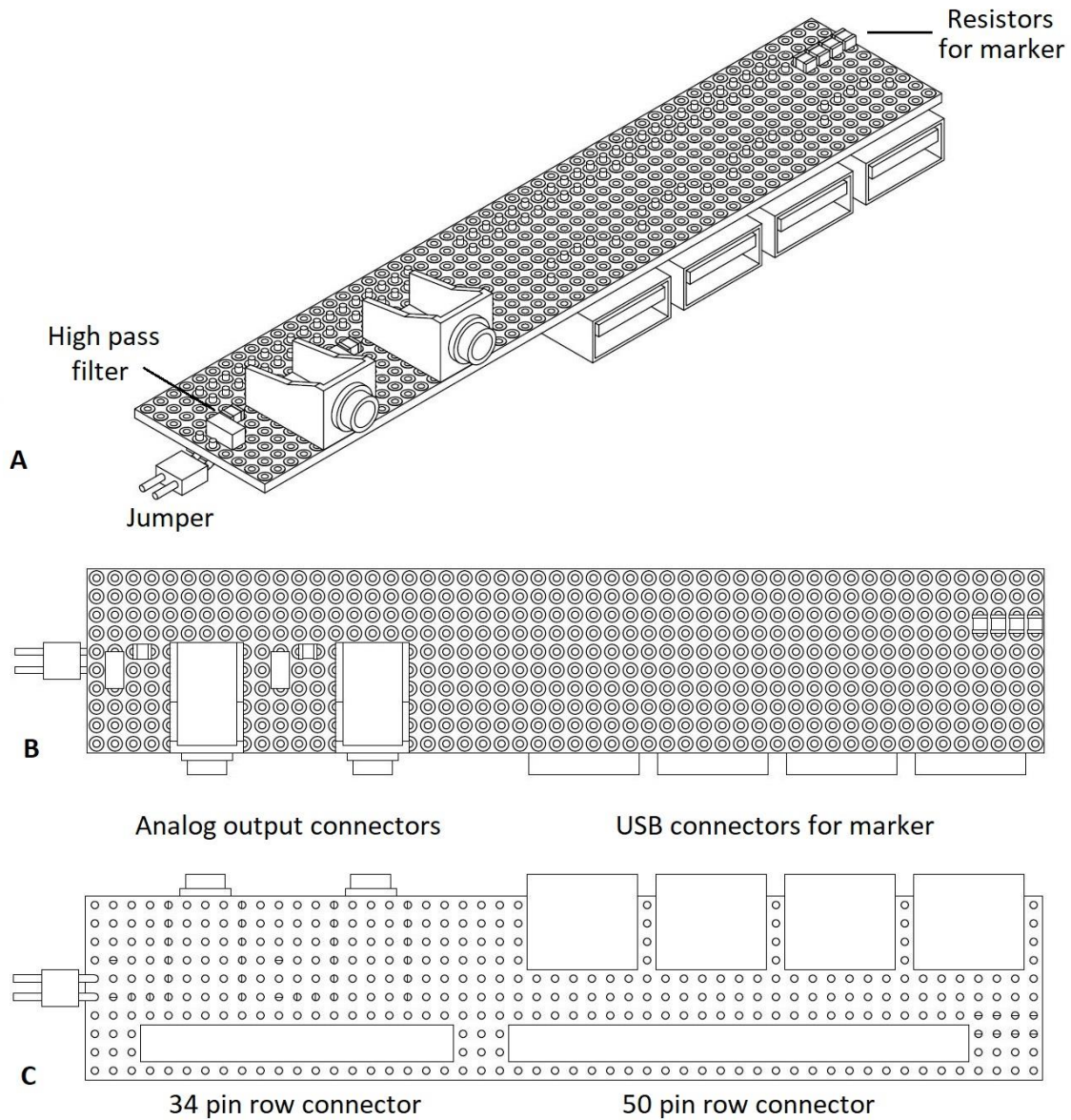
Figure 3.7: Connector head component scheme illustrated in **A)** isometric, **B)** top and **C)** bottom view.

3.1.3 Marker hardware

To mark specific events during the measurement procedure, such as passive movement of the lower extremities or manual stimulation of the plantar reflex, we implement optional marker hardware. A simple circuit connects the +5 V signal of the digital connector block over a 10 kΩ resistance with a digital input (Figure 3.8). This signal can be interrupted with the marker, a switch connected to the circuit when needed.
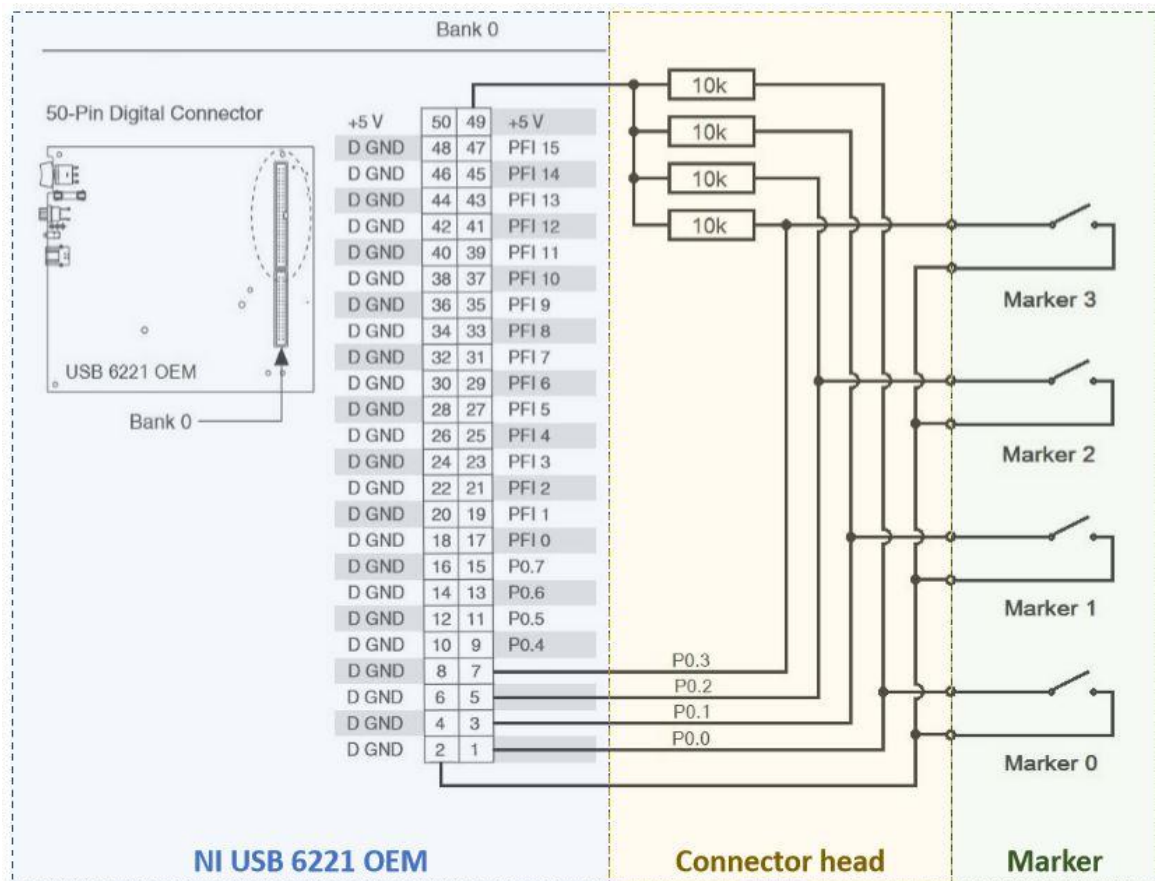
Figure 3.8: Marker circuitry, wired to the 50-pin digital connector of NI USB 6221 OEM (blue). The circuitry can be divided into the components soldered to the connector head (yellow), which is plugged on the NI device, and the detachable marker hardware(green). Adapted from (National Instruments™, 2008)

In case different events have to be marked within one measurement, four marker circuits have been implemented. To simplify the hardware, the markers are detachable and only connected to the recording device when needed (Figure 3.9).
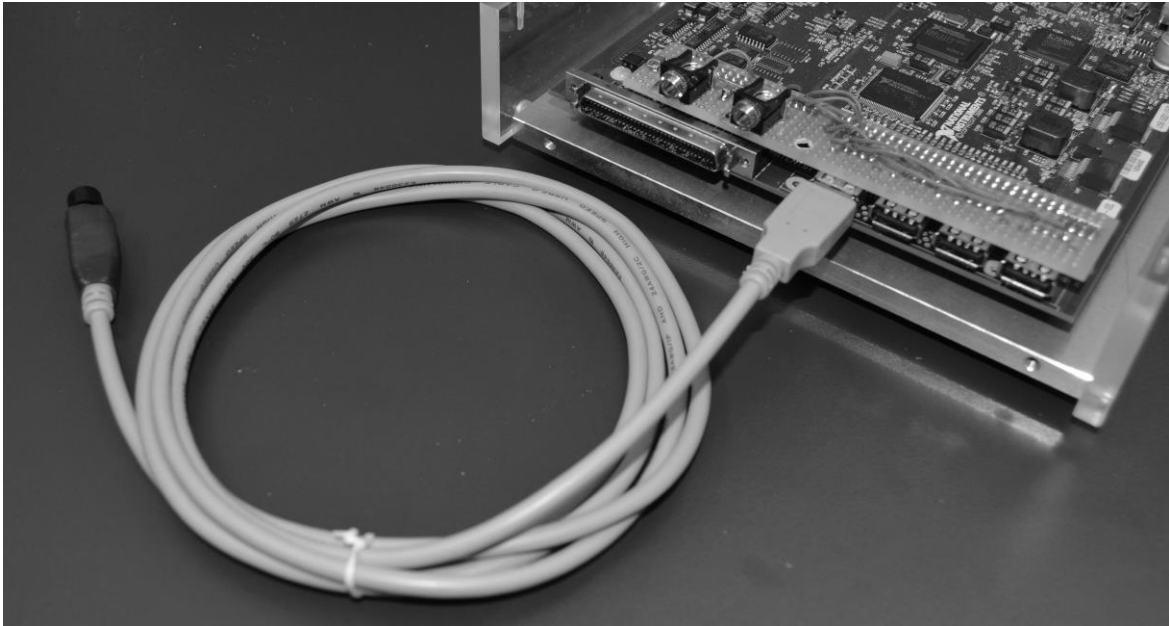
Figure 3.9: Marker attached via the connector head to the NI recording device.

3.2 Implementation of recording software

The recording software, written in LabVIEW™, serves two main purposes, the live visualization of the EMG measurements and, more importantly, the logging of the data.

3.2.1 About LabVIEW™

LabVIEW™ is a graphical programming environment used for system engineering, especially for measurement and control applications. A LabVIEW™ program is called VI (virtual instrument) and consists of a front panel and a block diagram. The front panel serves as the user interface for the program, here inputs can be made with e.g., Boolean or numeric controls and outputs can be visualized in form of graphs or other indicators. It interacts with the block diagram, which contains the functional graphical code of the VI. This program code may serve the purpose of processing software and/or hardware inputs to visualize them on the front panel or to write the desired data to a file. Furthermore, processed data can be sent as output to control external hardware.

3.2.2 Data logging

In order to access the analog input data of the NI USB 6221 OEM, a DAQ assistant was implemented to the block diagram and set up. First, the physical input channels of the I/O device were assigned (see Figure 3.10). This includes naming, ordering and configuration of input range and scaled units for each channel. Next, the sample rate for these channels is set to 10k samples per second. The DAQ assistant is capable of logging the measurement

data and saving them to a TDMS file, which can be easily imported to Excel or MATLAB® for data analysis.
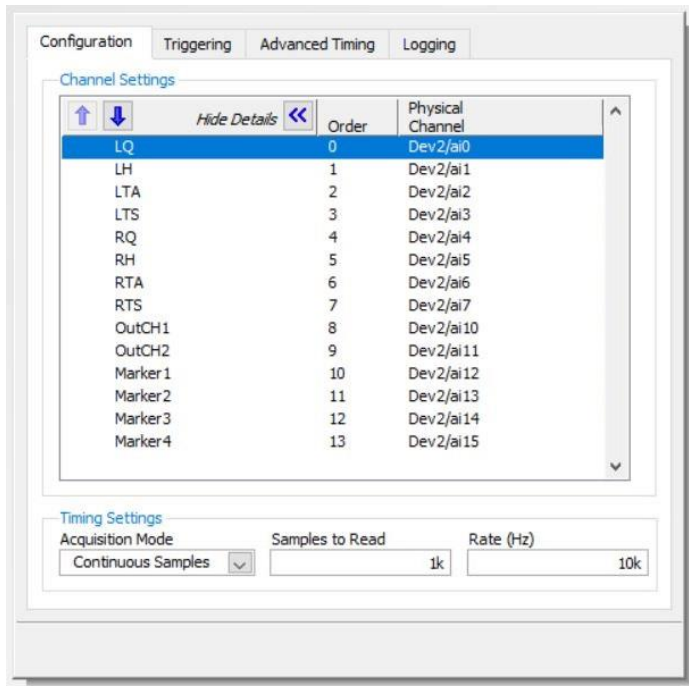
Figure 3.10: DAQ-assistant configuration: assignment, naming and ordering of physical channels.

The functional block diagram in Figure 3.11 shows the components for logging and visualization of the EMG data. The block diagram is located in a loop, which reads 1k samples per iteration and stops when the corresponding button on the front panel is pushed. These settings (1k samples read per iteration with 10kHz sampling rate) result in 10 iterations per second, which represents a well-balanced compromise between hardware performance and sufficient resolution for the live visualisation.
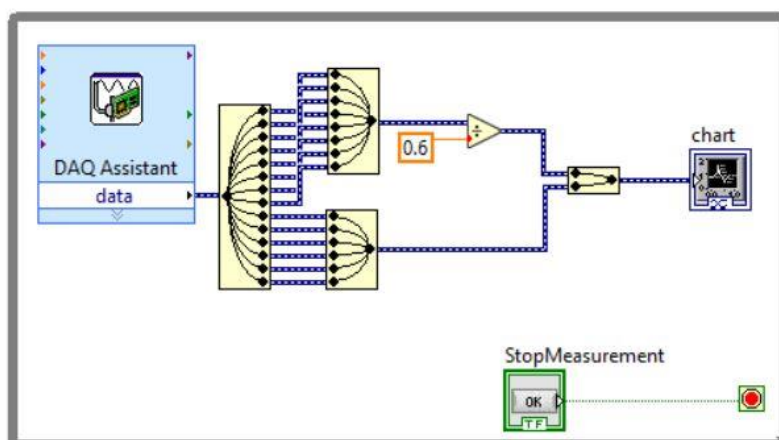
Figure 3.11: LabVIEW™ block diagram with the components for recording and visualization, allocated in a loop.

3.2.3 Live visualization

Simultaneously to the logging process, the data is extracted from the DAQ assistant (compare Figure 3.11) and is partly processed. The 14-channel input signal is split up into two groups, the EMG data and the other input signals. The EMG data is then divided by a constant of 0.6 in order to obtain even values on the waveform chart, where 1V equals 1mV of raw EMG signal:

$$Raw\ siganl \cdot \frac{amplification\ gain}{LabVIEW^{™}\ constant} = Visualized\ signal \qquad (3.1)$$

$$1mV \cdot \frac{600}{0.6} = 1V$$

After this modification, the two signal groups are merged again and connected to a waveform chart which visualizes it on the front panel in real time (Figure 3.12).
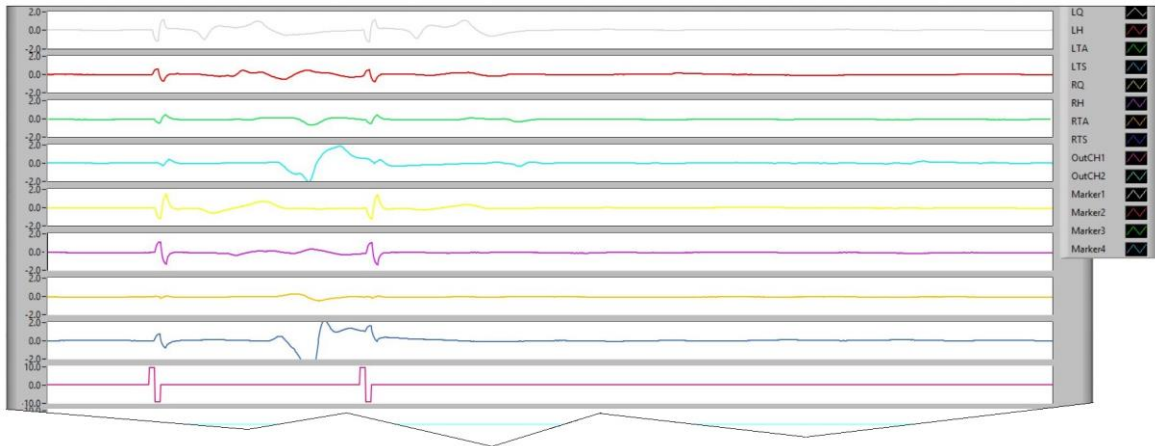
Figure 3.12: Data visualization on the front panel. This example shows a 100mA biphasic double pulse and the corresponding EMG responses.

3.3 Verification test

As the central device of the recording system, the main characteristics of the EMG amplifier, which was designed in an earlier project at the Center for Medical Physics and Biomedical Engineering, were tested. These parameters are the amplification gain, the operating linearity and the phase behaviour, all dependent on the frequency of the input signal.

3.3.1 Testing procedure

In order to conduct a frequency response test, a simple measuring circuit was designed (Figure 3.13). A signal generator, which emits a sinusoidal signal with an amplitude of about 1V and adjustable frequency, was connected to a voltage divider.
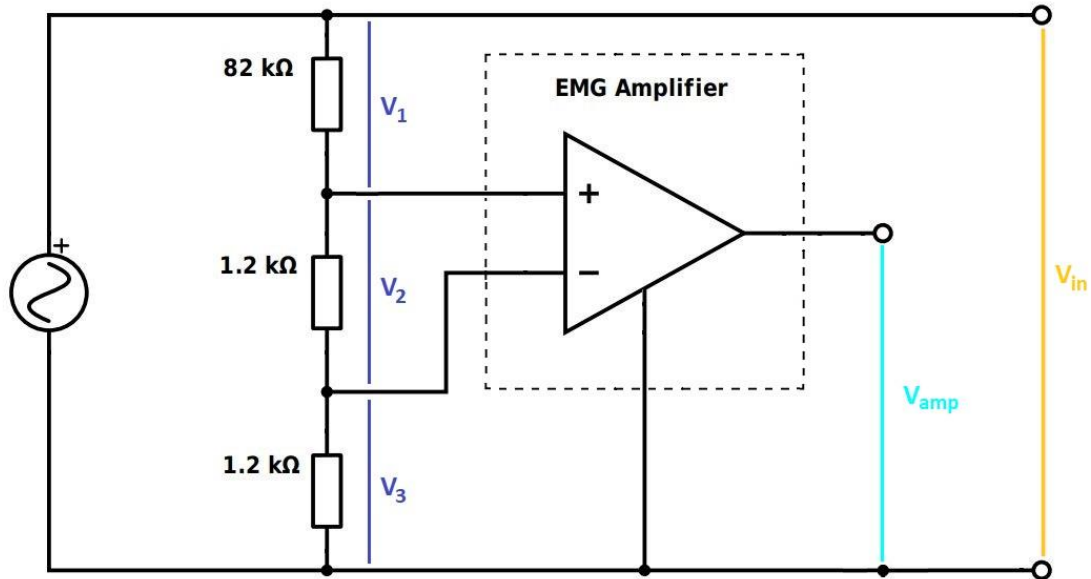
Figure 3.13: Verification circuit for EMG amplifier. A sinusoidal signal with an amplitude of approximately 1V is generated and applied to a voltage divider. The voltage fraction V_2 is then amplified by the EMG device to V_{amp}. V_{in} and V_{amp} are measured with an oscilloscope.

The two inputs of the specific channel of the EMG amplifier, as well as the ground reference are connected to the voltage divider. Now the input voltage V_{in} is measured with an oscilloscope as a reference signal. The amplified signal (V_{amp}) of voltage fraction V_2 is visualized using the second channel of the oscilloscope. Three parameters are measured for every frequency setting: The input Voltage V_{in}, which was set to a value of 1V in the beginning of the measurements, but with every change of frequency this value also changed. Therefore, it is measured separately for every frequency value. The second quantity measured is the amplitude of the amplified signal V_{amp}. Lastly the time offset between V_{in} and V_{amp} is measured in ms. Also, the pulse shapes of both signals are compared and checked for any distortions. These measurements enable the verification of several different instrument parameters.

Gain

Gain is the relation of input signal amplitude to output signal amplitude. It can either be described as a linear value or in a logarithmic (decibel) form.

$$gain_{linear} = \frac{V_{out}}{V_{in}}$$ (3.2)

$$gain_{dB} = 20 \, log_{10}(gain_{linear})$$ (3.3)

Signals resulting from electrophysiological activity typically have amplitudes in the range of a few µV to a few mV. In order to properly display and/or record these signals, their

amplitudes have to be amplified about three orders of magnitude. Therefore, biopotential amplifiers typically have gains of 1000 or greater (Prutchi & Norris, 2005).

Frequency response

The main frequency response parameter of an amplifier is the frequency bandwidth (Figure 3.14). The bandwidth of an amplifier is the optimal working range and is defined as the frequency interval between the lower and the upper cut off frequency.
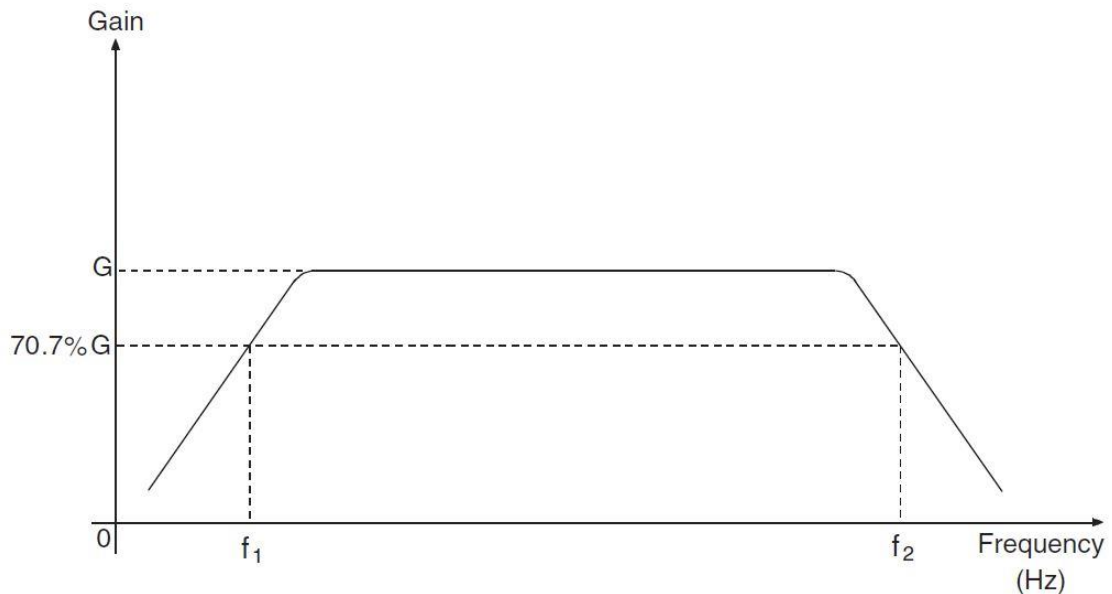
Figure 3.14: Frequency response of a biopotential amplifier. (Prutchi & Norris, 2005)

The gain at these cut off frequencies is 70.7% of the maximum gain at the plateau in the middle. Due to the fact, that the signal power at these points is half the maximum signal power $[(0.707)^2 = 0.5]$, they are also referred to as half-power points.

Linearity

Linearity in an amplifier is a measure of how proportional input and output signals are. In the verification method described above, this can be tested by comparing the shape of the amplified signal to the sinusoidal input signal. When the output signal exhibits a pure, undistorted sinusoidal shape, regardless of the difference in amplitude, linearity is given.

Phase difference

The position of a point on a waveform cycle, at an instant, is defined as phase (Figure 3.15). A signal is called "zero phase", when the beginning/end the relevant waveform cycle goes through the origin of the graph.
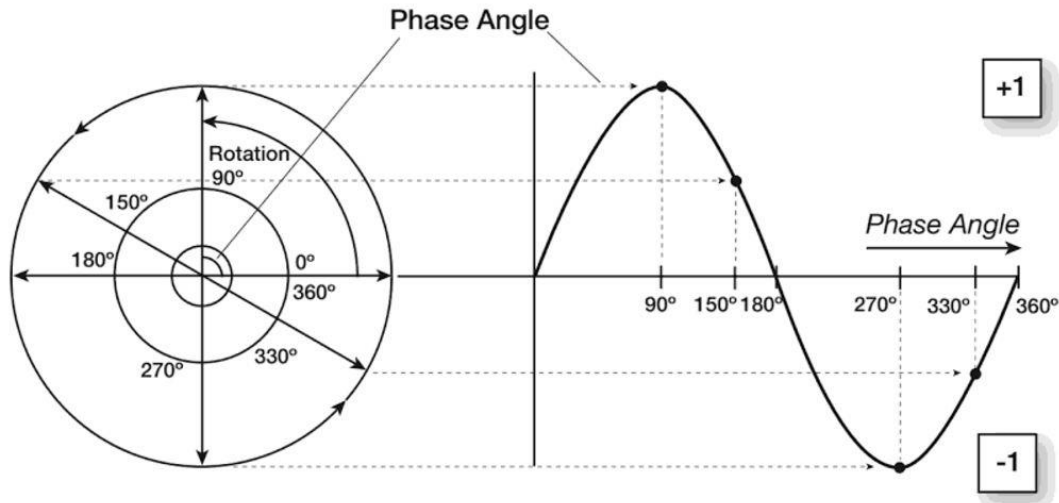
Figure 3.15: Sine wave phase angles for sin θ = (y/r) across one cycle (360° of phase). Reprinted from (Angus & Howard, 2006).

The term phase shift describes the offset of a signal from this 0° phase. Since the termini phase and phase shift are only used in cyclic waveforms, such as sinusoidal waves, they are most commonly measured in degrees or radians (Figure 3.16). When two or more cyclic waveforms are compared to one another, and none of them is the zero phase, the term phase difference is used to describe their phase behaviour.
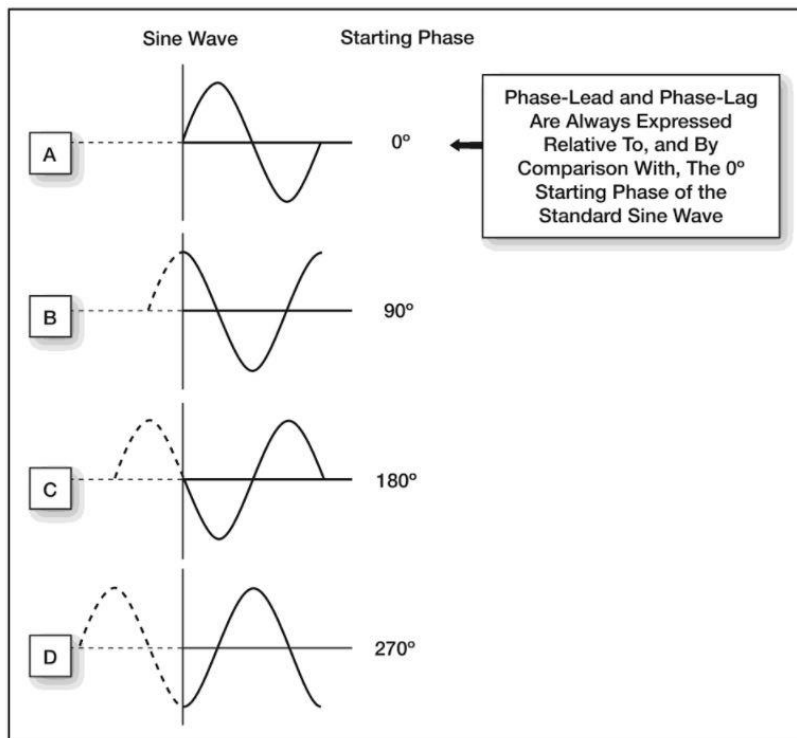
Figure 3.16: Four examples of sine waves. A. The zero phase with a starting phase of 0°. **B.- D.** examples of phase shifted sine waves with different starting phases (Sahley & Musiek, 2015).

3.3.2 Results

Direct measurements

The measurements explained above have been made on all 16 channels of the EMG amplifier. For every channel, frequency responses have been measured at 1, 2, 5, 10, 20, 50, 100, 200, 500, 1000 and 10000Hz (Figure 3.17).
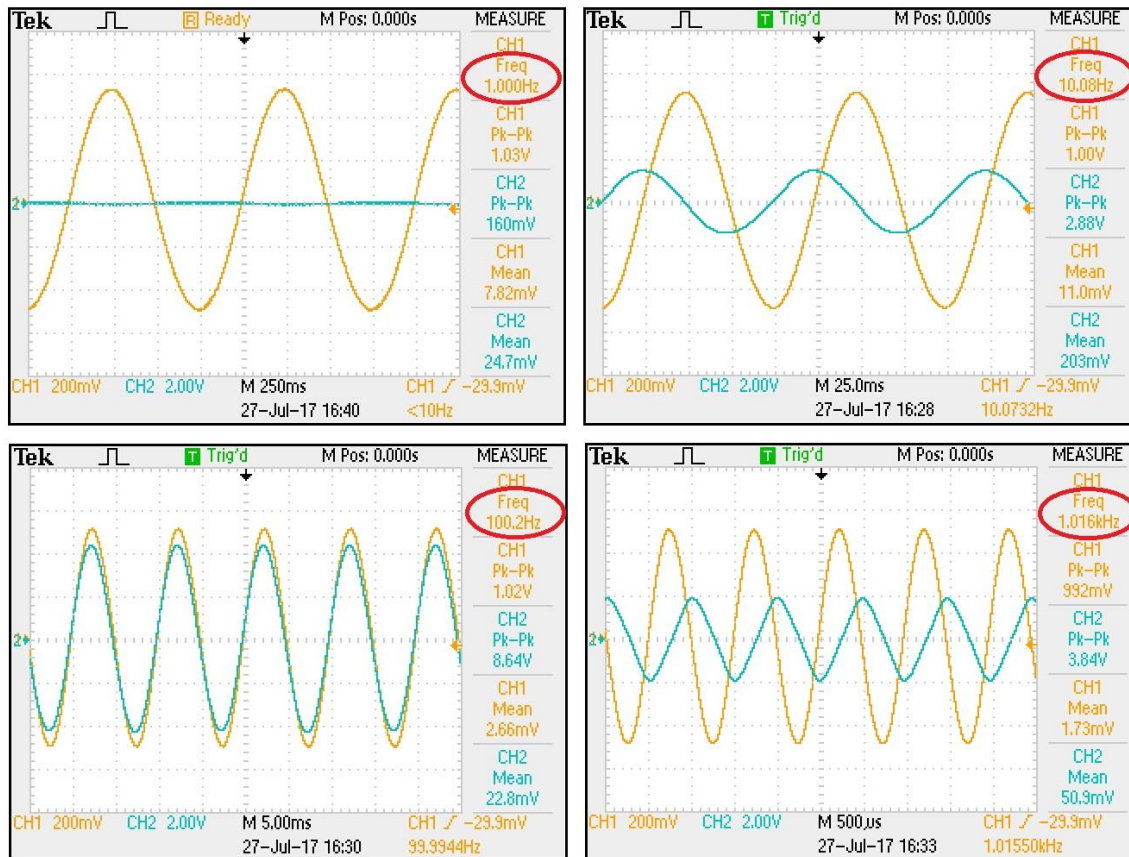
Figure 3.17: Example of four measurements on EMG channel 1. Oscilloscope channel 1 (orange) visualizes V_{in}, channel 2 (cyan) shows the amplified signal V_{amp}.

Derived parameters

First the phase difference φ in radians is calculated from the measured phase shift θ in ms at the zero line:

$$\boldsymbol{\varphi} = \boldsymbol{\theta} \cdot \frac{\boldsymbol{f}}{\boldsymbol{1000}} \cdot \boldsymbol{2\pi} \qquad (3.4)$$

This conversion leads to following graph, showing the frequency dependency of the phase difference φ:
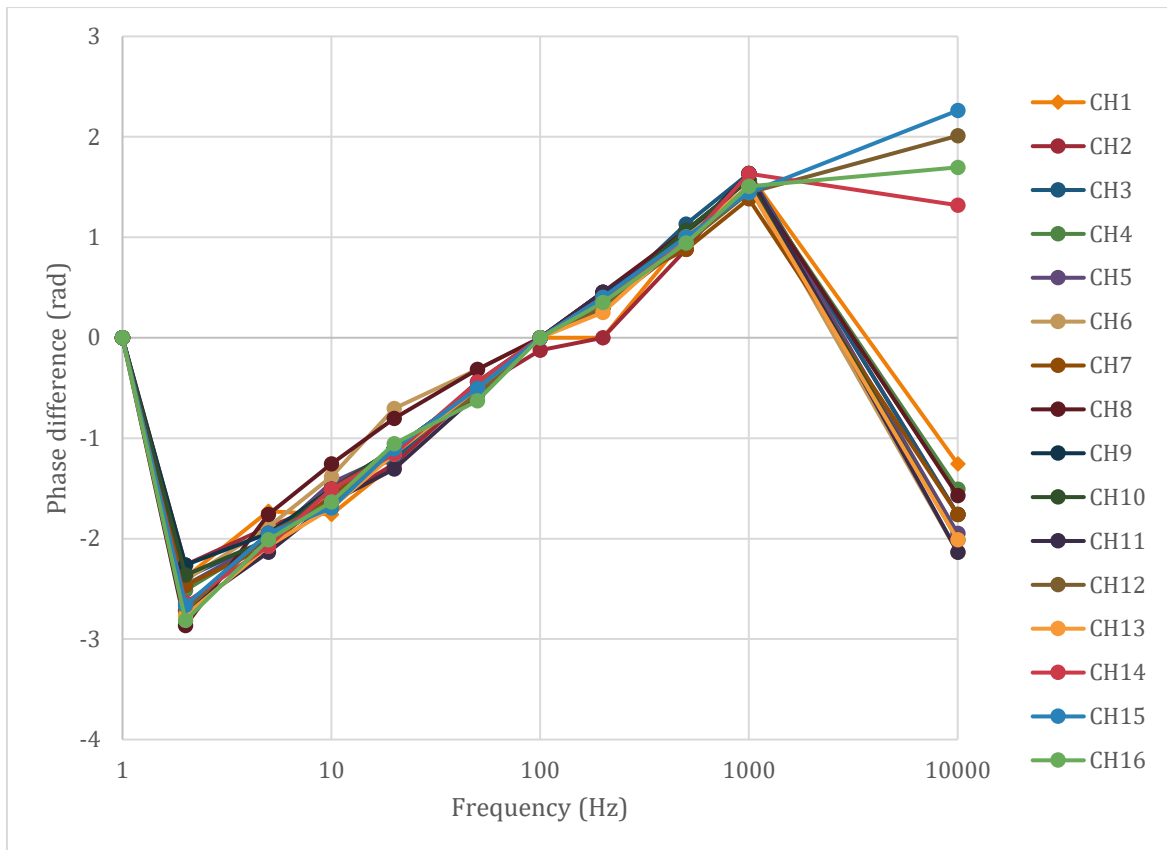
Figure 3.18: Frequency dependency of the phase difference φ of the amplified signal V_{amp} with respect to the input signal V_{in}.

The second parameter, that can be calculated from the measured values is the gain of the amplifier. Therefore, first the voltage fraction V2, which is the amplifier input signal (compare Figure 3.13) is calculated:

$$V_2 = V_{in} \cdot \frac{R_2}{R_1 + R_2 + R_3} \tag{3.5}$$

$$V_2 = V_{in} \cdot \frac{1.2k\Omega}{1.2k\Omega + 1.2k\Omega + 82k\Omega} = V_{in} \cdot \frac{1.2}{84.4}$$

Now with the pre-amplifier voltage fraction known, the gain can be calculated according to Equation (3.2).
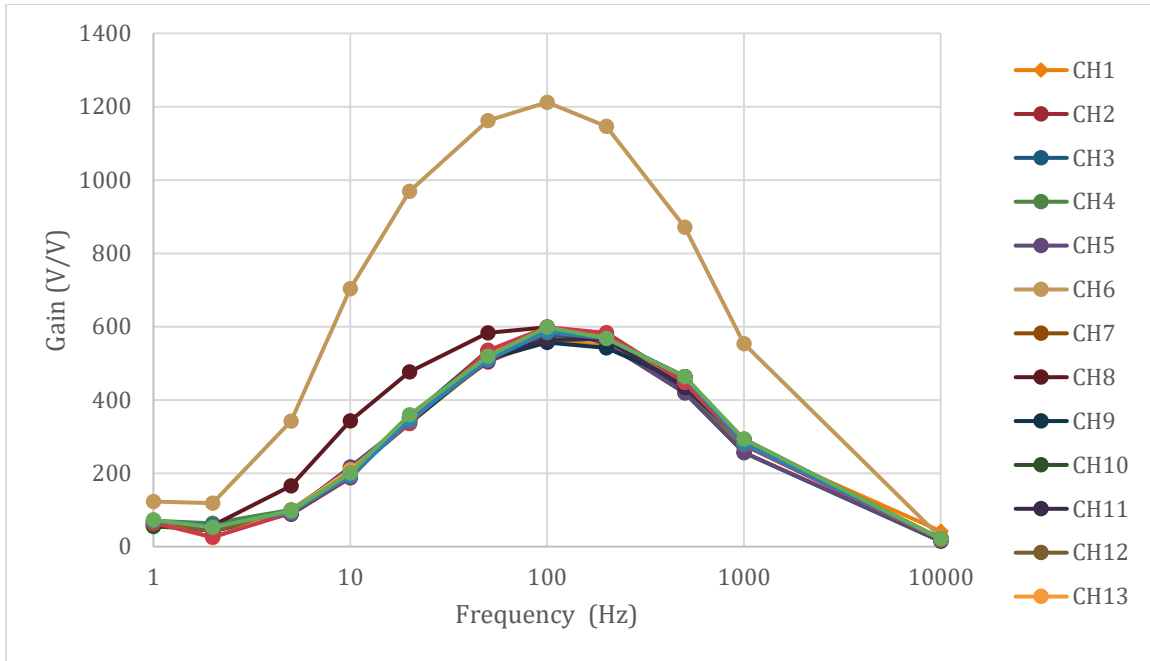
Figure 3.19: Frequency dependency of the gain of the amplified signal V_{amp} with respect to the input signal V_{in}.

Now the gain is averaged for each frequency value to determine the mean cut off frequencies and the bandwidth of the amplifier:
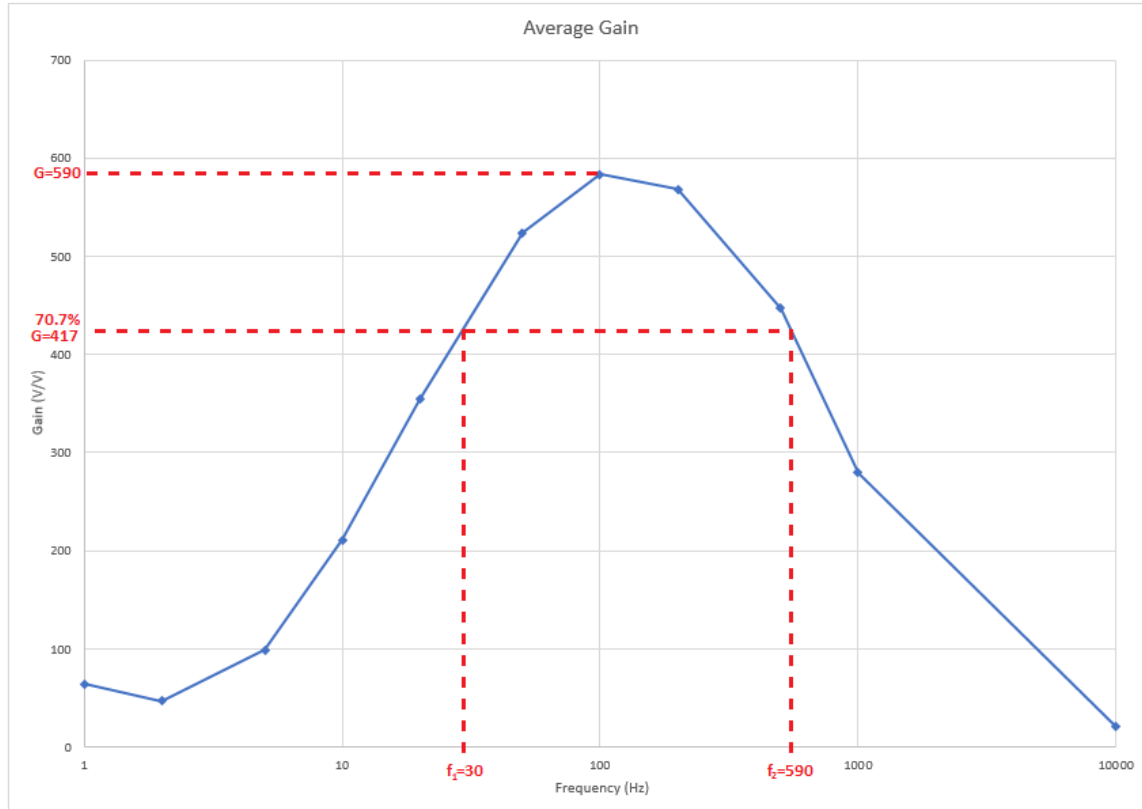
Figure 3.20: Mean cut off frequencies and bandwidth. Channel 6 was not included in the underlying averaging.

3.3.3 Conclusion

The technical evaluation of the recording system developed in this thesis proved, that the requirements (Chapter 1.2) are met and the system is capable of measuring surface EMG signals. The system has 16 EMG channels, of which 8 are required for the bilateral recording of the quadriceps, hamstrings, tibialis anterior and triceps surae muscle activities. All channels except channel 6 have a gain of G=590 V/V at f=100 Hz and a bandwidth of approximately 30-590 Hz (Figures 3.19 and 3.20). At the range of optimal amplification (50-200 Hz), the signals underlay the least phase shift (Figure 3.18). Channel 6 has exactly the twofold gain of the other channels and is not in use; more detailed evaluation/refurbishment of the circuitry of this channel is required. Furthermore, the recording system is capable of logging the manual marking of up to four different events during the recording session with the marker hardware, that was implemented. All measurement data is live visualized and written to a TDMS file.

The system is limited to the recording of EMG signals, since other biosignal measurements such as electrooculography (EOG) and electroencephalography (EEG) require different filter (Prutchi & Norris, 2005).

4 ELECTRICAL STIMULATION SYSTEM

In order to meet the wide range of system requirements mandated by the research objective (see Chapter 1.3), using a conventional and commonly available stimulation system is not possible. Therefore, freely programmable hardware was chosen, to allow the application of stimulation patterns with as few restrictions as possible. In this chapter, first the program, written to generate these stimulation patterns, is presented. Then the hardware chosen and the modifications made to it are shown, followed by a summary of the evaluation procedure, which was done under laboratory conditions.
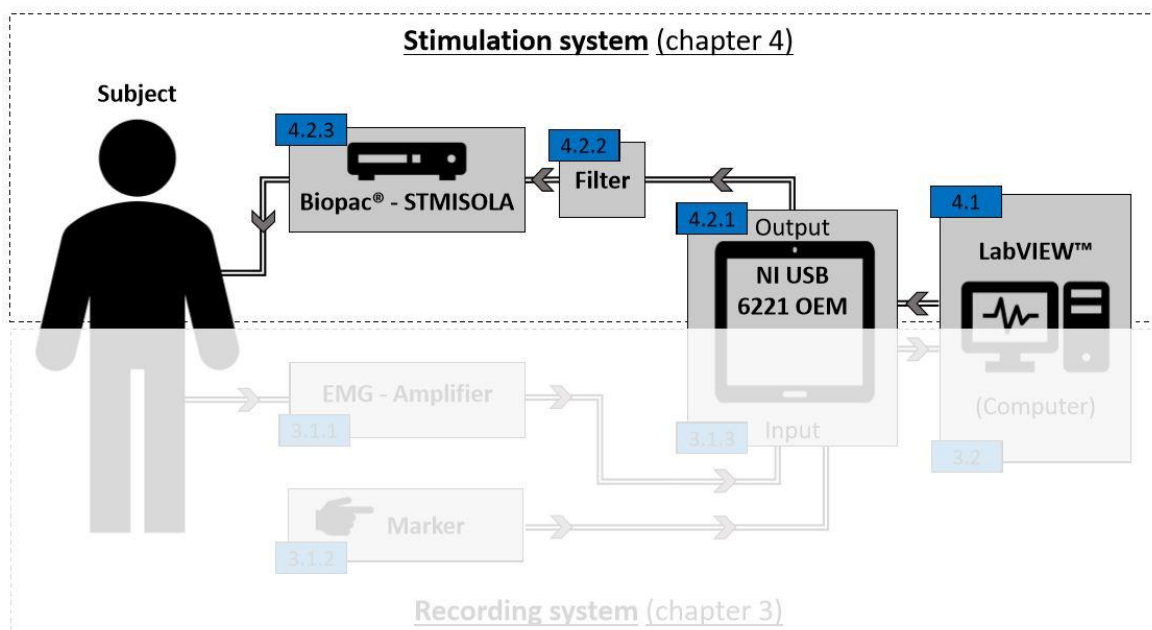
Figure 4.1: Schematic drawing of the stimulation system with numbers of relevant subchapters.

4.1 Implementation of stimulation software

Due to the easy operation of the National Instruments™ multifunctional I/O device with their own software, the main program used in the stimulation system is LabVIEW™. The generation of the stimulation data itself, was realized using an embedded MATLAB® script to maintain a maximum degree of freedom in terms of pulse shapes and stimulation patterns.

> **A brief explanation of the functionality of the program is given in the subsection "About LabVIEW™" in Chapter 3.2.1.**

The part of the LabVIEW™ program which is responsible for generating and sending stimulation data to the external hardware, can systematically be divided into the following three units: Input, Process and Output.
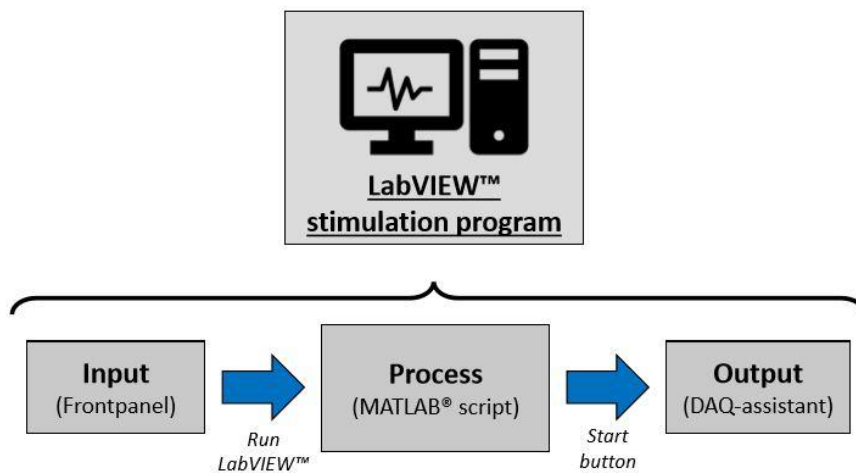
Figure 4.2: Systematic structure of the stimulation program.

Input

The main part of the front panel serves the purpose of giving input to the block diagram to generate the stimulation data. The system operator defines the stimulation settings with Boolean elements (switches, checkboxes, etc.) and numeric controls (Figure 4.3).
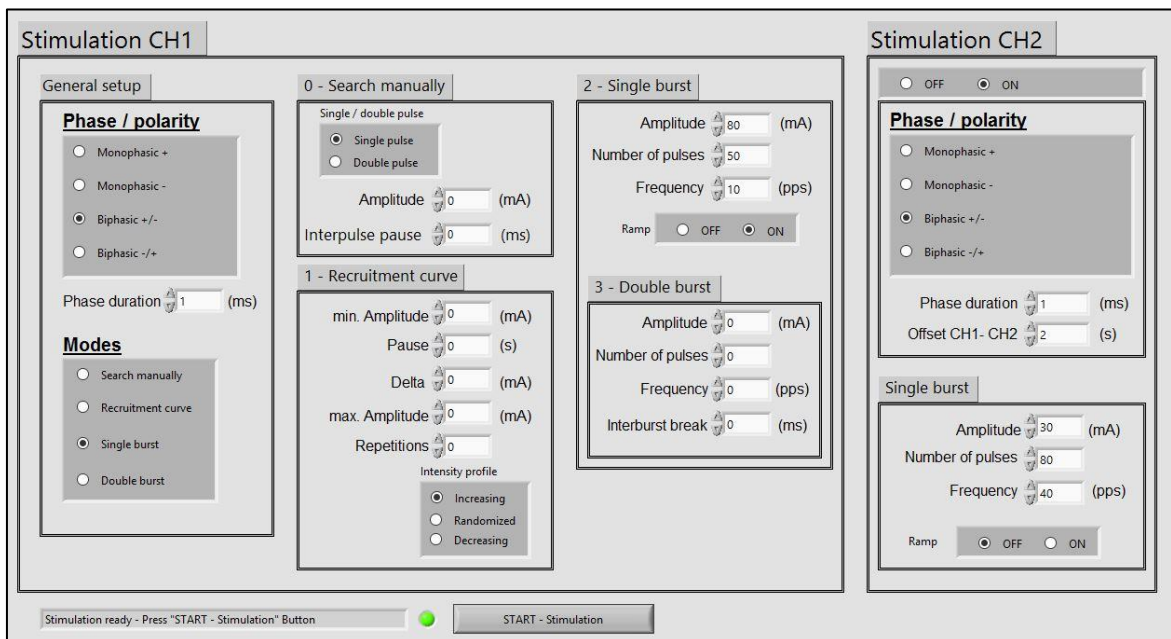
Figure 4.3: Front panel of LabVIEW™ stimulation program.

At first, general settings regarding pulse characteristics have to be made. This includes the polarity (+/-), the pulse shape (monophasic or biphasic) and the phase duration in milliseconds. Also, the basic stimulation mode is chosen in the beginning:

There are four stimulation modes implemented: (0) one single or double pulse to manually search the motor threshold of different muscle groups; (1) an automated collection of single pulses with different amplitudes, either increasing, decreasing or randomized, to gather more information about the muscle recruitment behaviour; (2) a single burst of stimulation pulses with adjustable frequency and number of pulses. There is also the option of a one-second ramp, where the amplitude smoothly builds up within the first second of stimulation to alleviate discomfort; (3) extends mode 2 by a second, independently defined stimulation burst. This second burst is delayed by a time span called inter-burst break.

Furthermore, the second stimulation channel can be enabled and set up just like the first. This channel only has one operation mode, which corresponds to mode (2) of channel one.

Process

Generation of variables

The input data is processed by a MATLAB® script, which is implemented in the block diagram (Figure 4.4). First of all, this requires the previously made settings to be imported to the script. The import function already defines the input as MATLAB® variables, so it is not necessary to do this programmatically.
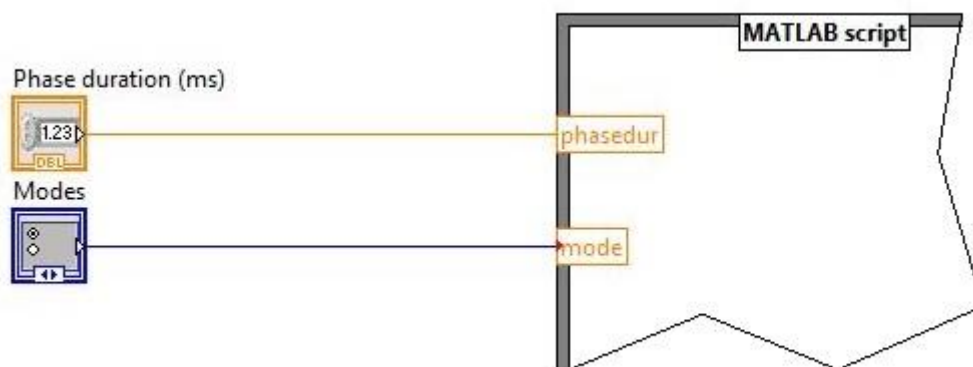
Figure 4.4: Import of settings from LabVIEW™ controls to MATLAB® variables. A sample section of the block diagram with one numeric control (Phase duration in ms) and one Boolean control (Modes), being imported to a MATLAB® script. The Boolean element corresponds to a radio button checkbox on the front panel.

Translation of input values

The operator feeds in the setting values, in units that are practical for it. Small time settings are made in milliseconds, while longer time spans are defined in seconds. Stimulation amplitudes are entered as milliampere values in a range of 1-100 and frequencies in pps (pulses per second). These units may be intuitive for the user, but they are not practical for the following mathematical operations, therefore they need to be translated in another format.

First, amplitude input values are divided by ten to convert them to the range of the physical output channels of the NI device, which is -10 to 10 volts. An amplitude input entered as 85 (mA), is translated to an internal value of 8.5.

```
amp_2=amp_2/10;
```

In the same way, time values are converted from seconds / milliseconds to a sample number. The device is working with a sample rate (fs) of 100000 samples per second. A time span keyed in as 50 (ms) is translated to the corresponding number of 5000 samples.

```
phasedur=round((phasedur/1000)*fs);
```

Generation of basic pulse shape

After converting all input data in practical units, a basic pulse shape is generated (Figure 4.5). So far, this only uses the first two settings, the phase mode and the phase duration. A rectangular pulse is built with ones:

```
pulse = ones(1,phasedur);        %Monophasic (+) pulse shape
if phasemode==1
    pulse=pulse*-1;              %Monophasic (-) pulse shape
elseif phasemode==2
    pulse=[pulse,pulse*-1];      %Biphasic (+/-) pulse shape
elseif phasemode==3
    pulse=[pulse*-1,pulse];      %Biphasic (-/+) pulse shape
end
```
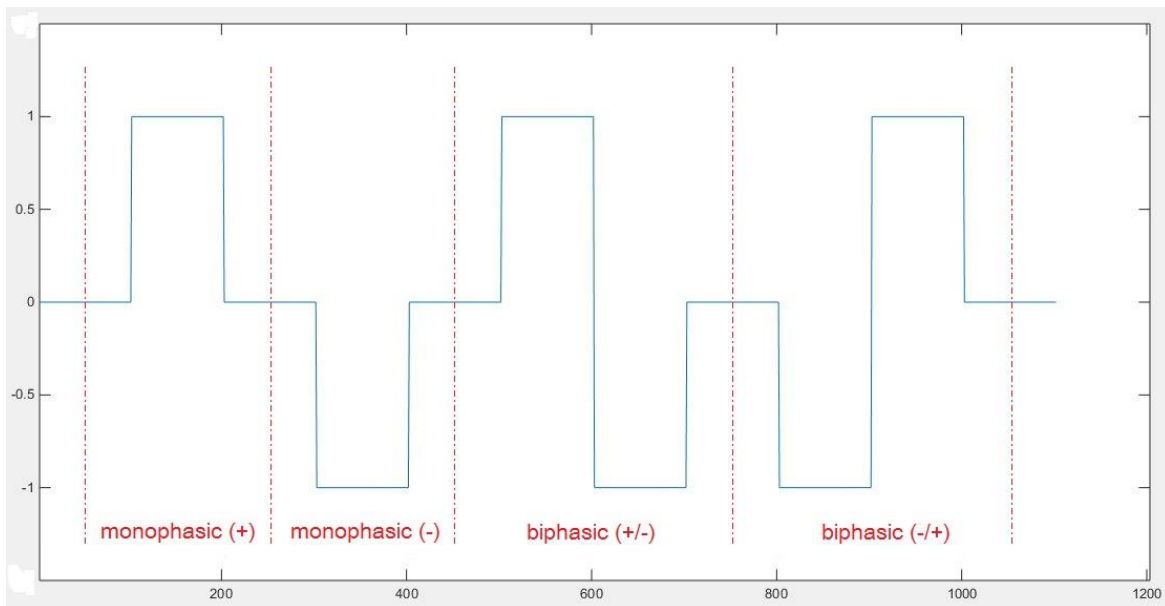
Figure 4.5: Basic pulse shapes with an amplitude of 1/-1 and a phase width of 100 samples, which equals a phase duration of 1 millisecond. From left to right, these shapes correspond to the phase modes 0, 1, 2 and 3 in the LabVIEW™ program.

Modification and replication of basic pulse according to operation mode

This basic pulse is then multiplied by the corresponding amplitude and, if appropriate, modified and replicated according to the chosen stimulation mode.

Mode 0 – Search manually

```
%% CH1 MODE0 - search manually
if mode==0
    if doublepulse_0==0
    output = [pulse*amp_0];
    elseif doublepulse_0==1
    output = [pulse*amp_0,zeros(1,pause_0),pulse*amp_0];
    end
```

For a single stimulation pulse, the basic pulse generated before is simply multiplied by the set amplitude. In case of a double pulse, the output is built of two single pulses, separated by a row of zeros with the length of the pause (Figure 4.6).
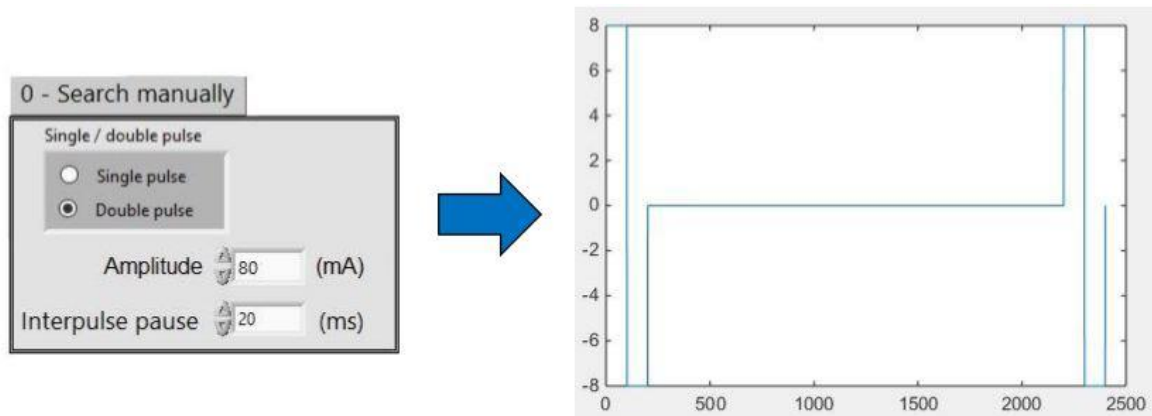
Figure 4.6: Example for mode 0: double pulse with an amplitude of 80 mA and an interpulse pause of 20 ms (General settings: biphasic +/-, phase duration = 1 ms).

Mode 1 – Recruitment curve

```
%% CH1 MODE1 - recruitment curve
elseif mode==1
    amp_1=ampmin_1:delta_1:ampmax_1;
    amp_1=repmat(amp_1,1,rep_1);
    if profile_1==1
        amp_1=amp_1(randperm(length(amp_1)));
    elseif profile_1==2
        amp_1=fliplr(amp_1);
    end
    for n = 1:length(amp_1)
        output = [ output, amp_1(n)*pulse,zeros(1,pause_1)];
    end
```

First an array is created with the required amplitude values from the minimum to the maximum in the defined step width. For stochastic reasons, this array is then replicated as often, as repetitions are set. For example: Three repetitions (rep_1=3) would mean, that every amplitude value will appear three times in this array. Now these values are reordered according to the chosen intensity profile (in case of increasing intensities, no permutation is necessary). Finally, the output data is assembled using a for loop. Within every loop execution, one basic pulse (ones) multiplied by the correlating element in the amplitude array, and one pause (zeros) is added to the output (Figure 4.7).
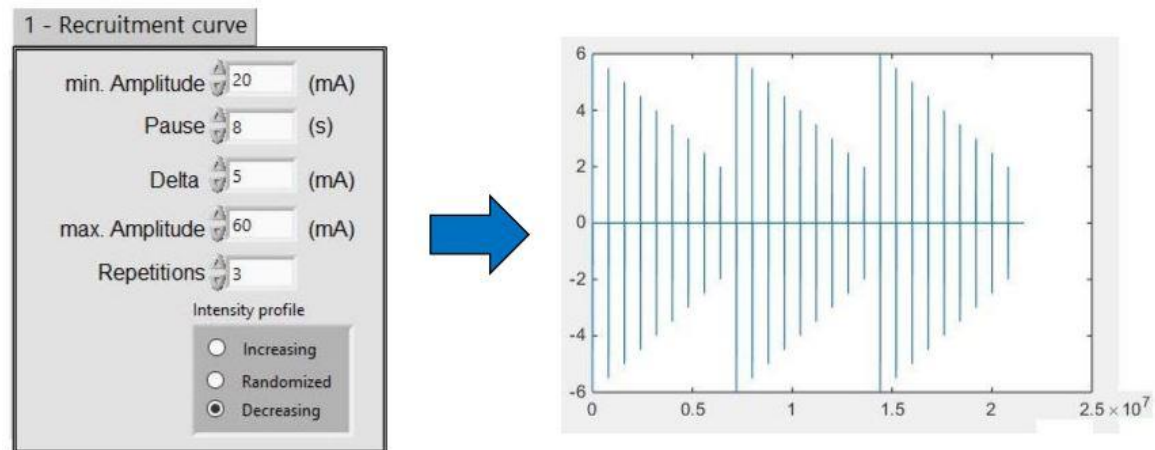
Figure 4.7: Example for mode 1: decreasing intensity profile with amplitudes from 60 to 20 mA, with a step width of 5 mA. Three repetitions of every amplitude value and eight seconds pause after every stimulation impulse (General settings: biphasic +/-, phase duration = 1 ms).

Mode 2 – Single burst

```
%% CH1 MODE2 - single burst
elseif mode>=2
pulse_2=[pulse,zeros(1,(round(fs/freq_2))-length(pulse))];
    if ramp_2==1
        ramp_delta=round(amp_2/freq_2,3);
        amp_2r=ramp_delta:ramp_delta:amp_2;
            for n = 1:length(amp_2r)
            output = [output, amp_2r(n) .* pulse_2];
            end
    end
output=[output,repmat(pulse_2*amp_2,1,pulsenum_2)];
end
```

To generate a single stimulation burst with a defined frequency, the basic pulse is extended by a number of zeros, according to the time between two impulses. This sequence of a basic pulse and a break is then multiplied by the amplitude and repeated as many times, as numbers of pulses are set. If the optional one second ramp is enabled, similar to mode 1, a stepwise increasing amplitude array is created. This array contains as many elements as are necessary to result in one second of stimulation with the given frequency. For example, a ramp for a stimulation with 10 pps frequency will contain ten elements (Figure 4.8). This ramp is placed before the stimulation burst itself to alleviate discomfort at the beginning of more intense stimulations.
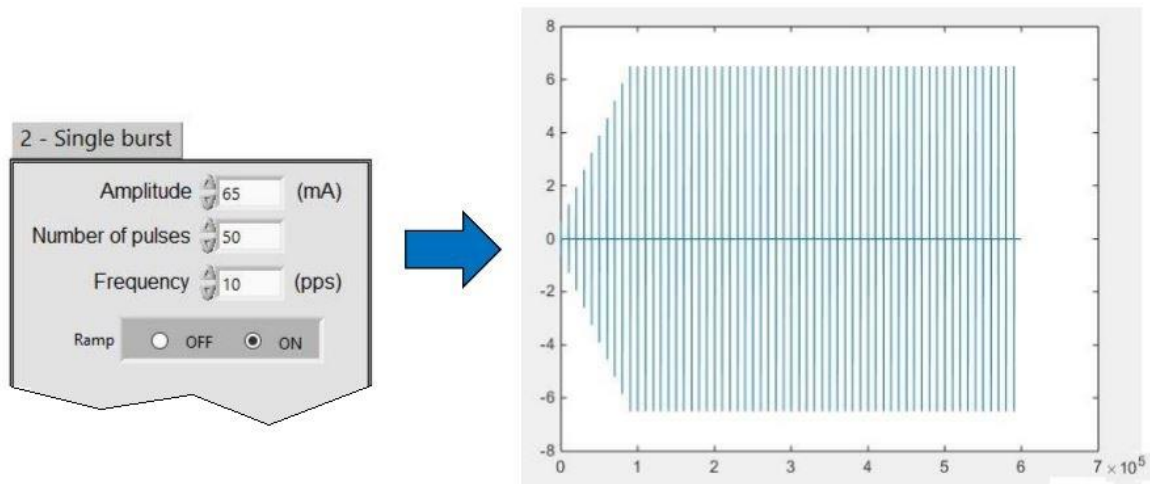
Figure 4.8: Example for mode 2: single burst with one second ramp and 50 pulses with an amplitude of 65 mA and 10 pps frequency. (General settings: biphasic +/-, phase duration = 1 ms).

Mode 3 – Double burst

```
%% CH1 MODE3 - double burst
if mode==3
    pulse_3=[pulse,zeros(1,(round(fs/freq_3))-length(pulse))];
    output=[output,zeros(1,pause_3-(round(fs/freq_2))-
length(pulse)),repmat(pulse_3*amp_3,1,pulsenum_3)];
end
```

Mode 3 is an extension of the single burst, as described before. After generating the first burst (mode 2), again a sequence of a basic pulse and break time according to the frequency is put together. The sequence is replicated and multiplied by the corresponding amplitude to form the second stimulation burst. Both bursts are now put together with the inter-burst break in between (Figure 4.9).
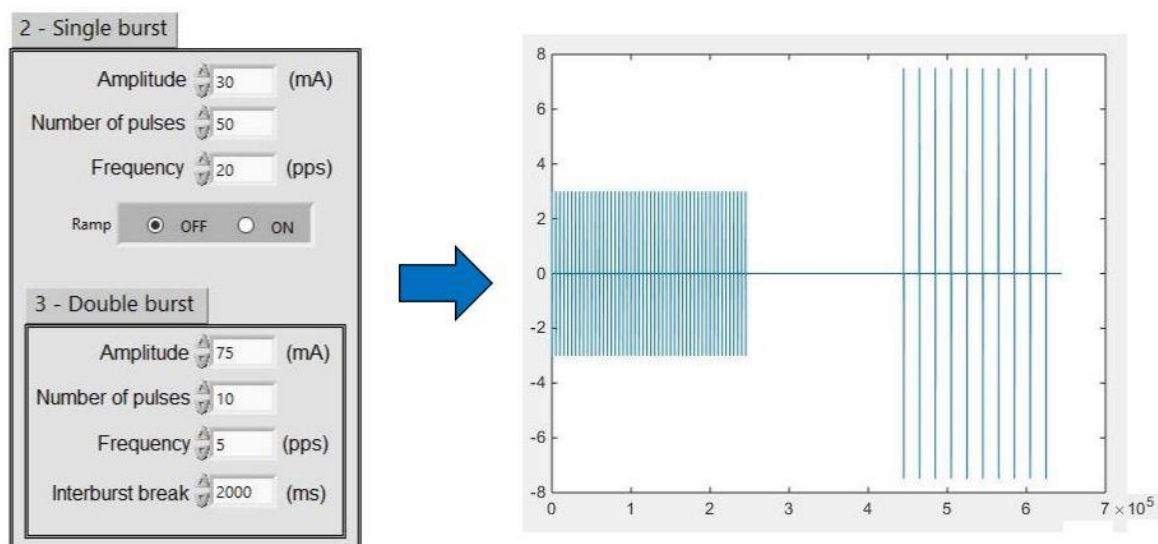
Figure 4.9: Example for mode 3: double burst. The first burst consists of 50 pulses with 30 mA and a frequency of 20 pps. Two seconds later the second burst starts, with ten 75 mA pulses at a frequency of five pps (General settings: biphasic +/-, phase duration = 1 ms).

Stimulation channel 2

The generation of the stimulation data for channel 2 is in principle the same as for the first channel. To enable a timewise separated starting of the channels, an offset of channel 1 to channel 2 can be set. The offset set in seconds is the time, which the second channel starts delayed relative to the first (Figure 4.10).

Also, for channel 2 there is only one operation mode implemented, a single burst of stimuli. This mode corresponds exactly to mode 2 of channel 1.
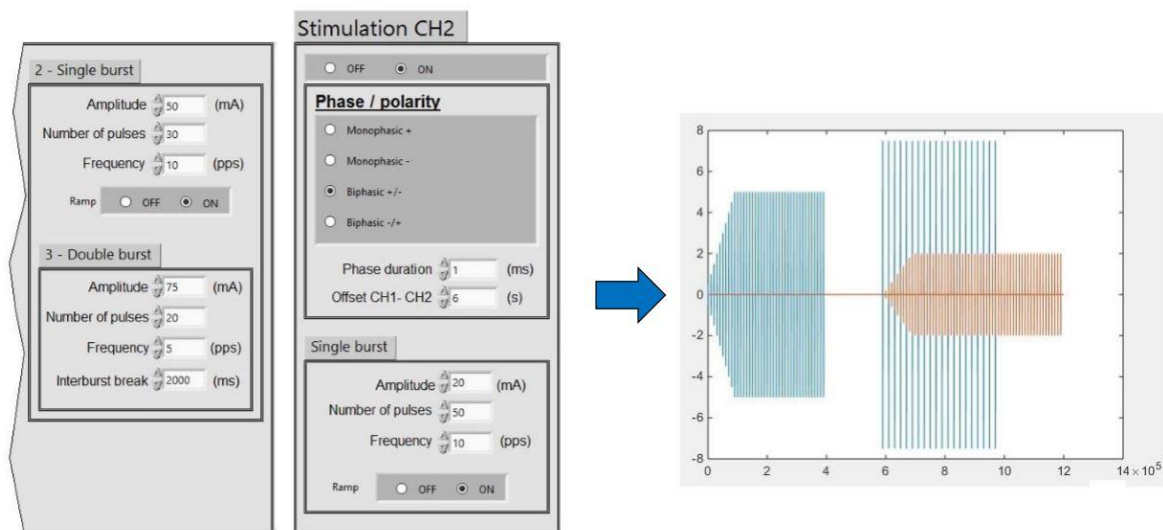
Figure 4.10: Example for a two channels stimulation: Channel 1 (blue): Double burst mode, the first burst consists of 30 pulses with 50 mA and a frequency of 10 pps with a one second ramp before. Two seconds later the second burst starts, with twenty 75 mA pulses at a frequency of five pps. Channel 2 (orange): One ramped stimulation burst with fifty 20 mA pulses at a frequency of 10pps, delayed to CH1 by six seconds (General settings for both channels: biphasic +/-, phase duration = 1 ms).

Combining both stimulation channels

The last step in processing the stimulation data with the MATLAB® script is the combination of both channels. This results in an output array with two rows, the first for channel 1, the second for channel 2.

```
output(2,1:numel(output_CH2)) = output_CH2;
```

Output

When the stimulation data was generated, on the front panel "Stimulation ready" is indicated and the program waits for a button push. This is due to the reason, that depending on the performance of the computer system, generation long arrays may take some seconds. Therefore, without the additional start button, the stimulation session would not start at a clearly defined time. After the button push, the two-rowed stimulation array is sent via a

DAQ assistant to the physical channels ao0 and ao1 (analog outputs) of the NI device. The DAQ assistant is a functional program block, to enable efficient communication of LabVIEW™ with NI DAQ (Data Acquisition) devices.

4.2 Implementation of stimulation hardware

The hardware of the stimulation-related part of the system, developed in this thesis, can be divided into three parts: First, the digital stimulation data is analogized at the output side of the NI multifunctional I/O device, resulting in a +/- 10V signal. Then, to ensure no DC currents are being applied to the subject, a high-pass filter was implemented. This filter circuitry is placed in between NI device and the stimulator, the third hardware component of this system.

4.2.1 Analogization of stimulation data

> **This section deals exclusively with the analog output of the NI USB 6221 OEM. A general introduction of the device is given in Subsection 3.1.2.**

The National Instruments™ USB 6221 OEM device has two analog output channels, that can be software-controlled independently from one another. The digital data is converted to an analog voltage signal with a range of +/- 10V and a DAC (Digital-Analog-Conversion) resolution of 16 bits (National Instruments^{TM}, 2016). The output has a high slew rate of 15V/μs, which is important for the generation of an accurate input for the stimulator. Within the voltage output range, the analog output channels are freely programmable. That means, there are no restrictions to single pulse shapes/characteristics or frequencies/ pattern of stimulation bursts. Also signals with a direct current offset or even a pure direct current signal can be output.

4.2.2 DC current protection

Exposure of the human body to electricity can lead to a variety of injuries, such as electric shock, ventricular fibrillation and burns. The low amount of charge applied to the patient in spinal cord stimulation and the distance of the stimulation site to the heart, exclude the possibility of most of these injuries. However, there is a risk of tissue damage, primarily caused by conversion of electrical currents into thermal energy. The thermal load is proportional to the amperage squared, the resistance and the time. Since the skin exhibits a much higher impedance, than the internal structures of the human body, most of the heating

will occur here. Normal stimulation impulses, with a pulse width of few milliseconds, will hardly cause any pathologic tissue heating because of the low time of exposure. On the other hand, very long stimulation impulses or DC voltage components applied to the patient, show a high risk of thermal tissue damage.

Since the analog output signal of the NI-USB 6221 OEM device has no restrictions in terms of shape properties, a pure DC signal, or a pulsating signal with a DC offset could be generated and transmitted to the stimulator (Figure 4.11). Furthermore, the stimulation device used in this application is freely programmable, meaning it amplifies any input signal, even a DC voltage, and sends it to the patient.
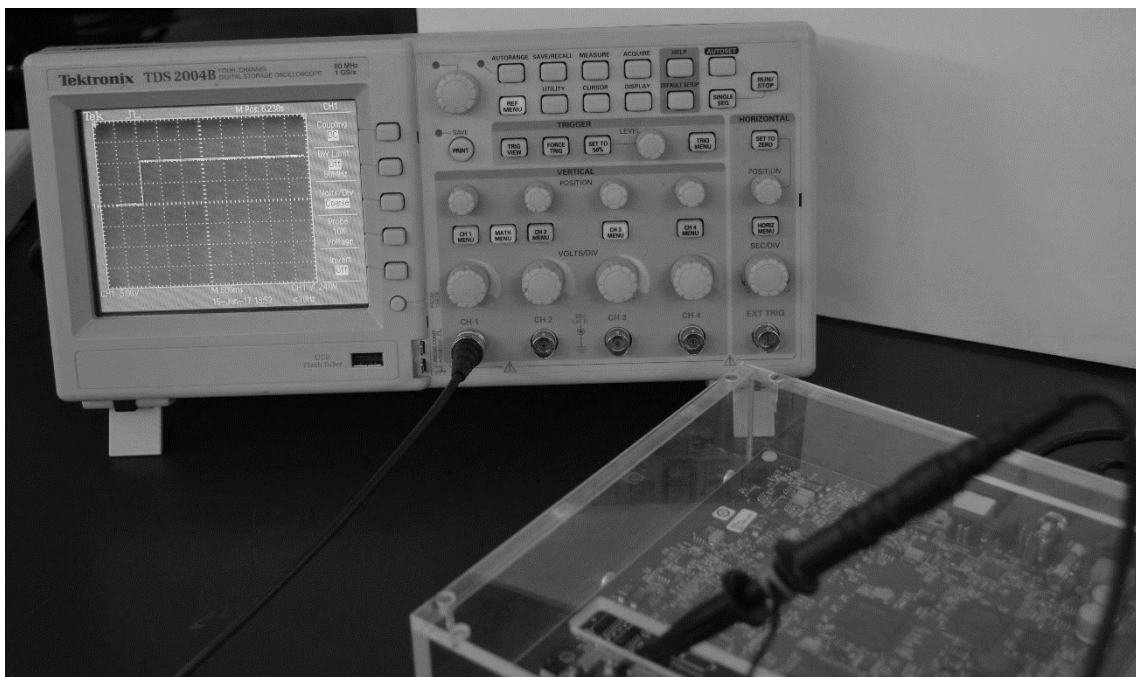
Figure 4.11: NI USB 6221 OEM generating a 10V DC output signal. Horizontal scale: 1 square equals 500ms. Vertical scale: 1 square equals 5V.

To eliminate the risk of direct current injuries, a first order high pass filter was implemented in between NI-DAQ device and the stimulator. This simple circuit is made up of a resistor and a capacitor (Figure 4.12), and its impedance is frequency dependent, due to the reactance X_C of the capacitor. For signals with high frequency, X_C is very small, and therefore the capacitor hardly influences the overall impedance; the signal passes. When the input frequency is very low, the reactance X_C gets big and increases the impedance of the high pass; the signal is cut off. The frequency where the reactance X_C equals the resistance R is called cut off frequency f_C and is an important value for the dimensioning of the high pass components. Here the high pass circuit causes a 45° phase shift, which leads to a reduction of the output signal amplitude to 70.7% of the input.
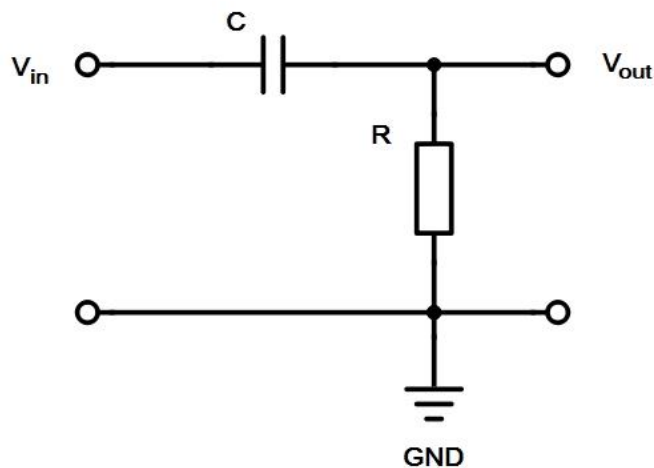
$$X_C = \frac{1}{2\pi f C}$$

$$f_C \Rightarrow X_C = R$$

$$f_C = \frac{1}{2\pi R C}$$

Figure 4.12: 1ˢᵗ Order high pass filter and important equations for dimensioning of the components. Low frequencies f result in high capacitive reactance X_C and are cut off. High frequencies pass the circuit due to the low influence of the capacitor on the overall impedance.

To only cut off a possible DC offset, without modifying the rectangular stimulation pulses too much, a very low cut off frequency of approximately 2 Hz was chosen for the filter. To avoid causing too much voltage drop at the filter circuitry, the resistor was chosen with a high value of 33 kΩ. With a capacitor with C=2.2 µF, the high pass filter exhibits a cut off frequency f_C = 2.2 Hz. In case future projects require very long stimulation pulses (which would be cut off with this filter), a jumper was implemented to bridge the capacitor.

4.2.3 BIOPAC® STMISOLA

The BIOPAC® STMISOLA linear isolated stimulator (see Figure 4.13) is a universal electrical stimulation device. It can be controlled by any analog input signal (±10 V), to generate stimulation signals with arbitrary wave shapes. This input is connected via the high pass filter to the output of the NI USB 6221 OEM device. The incoming voltage signal is now amplified according to the chosen operation mode of the stimulator and then sent to the subject. There are two stimulation modes:

Voltage (V) mode

When operating in voltage mode, the STMISOLA amplifies the voltage input signal (±10 V) by a factor of 20 to result in a ± 200 V output signal. To limit the maximum current applied to the subject, the output impedance can either be set to 100 Ω or 1 kΩ.

Current (I) mode

Run in the current mode, the output impedance settings have a high influence on the output amplitude. If the 100 Ω impedance is set, the stimulator operates in the high current mode, with a gain of 10 mA/V. With the input voltage of ±10 V, this results in an output signal range of ± 100 mA. With the 1 kΩ impedance setting, the device is operated in the low current mode. Here it exhibits a gain of 1 mA/V, which leads to a maximum output of ±10 mA. This mode is advantageous, when small amplitudes have to be output very precisely. Both current modes are compliant with a maximum voltage output of ± 200 V (BIOPAC® Systems Inc, 2016b).

Figure 4.13: BIOPAC® STMISOLA linear isolated stimulator. Shown in current mode (I) with high output range of ± 100 mA (Z_{out} = 100 Ω). The cable in the back inputs the control signal, the BNC cable in front is the stimulation output.

4.3 Evaluation

To evaluate the stimulation system under laboratory conditions, instead of applying stimulation pulses to a human subject, an equivalent circuit was designed. A multitude of settings and different single pulses and stimulation bursts have been measured, using this model circuitry. The obtained measurement data allowed the conclusive evaluation of the system, as described in the end of this chapter.

4.3.1 Testing procedure

The skin-electrode interface is very complex, which makes accurate direct impedance measurements impossible (Lyrken & Venables, 1971). However, a simplified RC-circuit can be used to model this interface (van Boxtel, 1977; Vargas Luna, Krenn, Cortés Ramírez,

& Mayr, 2015); the chosen component values have been empirically determined for modelling the specific case of transcutaneous spinal cord stimulation (Figure 4.14). This simplified model accounts for the impedance of the electrodes with the parallel elements (470 nF capacitor and 2.2 kΩ resistor), as well as for the lumped skin and body resistance with the 220 Ω resistor in series.
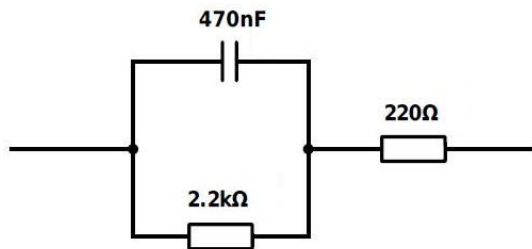
Figure 4.14:Skin-electrode interface equivalent circuit. Widely used, simplified model. Capacitor C_e = 470 nF and Resistor R_e = 2.2 kΩ account for the electrode impedance, whereas resistor R_s = 220 Ω models the lumped skin/body resistance.

The instrumentational setup for evaluating the stimulation system is the same, as is planned for the final application for spinal cord stimulation in human subjects (see also Figure 4.1). The stimulation data is generated with a LabVIEW™ program and sent via the analog output channels (AO0 and AO1) of the multifunctional I/O device. This output signal is measured with an oscilloscope (Channel 4) and further passes the high pass filter (Figure 4.15).
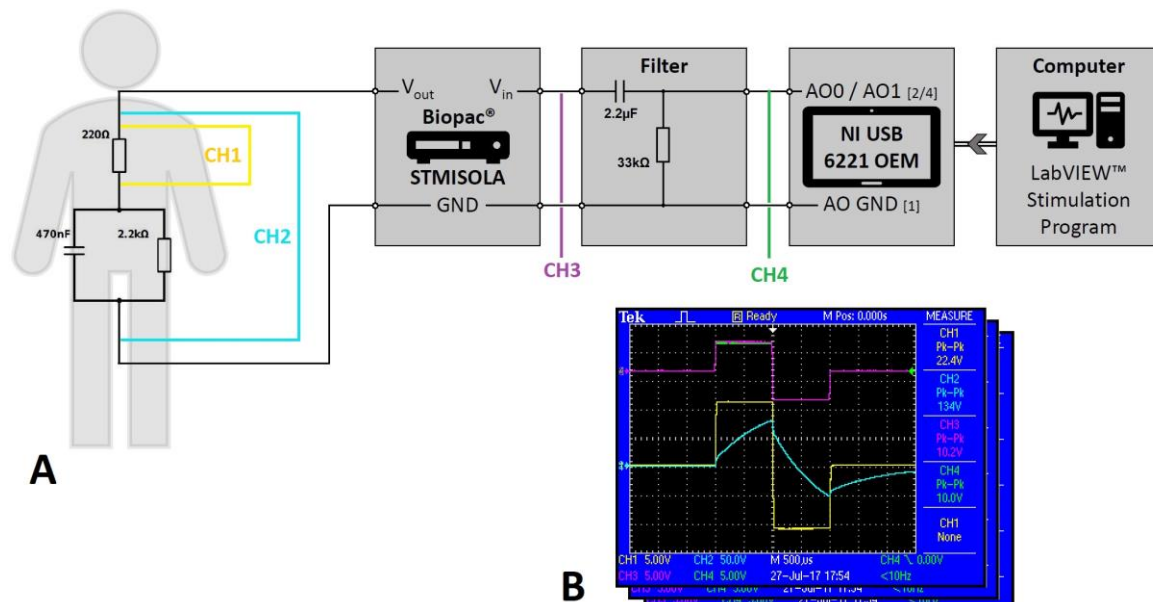
Figure 4.15: Measurements to evaluate the stimulation system.A) Experimental setup with measurement points and corresponding channels indicated. **B)** An example of the measurements, obtained while stimulation with a biphasic single pulse (1ms phase width, 50mA amplitude) Channels 3 and 4 are perfectly overlapping, therefore the green line of channel 4 can hardly been seen.

The filtered stimulator input data is measured with channel 3 of the oscilloscope. The stimulator output is then connected to the skin/electrode equivalent circuit model, where the voltage at the whole circuit is measured with channel 2. Also, the voltage at the resistor R_s, which accounts for the lumped skin/body resistance, is measured with channel 1 of the oscilloscope.

These measurements have been made with a variety of single stimulating pulses, with different shapes, amplitudes and widths. Also, different kinds of stimulation bursts have been tested. Lastly, to evaluate the function of the high pass filter, a 100mA DC signal was generated and sent to the hardware.

4.3.2 Results – Figures

For each type of measurements (single pulse, stimulation burst and DC current), there will be given one representative oscilloscope figure in this section. A general discussion of these results is subject of the following section.
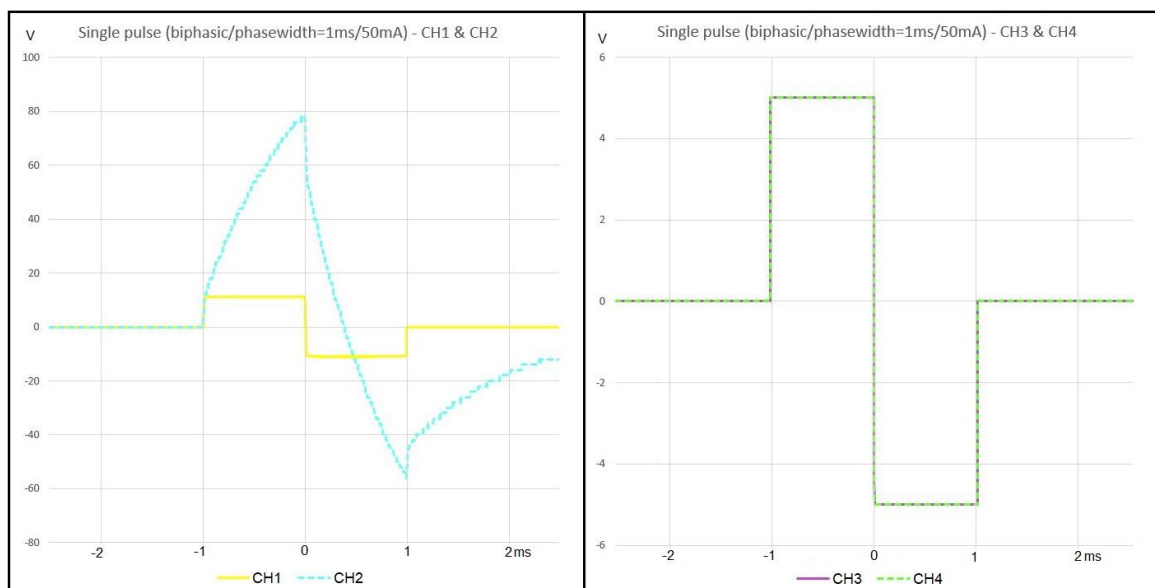
Figure 4.16: Measurement results: Single pulse, biphasic with a phase width of 1ms and 50mA amplitude. The left graph shows the measurements made at the equivalent circuit, the right graph shows measurements made on the stimulator input side.
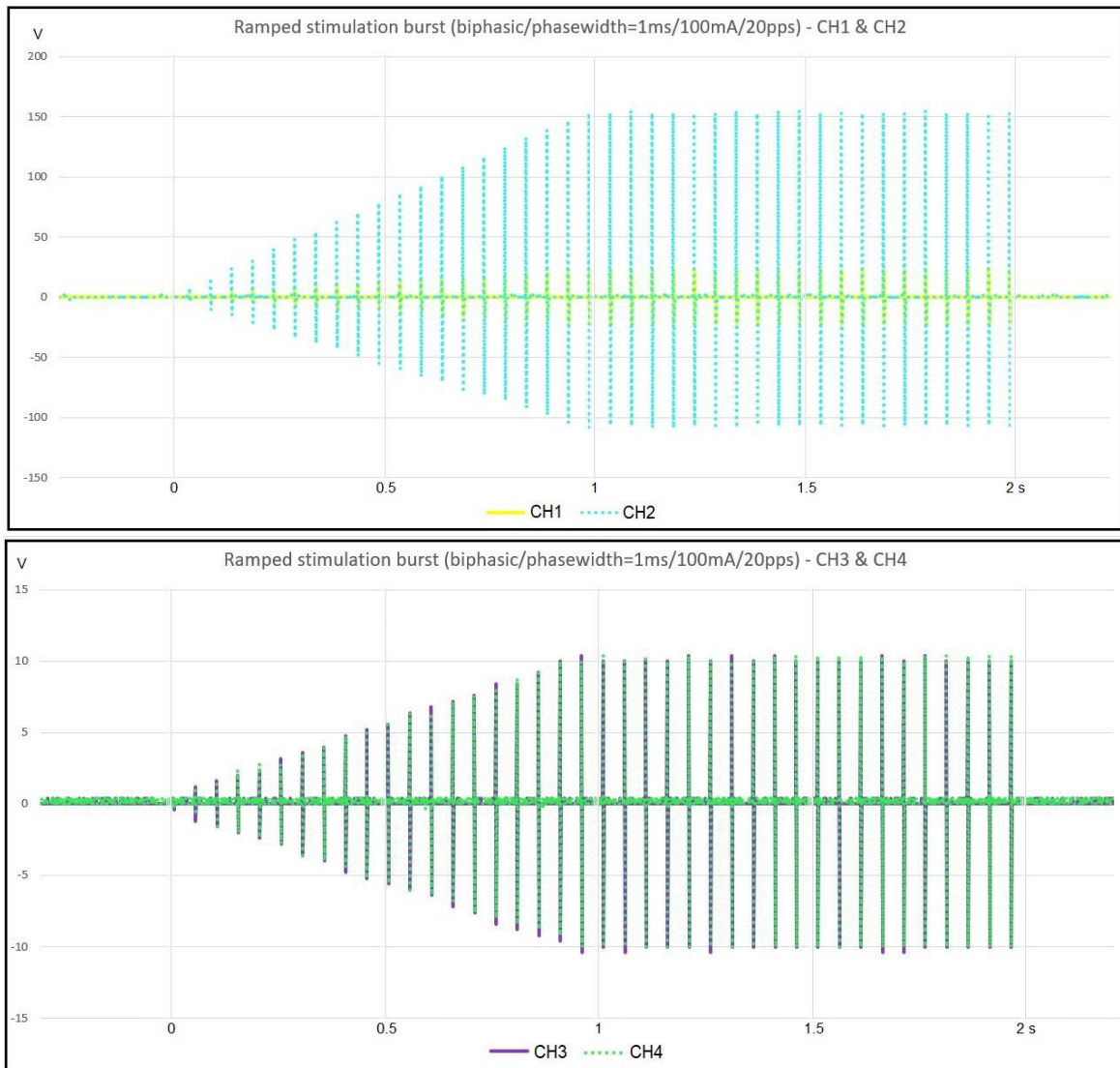
Figure 4.17: Measurement results: Ramped stimulation burst, biphasic pulses with a phase width of 1ms and 100mA amplitude with a frequency of 20pps. The upper graph shows the measurements made at the equivalent circuit, the lower graph shows measurements made on the stimulator input side.
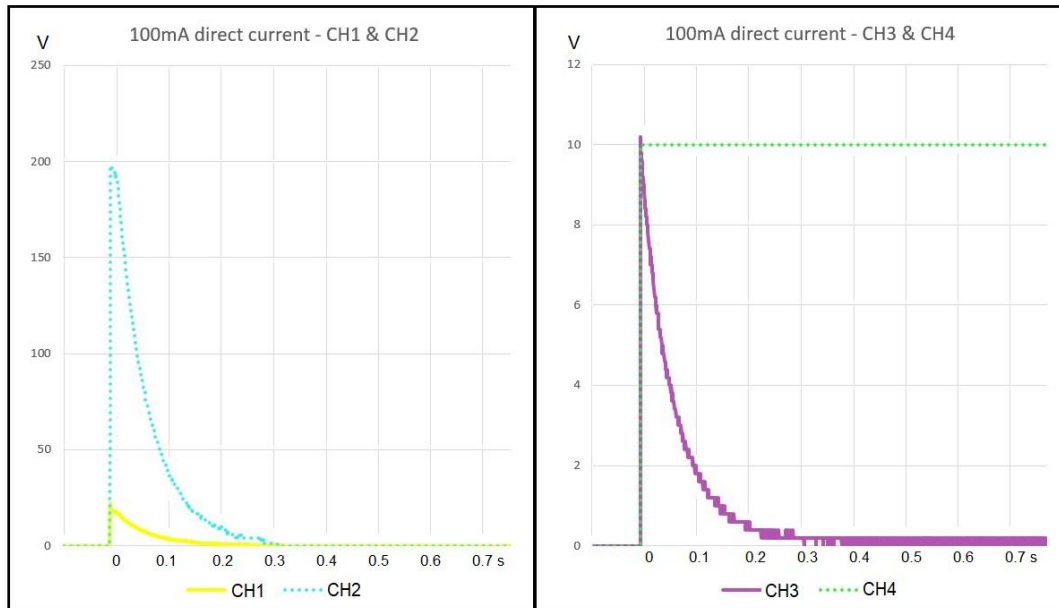
Figure 4.18: Measurement results: Direct current with 100mA amplitude. The left graph shows the measurements made at the equivalent circuit, the right graph shows measurements made on the stimulator input side.

4.3.3 Conclusion

The stimulation system developed in this thesis meets the requirements (Chapter 1.2) of the research application. The system has two independent and freely programmable stimulation channels. In terms of hardware, both channels can emit any pulse shapes in a range of +/-100 mA. The implemented high pass filter is effective protecting the subject from DC currents being applied (Figure 4.18). Also, the filter circuitry was evaluated for the longest clinically relevant stimulation pulses of 1 ms phase duration and showed no distortion of the rectangular pulse shape (Figure 4.16). All basic operation modes (Chapter 4.1) have been tested under laboratory conditions on an equivalent circuit, and could be verified to emit the desired stimulation pattern. Figure 4.17 shows an example of such a verification for a single ramped stimulation burst - biphasic pulses with a phase width of 1ms and 100mA amplitude with a frequency of 20pps.

On the hardware side, the system is limited to emit stimulation pulses in the range of +/-100 mA, whereas some other commonly available stimulation devices are able to emit pulses of up to +/- 120 mA. Due to the reason, that the software was designed for the very specific application in research studies on trans-spinal electrical stimulation, the operation modes implemented may not be practical for other applications. Also, only rectangular pulse shapes are possible to generate with this software. If required for other applications, both software limitations can easily be overcome by an adjustment of the MATLAB® script.

5 ELECTRICAL STIMULATION OF POSTERIOR ROOTS AND PERIPHERAL NERVES

Posterior root stimulation is capable of augmenting restricted movements or evoking lost motor functions in chronic spinal cord injured subjects (Dimitrijevic, Gerasimenko, & Pinter, 1998). After successful technical evaluation of recording (Chapter 3.3) and stimulation system (Chapter 4.3) under laboratory conditions, the system is used in a research study in the field of posterior root stimulation in clinical environment. The aim of this preliminary study is to test the system developed in this thesis and investigate the influence of peripheral nerve conditioning stimulation on the excitability of the spinal cord.

5.1 Method

5.1.1 Subject

Due to the reason, that this preliminary study mainly serves the purpose of testing the recording and stimulation system, the measurements are only carried out on a single subject (n=1, female, 24 years). The subject is spinal cord injured (motoric complete) with the lesion at vertebra C5.

5.1.2 Materials

The instrumentational setup of the recording and stimulation system used in this study is the same as described in chapter 3 and 4: in this subchapter, the main devices will be relisted together with an exact description of the electrode placement.

Two stimulators (BIOPAC® STMISOLA linear isolated stimulator) are controlled by a multifunctional I/O device (National Instruments™ USB 6221 OEM). The first stimulator is used for eliciting the PRM reflexes. The stimulation electrodes are placed in a bipolar setup on the back of the subject. The cathode is placed at the level of vertebrae T11/T12, the anode is located over vertebrae L4/L5 (Figure 5.1).
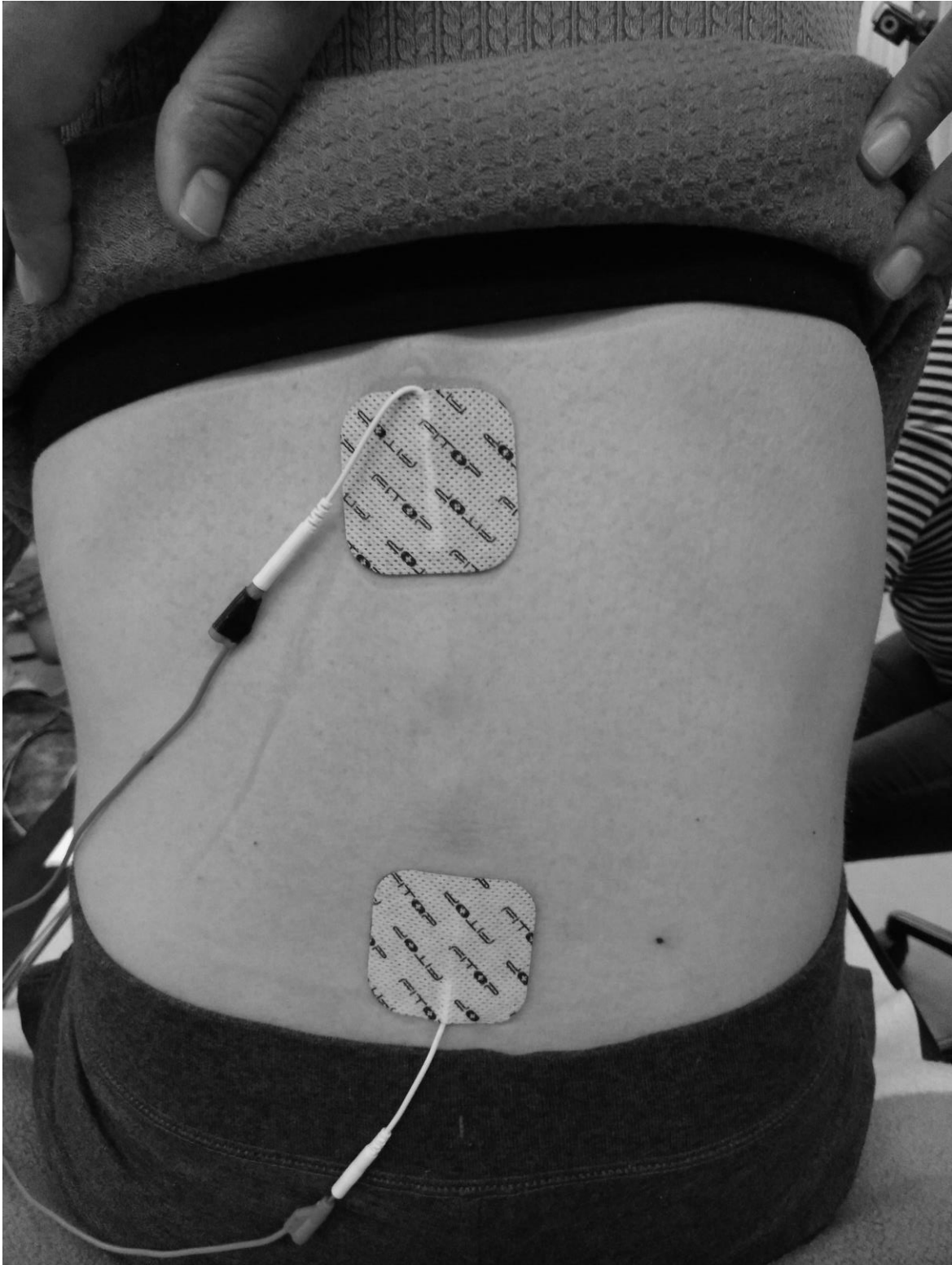
Figure 5.1: Bipolar stimulation electrode placement. Two surface electrodes (5x5cm) are placed over the spine of the subject. The cathode is located over vertebrae T11/T12, the anode is placed at level of L4/L5.

The electrodes of the second stimulation device are located at the left ankle of the subject, in order to apply conditioning pulses to the sural nerve (see Figure 5.2). The sural nerve is purely afferent peripheral nerve.
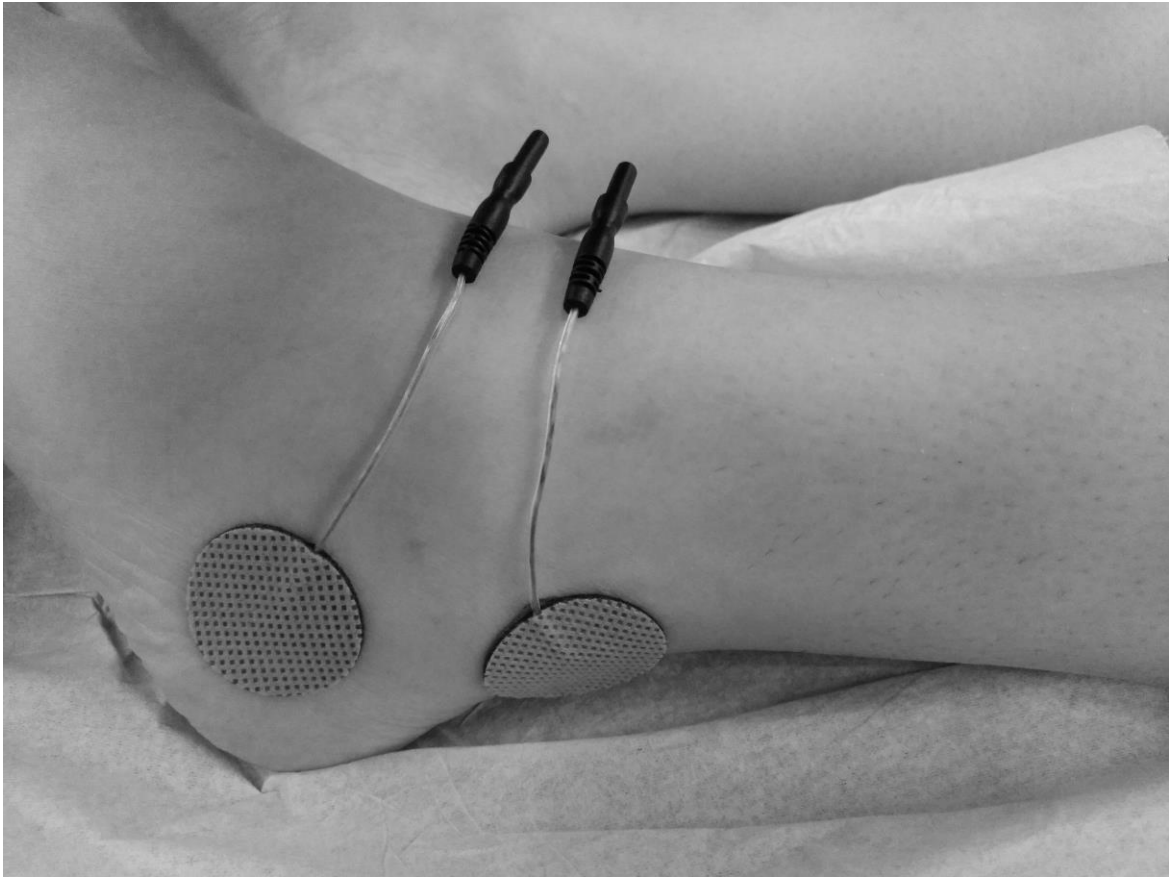
Figure 5.2: Bipolar conditioning electrode setup at the left ankle of the subject. The electrodes are placed over the sural nerve with the cathode being more proximal.

The EMG signals are recorded bilaterally at the four big synergistic muscle groups of the lower limb: the knee extensor (quadriceps) and flexor (hamstrings) and the ankle extensor (triceps surae) and flexor (tibialis anterior). The recording electrodes are placed centrally on the muscle bellies, with a distance of approximately 3 cm between the single electrodes of each pair. Signals are amplified with a gain of 590 and filtered with a bandwidth of 30-590 Hz.

5.1.3 Measurements

(A) - Single pulses

First single stimulation pulses are applied to the subject via the first set of electrodes, located at the spine below the level of lesion (recall Figure 2.25). Here the influence of different pulse shapes (monophasic and biphasic) and different polarities (+/-) on eliciting PRM reflexes is investigated.

(B) - Double pulses

To study the recovery behaviour of the monosynaptic neuronal interconnection in the spinal cord (Figure 5.3), double pulses with different intensities are applied to the subject. Biphasic rectangular stimulation pulses with phase widths of 1ms, intensities of 50, 60 and 75 mA and an inter-pulse time of 35 ms are emitted. Still this measurement only incorporates the first electrode set at the spine.
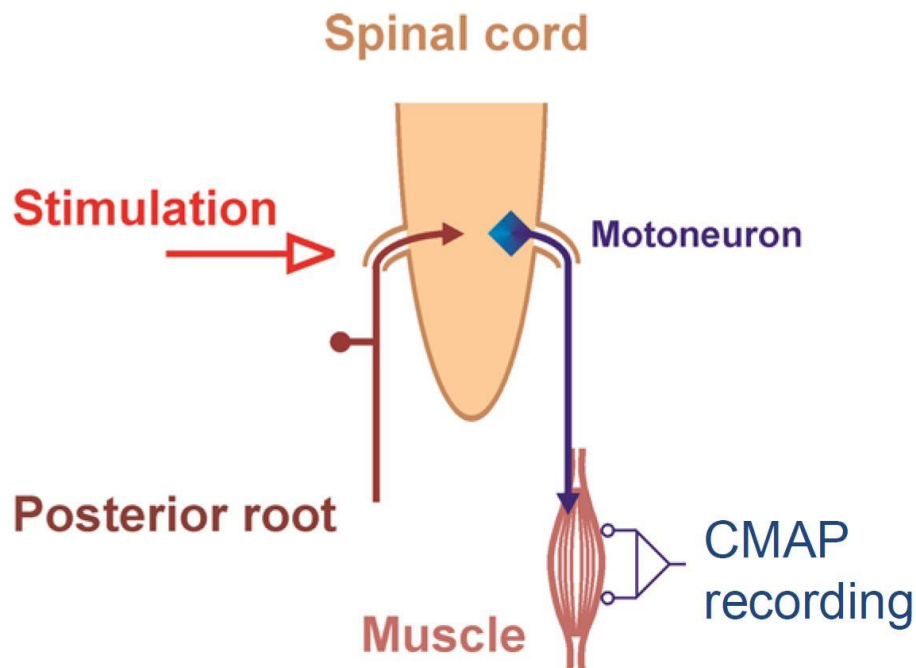
Figure 5.3: Schematic of PRM reflex measurement. The reflexes are initiated via a stimulation impulse in the posterior roots and transmitted over a monosynaptic connection to a motoneuron. The resulting compound muscle action potentials (CMAP) are measured using EMG (Krenn M, Danner SM, Schlaff C, Hofstoetter US, Minassian K, Mayr W, 2014).

(C) – Conditioning with peripheral nerve stimulation

This measurement serves the purpose of investigating the possibility of altering the spinal cord excitability by conditioning via stimulation of an afferent peripheral nerve (Figure 5.4). The first channel delivers single stimulation pulses to the posterior roots to elicit PRM reflexes, that serve as a probe. Here, the pulse shape and polarity is used, that was found to evoke the biggest PRM response in measurement A. The second channel stimulates the sural nerve of the subject with different stimulation patterns in order to study the different influence on excitability of the spinal cord.
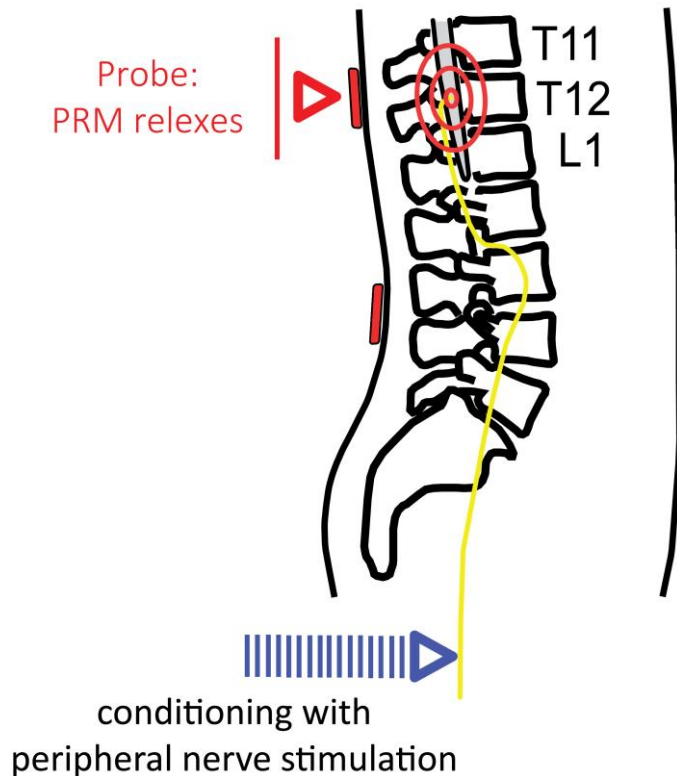
Figure 5.4: Schematic of two-channel PRM reflex elicitation with peripheral nerve stimulation. The first channel serves to elicit PRM reflexes as probe, whereas the second channel delivers conditioning stimulation to a peripheral nerve. (Krenn M, Danner SM, Schlaff C, Hofstoetter US, Minassian K, Mayr W, 2014).

(C1) - PRM reflex peak-to-peak control measurements

Due to the reason, that the following measurements (C2 & C3) will take about 20 minutes and involve a large number of stimulation impulses applied to the posterior roots and the peripheral nerve, control measurements are required in between the different stimulation protocols. Therefore, the peak-to-peak response of PRM reflexes, elicited using single stimulation pulses at the spinal electrodes, are measured. This is done five time prior to protocols C2 and C3 and three times after C3. These values serve as baseline values for the following measurements and provide a general stability control.

(C2) – Peripheral nerve conditioning with a single pulse

Here the conditioning influence of a single stimulation pulse (20 mA, biphasic rectangular 2 x 1ms) applied to the sural nerve 20ms prior to the elicitation of a PRM reflex (with a 65mA, biphasic rectangular 2 x 1ms pulse) is studied. These measurements are compared to the control values obtained from C1.

(C3) – Peripheral nerve conditioning with an 80pps stimulation train

Further the conditioning effect of a five second stimulation train with 80 pps applied to the sural nerve is studied. Stimulation intensities of 1, 2.5, 5, 10 and 20 mA are tested. The time offset between peripheral conditioning and spinal test stimulation (65 mA, biphasic rectangular 2 x 1ms) is 20ms. Again, the EMG peak-to-peak values are set in relation to the previously obtained control values.

5.1.4 Data analysis

The raw measurement data, which is logged to a TDMS file by the LabVIEW™ program (recall Chapter 3.2), is read in and analysed with MATLAB® R2017a. The plots of the PRM reflex responses are generated by detecting the stimulation artefact and plotting the relevant time interval around it. In case of single pulses this time frame is set to 5 ms before and 45/50 ms after the stimulation impulse, for double pulses respectively this time frame is expended to 90 ms after the first stimulation artefact.

The peak-to-peak values are calculated by a simple subtraction of the minimal voltage value from the maximal value of a reflex response. The relative change in peak-to-peak responses is obtained by division of the conditioned PRM reflex magnitude by the control measure.

5.2 Results

Here the measurement data obtained during the stimulation protocols A, B and C1-C3, as described above, is given in a graphical form without further description. Contemplation and discussion of these plots is objective of the next chapter.

(A) Single pulses
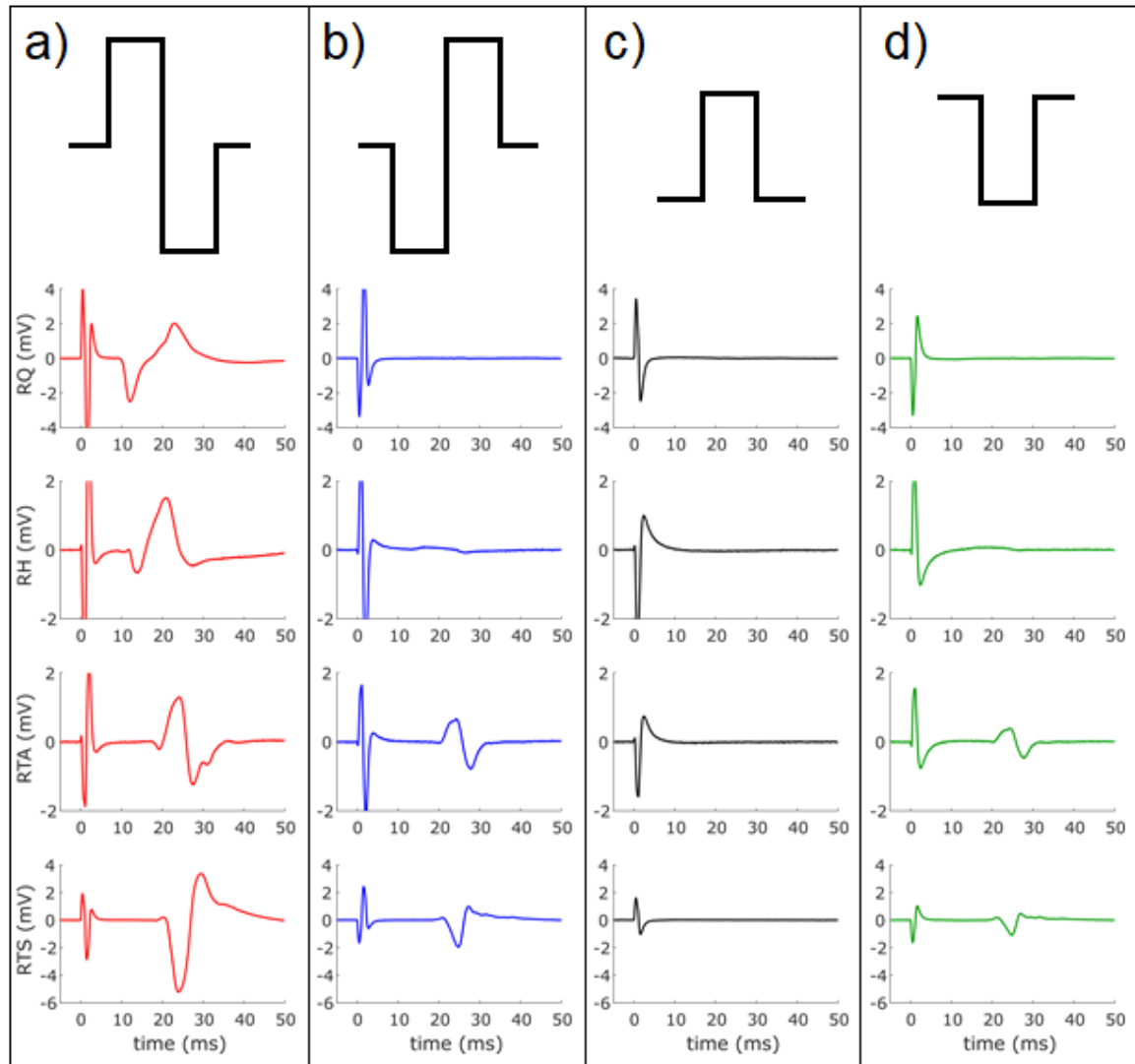
Figure 5.5: PRM reflex elicited with different stimulation pulses. EMG measurements of PRM reflexes at the muscles (Q = quadriceps, H = hamstrings, TA = tibialis anterior, TS = triceps surae) of the right (R) leg. **a)** Biphasic rectangular, cathode polarity +/-. **b)** Biphasic rectangular, cathode polarity -/+. **c)** Monophasic rectangular, cathode polarity +. **d)** Monophasic rectangular, cathode polarity -.

(B) Double pulses
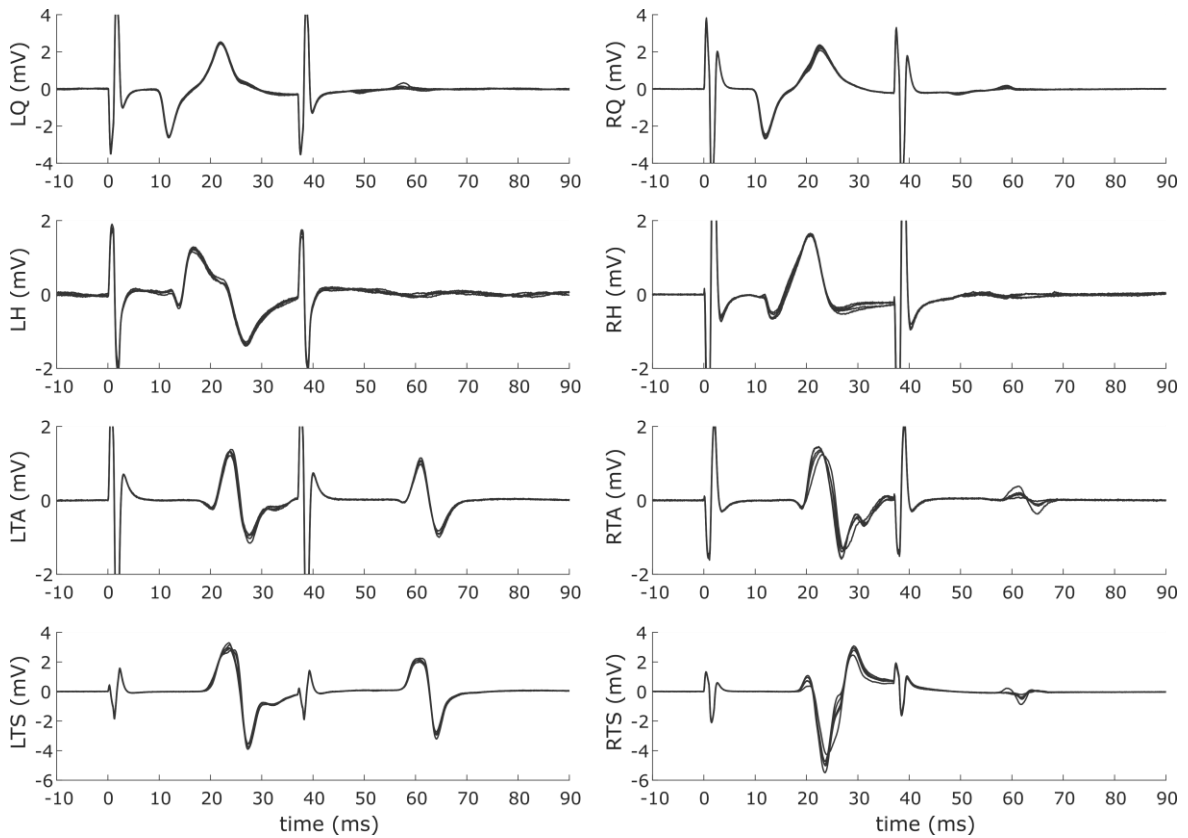
Figure 5.6: Recovery behaviour of PRM reflex elicitability measured bilaterally in the muscles of lower extremities after inducing two biphasic (+/-) rectangular stimulation pulses with 75 mA and an inter-pulse time of 35 ms.
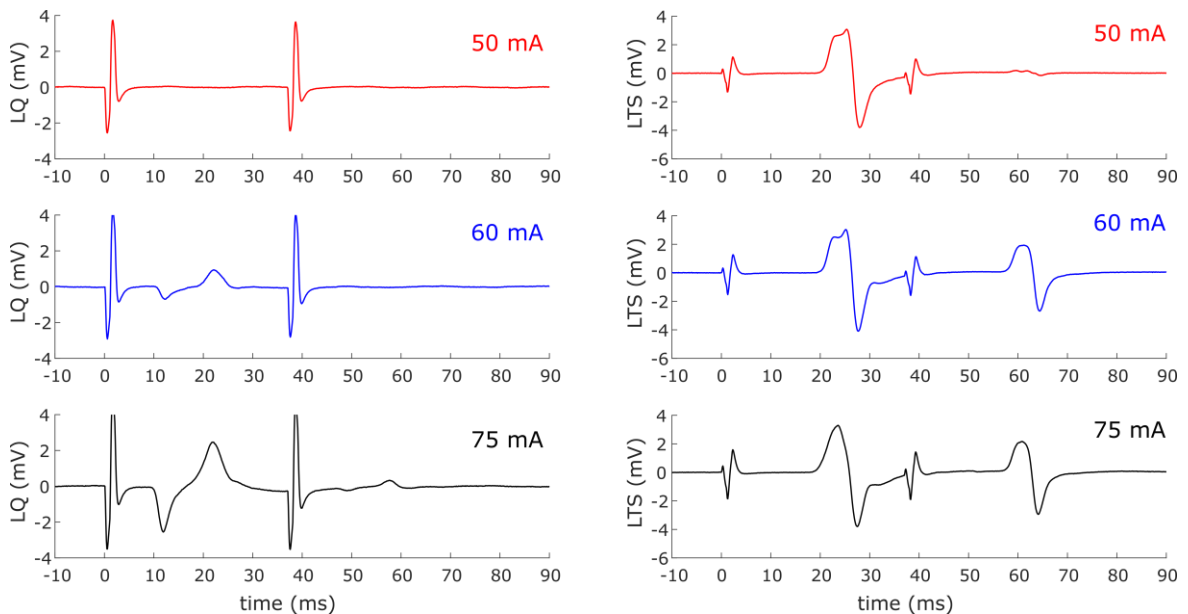
Figure 5.7:Influence of stimulation intensity on recovery behaviour of PRM reflex elicitability. Example of Measurements obtained in the quadriceps (Q) and triceps surae (TS) of the left (L) leg after applying biphasic (+/-) rectangular pulses of 50, 60 and 75 mA.

(C1) PRM reflex peak-to-peak control measure
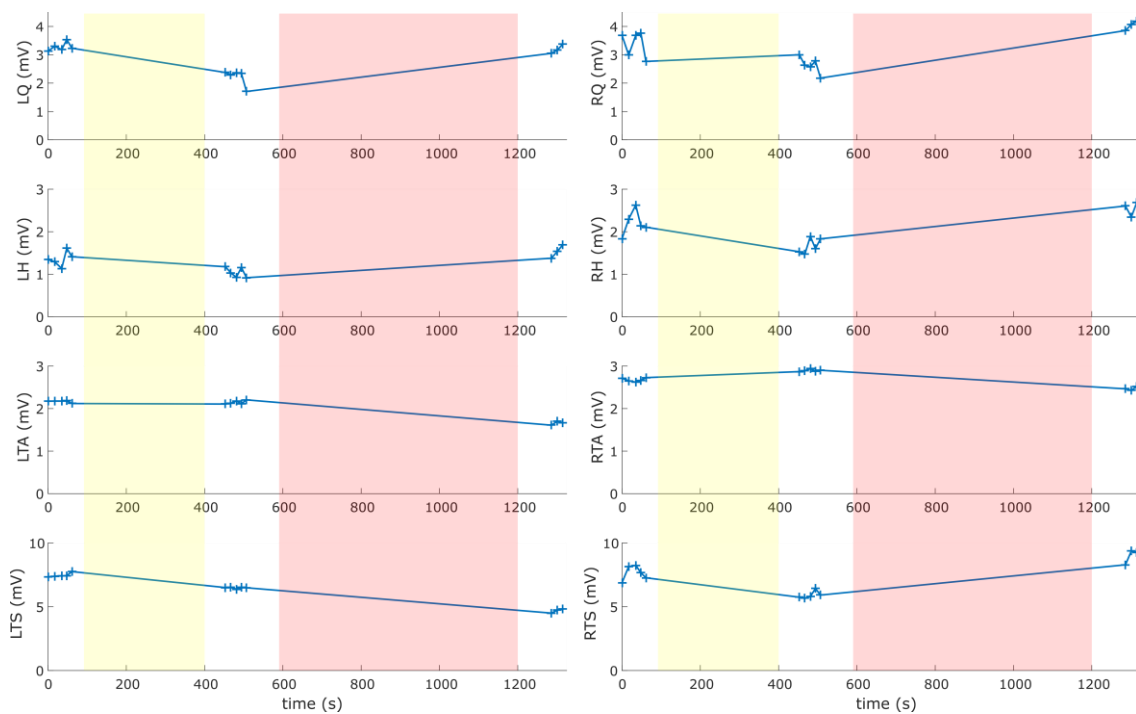
Figure 5.8: Stability of control measurements of PRM reflex peak-to-peak values. Yellow section visualizes conditioning test measurements with single pulses (C2); during red section conditioning with 5s stimulation trains of 80pps was tested (C3).

(C2) Peripheral nerve conditioning with a single pulse
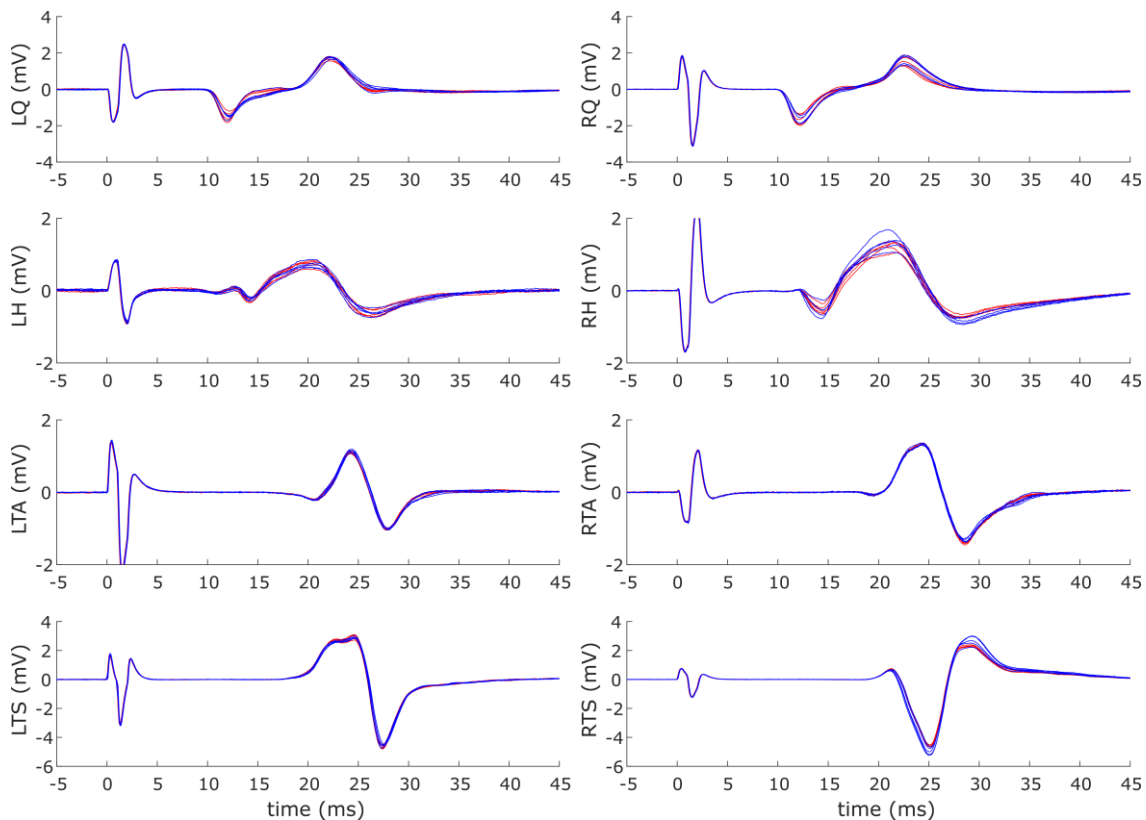
Figure 5.9: PRM reflex elicited after a single stimulation of the sural nerve at the left ankle. Blue traces show the control measurements prior to the peripheral nerve stimulation; red traces show PRM reflexes after conditioning. Conditioning-test interval is 20 ms. Sural nerve

stimulation parameter: 20 mA, biphasic rectangular 2 x 1ms, single pulse; transcutaneous spinal cord stimulation parameter: 65 mA, biphasic rectangular 2 x 1ms.

(C3) Peripheral nerve conditioning with an 80pps stimulation train
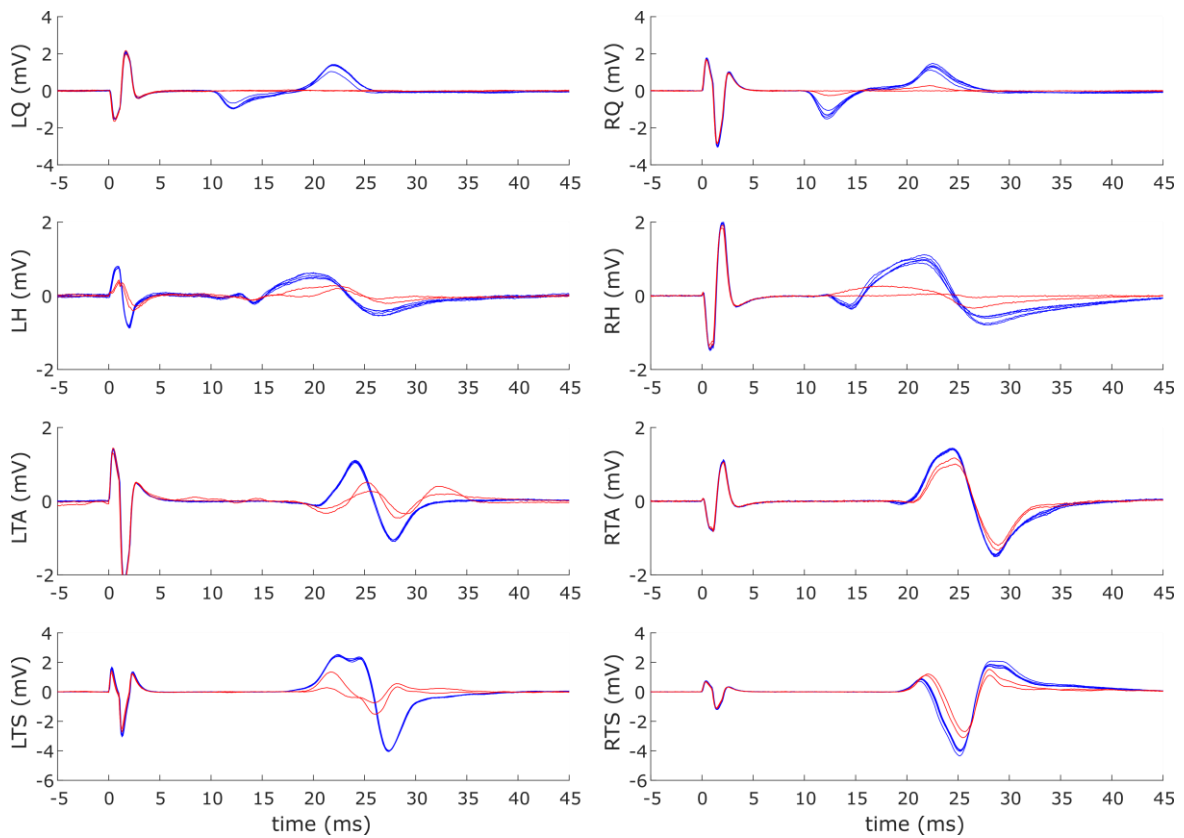
Figure 5.10: PRM reflex elicited after a 5s 80pps stimulation of the sural nerve at the left ankle. Blue traces show the control measurements prior to the peripheral nerve stimulation; red traces show PRM reflexes after conditioning. Conditioning-test interval is 20ms. Sural nerve stimulation parameter: 20 mA, biphasic rectangular 2 x 1ms, 80pps, 5 s burst duration; transcutaneous spinal cord stimulation parameter: 65 mA, biphasic rectangular 2 x 1ms.
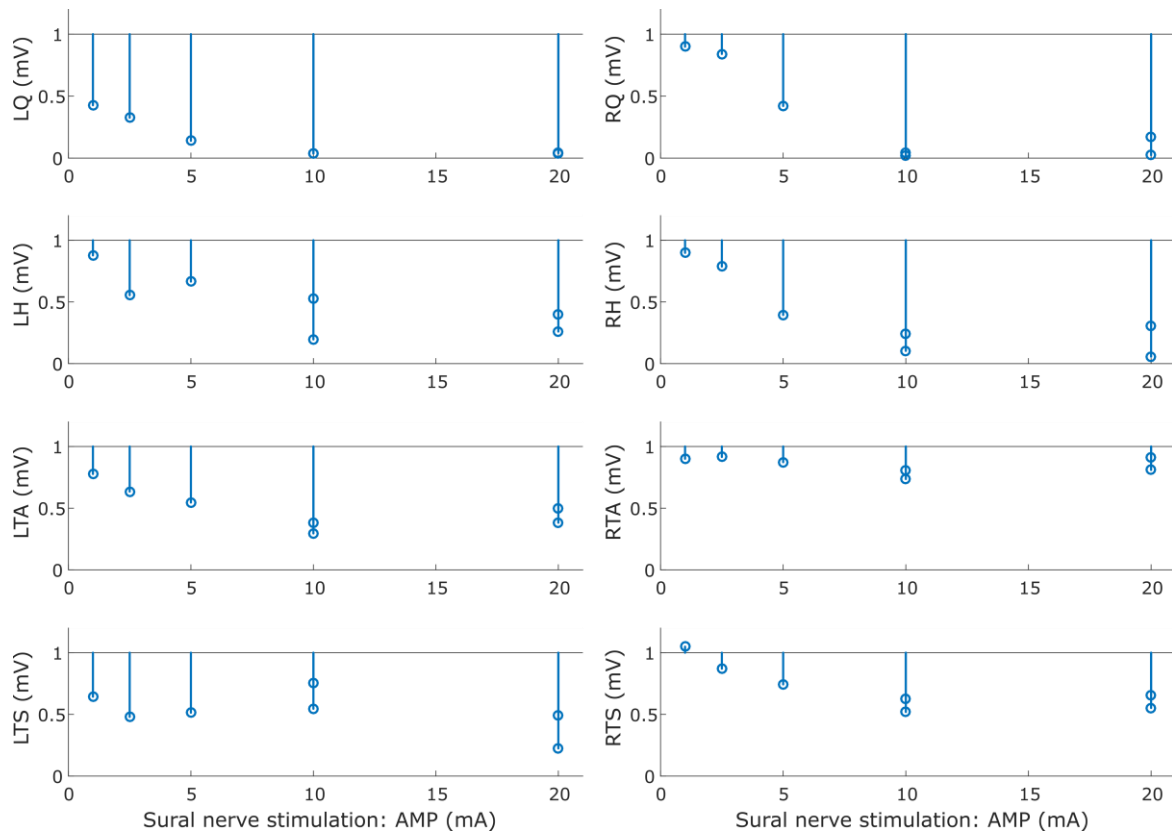
Figure 5.11: Relative change of PRM reflex peak-to-peak values after 80pps stimulation of the sural nerve at the left ankle with 1, 2.5, 5, 10 and 20mA, compared to the control measurement. EMG measurements obtained from muscles of the left (ipsilateral) and right (contralateral) leg. Transcutaneous spinal cord stimulation parameter: 65 mA, biphasic rectangular 2 x 1ms; conditioning-test interval 20ms.

5.3 Conclusion

The initial pulse shape and polarity evaluation measurements A (Figure 5.5), clearly show that biphasic rectangular stimulation pulses, starting with a cathodic positive phase, best elicit PRM reflexes in all measured muscle groups. All following measurements (B & C1-C3) incorporated these impulse parameters. This finding is of course only valid for the specific setup and electrode placement used in this study.

The double pulse measurements B showed difference in the recovery behaviour of PRM reflexes in distal (TA and TS) and proximal (Q and H) muscles. Motoneurons innervating more distal muscle groups seemed to recover faster, so that a second PRM reflex response could be measured in these muscles, whereas this was not the case in the quadriceps and hamstrings (compare Figure 5.6). Also, the intensities of the double pulses influence the recovery behaviour (Figure 5.7), with lower intensities (50 mA) being more effective in suppressing the elicitation of a second PRM reflex than high intensities (75 mA).

The control measurements of peak-to-peak values of PRM reflexes elicited without peripheral nerve stimulation (Figure 5.8) shows stability in every block of five probe-impulses, as well as in between the different measurement protocols. While peripheral nerve stimulation with single stimulation pulses (Figure 5.9) has little conditioning effect on the excitability of the spinal cord, stimulation with 5s trains of 80pps (Figure 5.10) shows significant reduction in PRM reflex magnitudes. Similar to the observation made on the double pulses, this suppression appears more prominent in distal muscle groups compared to more proximal muscles (Figure 5.11). A big difference in conditioning effect is observable when comparing the strongly suppressed ipsilateral (left) and the less influenced contralateral (right) leg muscle responses. Latter are influenced by the irradiation of the neuronal network more in the thigh muscle reflexes.

It shall be stressed out, that this is a preliminary study with only one subject, which mainly serves the purpose of testing the device developed in this thesis in a clinical environment. Nevertheless, the results concluded above are in remarkable accordance to the work of Krenn et al. (2014), who suggest presynaptic inhibition as explanation for the suppressive effect.

This study will enable a deeper understanding of functional profiles below the level of lesion in individuals with incomplete, discomplete, and clinically complete spinal cord injury and thereby substantially support rehabilitation therapy guidance.

6 REFERENCES

Angus, J., & Howard, D. (2006). *Acoustics and psychoacoustics* (3rd ed.). New York: Elsevier.

Arbuthnott, E. R., Boyd, I. A., & Kalu, K. U. (1980). Ultrastructural dimensions of myelinated peripheral nerve fibres in the cat and their relation to conduction velocity. *The Journal of Physiology*, *308*, 125–57. https://doi.org/10.1113/jphysiol.1980.sp013465

Basmajian, J. V, & De Luca, C. J. (1985). *Muscles alive. Williams and Wilkins*. Retrieved from http://rheumatology.oxfordjournals.org/content/7/4/local/back-matter.pdf

BIOPAC® Systems Inc. (2016a). *Product Sheet EL500-Series Disposable Electrodes*.

BIOPAC® Systems Inc. (2016b). *Product Sheet STMISOLA Linear Isolated Stimulator*.

Blair, E., & Erlanger, J. (1933). A comparison of the characteristics of axons through their individual electrical responses. *Am J Physiol*.

Brodal, P. (2010). *The central nervous system. structure and function*. Retrieved from http://books.google.com/books?id=iJjI6yDNmr8C

Compton, A. K., Shah, B., & Hayek, S. M. (2012). Spinal cord stimulation: A review. *Current Pain and Headache Reports*. https://doi.org/10.1007/s11916-011-0238-7

Dimitrijevic, M. R., Gerasimenko, Y., & Pinter, M. M. (1998). Evidence for a spinal central pattern generator in humans. In *Annals of the New York Academy of Sciences* (Vol. 860, pp. 360–376). https://doi.org/10.1111/j.1749-6632.1998.tb09062.x

Dy, C. J., Gerasimenko, Y. P., Edgerton, V. R., Dyhre-Poulsen, P., Courtine, G., & Harkema, S. J. (2010). Phase-dependent modulation of percutaneously elicited multisegmental muscle responses after spinal cord injury. *Journal of Neurophysiology*, *103*(5), 2808–2820. https://doi.org/10.1152/jn.00316.2009

Gerasimenko, Y., Roy, R. R., & Edgerton, V. R. (2008). Epidural stimulation: Comparison of the spinal circuits that generate and control locomotion in rats, cats and humans. *Experimental Neurology*. https://doi.org/10.1016/j.expneurol.2007.07.015

Gillies, A. R., & Lieber, R. L. (2012). Structure and function of the skeletal muscle extracellular matrix. *Muscle Nerve*, *44*(3), 318–331. https://doi.org/10.1002/mus.22094.Structure

Henneman, E. (1981). Recruitment of motorneurons: the size principle. *Prog Clin Neurophysiol*.

Hodgkin, a L., & Huxley, a F. (1952). Currents carried by sodium and potassium ions through the membrane of the giant axon of Loligo. *The Journal of Physiology*, *116*(4), 449–472. https://doi.org/10.1113/jphysiol.1952.sp004717

Hoffmann, P. (1922). *Untersuchungen über die Eigenreflexe (Sehnenreflexe) menschlicher Muskeln.* Berlin: Springer.

Kandel, E. R., Schwartz, J. H., & Jessell, T. M. (2013). *Principles of Neural Science*. *Neurology* (Vol. 4). https://doi.org/10.1036/0838577016

Konrad, P. (2005). *The ABC of EMG A Practical Introduction to Kinesiological Electromyography*. *Noraxon INC. USA. A*. https://doi.org/10.1016/j.jacc.2008.05.066

Krenn M, Danner SM, Schlaff C, Hofstoetter US, Minassian K, Mayr W, D. M. (2014). Altering spinal cord excitability by peripheral nerve stimulation. *Society of Neuroscience*.

Kumar, S., & Mital, A. (1996). *Electromyography in Ergonomics*. London: Taylor&Francis.

Lodish, H., Berk, A., Zipursky, S. L., Matsudaira, P., Baltimore, D., & Darnell, J. (2000). *Molecular Cell Biology. 4th edition*. *New York: W. H. Freeman*. https://doi.org/10.1017/CBO9781107415324.004

Lyrken, D. T., & Venables, P. H. (1971). Direct Measurement of Skin Conductance: A Proposal for Standardization. *Psychophysiology Sep1971*, *8*(5), 656. https://doi.org/10.1111/j.1469-8986.1971.tb00501.x

McComas, A. J. (1996). *In skeletal muscle form and function. Human kinetics publishers.*

McNeal, D. R. (1976). Analysis of a Model for Excitation of Myelinated Nerve. *IEEE Transactions on Biomedical Engineering*, *BME-23*(4), 329–337. https://doi.org/10.1109/TBME.1976.324593

McNeal, D. R. (1977). 2000 years of electrical stimulation. *Functional Electrical Stimulation - Application in Neural Prostheses*.

Minassian, K., Hofstoetter, U., & Rattay, F. (2012). Transcutaneous Lumbar Posterior Root Stimulation for Motor Control Studies and Modification of Motor Activity after Spinal Cord Injury. In *Restorative Neurology of Spinal Cord Injury*. https://doi.org/10.1093/acprof:oso/9780199746507.003.0010

Minassian, K., Persy, I., Rattay, F., Dimitrijevic, M. R., Hofer, C., & Kern, H. (2007). Posterior root-muscle preflexes elicited by transcutaneous stimulation of the human lumbosacral cord. *Muscle and Nerve*, *35*(3), 327–336. https://doi.org/10.1002/mus.20700

National Instruments™. (2008). *User Guide NI USB-622x/625x/628x OEM*.

National Instruments™. (2016). *Device Specification NI 6221*.

Nilsson, I., & Berthold, C. H. (1988). Axon classes and internodal growth in the ventral spinal root L7 of adult and developing cats. *Journal of Anatomy*, *156*, 71–96. https://doi.org/10.1210/jcem-41-2-332

Prutchi, D., & Norris, M. (2005). *Design and Development of Medical Electronic Instrumentation: A Practical Perspective of the Design, Construction, and Test of Medical Devices. Design and Development of Medical Electronic Instrumentation: A Practical Perspective of the Design, Construction, and Test of Medical Devices*. https://doi.org/10.1002/0471681849

Ramon y Cajal, S. (1906). The structure and connexions of neurons. *Nobel Lectures: Physiology or Medicine 1901-1921 (1976)*, 220–253.

Rattay, F. (1986). Analysis of Models for External Stimulation of Axons. *IEEE Transactions on Biomedical Engineering*, *BME-33*(10), 974–977. https://doi.org/10.1109/TBME.1986.325670

Rattay, F. (1990). Electrical Nerve Stimulation. *Antimicrobial Agents and Chemotherapy*, *58*(12), 7250–7257. https://doi.org/10.1007/978-3-7091-3271-5

Robert F. Schmidt, K. U. (2003). *Lehrbuch Vorklinik Teil B*. Köln: Deutscher Ärzte-Verlag.

Sahley, T. L., & Musiek, F. E. (2015). *Basic Fundamentals in Hearing Science*. San Diego: Plural Publishing.

Shealy, C. N., Mortimer, J. T., & Reswick, J. B. (1965). Electrical inhibition of pain by stimulation of the dorsal columns: preliminary clinical report. *Anesthesia and*

Analgesia, *46*(4), 489–91. https://doi.org/10.3109/15360288.2012.678473

van Boxtel, A. (1977). Skin resistance during square-wave electrical pulses of 1 to 10 mA. *Medical & Biological Engineering & Computing*, *15*(6), 679–687. https://doi.org/10.1007/BF02457927

Vargas Luna, J. L., Krenn, M., Cortés Ramírez, J. A., & Mayr, W. (2015). Dynamic impedance model of the skin-electrode interface for transcutaneous electrical stimulation. *PLoS ONE*, *10*(5). https://doi.org/10.1371/journal.pone.0125609

Winter, D. a. (1990). *Biomechanics and Motor Control of Human Movement*. *Processing* (Vol. 2nd). https://doi.org/10.1002/9780470549148

7 APPENDICES

LABVIEW™ STIMULATION AND RECORDING PROGRAM

```matlab
%% translate amplitude values from 0-100 to 0-10 range
amp_0=amp_0/10;
ampmin_1=ampmin_1/10;
delta_1=delta_1/10;
ampmax_1=ampmax_1/10;
amp_2=amp_2/10;
amp_3=amp_3/10;
amp_CH2=amp_CH2/10;

output=[];
output_CH2=[];
%% translate timevalues from ms / s to samplenumbers
phasedur=round((phasedur/1000)*fs);
pause_0=round((pause_0/1000)*fs);
pause_1=round(pause_1*fs);
pause_3=round((pause_3/1000)*fs);
phasedur_CH2=round((phasedur_CH2/1000)*fs);
offset_CH2=round(offset_CH2*fs);
%% generating basic pulse w/o pause behind
pulse = ones(1,phasedur);       %Monophasic (+) pulse shape
if phasemode==1
    pulse=pulse*-1;             %Monophasic (-) pulse shape
elseif phasemode==2
    pulse=[pulse,pulse*-1];     %Biphasic (+/-) pulse shape
elseif phasemode==3
    pulse=[pulse*-1,pulse];     %Biphasic (-/+) pulse shape
end
%% CH1 MODE0 - search manually
if mode==0
    if doublepulse_0==0
    output = [pulse*amp_0];
    elseif doublepulse_0==1
    output = [pulse*amp_0,zeros(1,pause_0),pulse*amp_0];
    end
%% CH1 MODE1 - recruitment curve
elseif mode==1
    amp_1=ampmin_1:delta_1:ampmax_1;
    amp_1=repmat(amp_1,1,rep_1);
    if profile_1==1
        amp_1=amp_1(randperm(length(amp_1)));
    elseif profile_1==2
        amp_1=fliplr(amp_1);
    end
    for n = 1:length(amp_1)
        output = [ output, amp_1(n)*pulse,zeros(1,pause_1)];
    end
%% CH1 MODE2 - single burst
elseif mode>=2
pulse_2=[pulse,zeros(1,(round(fs/freq_2))-length(pulse))];
    if ramp_2==1
        ramp_delta=round(amp_2/freq_2,3);
        amp_2r=ramp_delta:ramp_delta:amp_2;
        for n = 1:length(amp_2r)
        output = [output, amp_2r(n) .* pulse_2];
        end
    end
output=[output,repmat(pulse_2*amp_2,1,pulsenum_2)];
end
%% CH1 MODE3 - sdouble burst
if mode==3
    pulse_3=[pulse,zeros(1,(round(fs/freq_3))-length(pulse))];
    output=[output,zeros(1,pause_3-(round(fs/freq_2))-length(pulse)),rep
end
%% CH2
if CH2==1
    %% generating basic pulse w/o pause behind
pulse_CH2 = ones(1,phasedur_CH2);       %Monophasic (+) pulse shap
if phasemode_CH2==1
    pulse_CH2=pulse_CH2*-1;             %Monophasic (-) pulse shape
elseif phasemode_CH2==2
    pulse_CH2=[pulse_CH2,pulse_CH2*-1];     %Biphasic (+/-) pulse shape
elseif phasemode_CH2==3
    pulse_CH2=[pulse_CH2*-1,pulse_CH2];     %Biphasic (-/+) pulse shape
end
pulse_CH2=[pulse_CH2,zeros(1,(round(fs/freq_CH2))-length(pulse_CH2)
    if ramp_CH2==1
        ramp_delta_CH2=round(amp_CH2/freq_CH2,3);
        amp_CH2r=ramp_delta_CH2:ramp_delta_CH2:amp_CH2;
        for n = 1:length(amp_CH2r)
        output_CH2 = [output_CH2, amp_CH2r(n) .* pulse_CH2];
        end
    end
output_CH2=[zeros(1,offset_CH2),output_CH2,repmat(pulse_CH2*amp_
end
output=[output,0];
output_CH2=[output_CH2,0];
output(2,1:numel(output_CH2)) = output_CH2;
M=length(output);
```

Input labels:

- Phase / polarity — phasemode
- Phase duration (ms) — phasedur
- Modes — mode
- Single / double pulse — doublepulse_0
- Amplitude (mA) — amp_0
- Interpulse pause (ms) — pause_0
- min. Amplitude (mA) — ampmin_1
- Pause (s) — pause_1
- Delta (mA) — delta_1
- max. Amplitude (mA) — ampmax_1
- Repetitions — rep_1
- Intensity profile — profile_1
- Amplitude (mA) — amp_2
- Number of pulses — pulsenum_2
- Frequency (pps) — freq_2
- Ramp — ramp_2
- Amplitude (mA) — amp_3
- Number of pulses — pulsenum_3
- Frequency (pps) — freq_3
- Interburst break (ms) — pause_3
- Stimulation CH2 — CH2
- Phase / polarity — phasemode_CH2
- Phase duration (ms) — phasedur_CH2
- Offset CH1- CH2 (s) — offset_CH2
- Ramp — ramp_CH2
- Amplitude (mA) — amp_CH2
- Number of pulses — pulsenum_CH2
- Frequency (pps) — freq_CH2

fs = 100000

...generating Stimulation Data — String

Outputs: output, M

MATLAB® SCRIPT FOR GENERATION OF STIMULATION DATA

```matlab
%% translate amplitude values from 0-100 to 0-10 range
amp_0=amp_0/10;
ampmin_1=ampmin_1/10;
delta_1=delta_1/10;
ampmax_1=ampmax_1/10;
amp_2=amp_2/10;
amp_3=amp_3/10;
amp_CH2=amp_CH2/10;

output=[];
output_CH2=[];
%% translate timevalues from ms / s to samplenumbers
phasedur=round((phasedur/1000)*fs);
pause_0=round((pause_0/1000)*fs);
pause_1=round(pause_1*fs);
pause_3=round((pause_3/1000)*fs);
phasedur_CH2=round((phasedur_CH2/1000)*fs);
offset_CH2=round(offset_CH2*fs);
%% generating basic pulse w/o pause behind
pulse = ones(1,phasedur);        %Monophasic (+) pulse
shape
if phasemode==1
    pulse=pulse*-1;              %Monophasic (-) pulse
shape
elseif phasemode==2
    pulse=[pulse,pulse*-1];      %Biphasic (+/-) pulse
shape
elseif phasemode==3
    pulse=[pulse*-1,pulse];      %Biphasic (-/+) pulse
shape
end
%% CH1 MODE0 - search manually
if mode==0
    if doublepulse_0==0
    output = [pulse*amp_0];
    elseif doublepulse_0==1
    output = [pulse*amp_0,zeros(1,pause_0),pulse*amp_0];
    end
%% CH1 MODE1 - recruitment curve
elseif mode==1
    amp_1=ampmin_1:delta_1:ampmax_1;
    amp_1=repmat(amp_1,1,rep_1);
    if profile_1==1
        amp_1=amp_1(randperm(length(amp_1)));
    elseif profile_1==2
```

```matlab
        amp_1=fliplr(amp_1);
    end
    for n = 1:length(amp_1)
        output = [ output,
amp_1(n)*pulse,zeros(1,pause_1)];
    end
%% CH1 MODE2 - single burst
elseif mode>=2
pulse_2=[pulse,zeros(1,(round(fs/freq_2))-
length(pulse))];
    if ramp_2==1
        ramp_delta=round(amp_2/freq_2,3);
        amp_2r=ramp_delta:ramp_delta:amp_2;
            for n = 1:length(amp_2r)
            output = [output, amp_2r(n) .* pulse_2];
            end
    end
output=[output,repmat(pulse_2*amp_2,1,pulsenum_2)];
end
%% CH1 MODE3 - double burst
if mode==3
    pulse_3=[pulse,zeros(1,(round(fs/freq_3))-
length(pulse))];
    output=[output,zeros(1,pause_3-(round(fs/freq_2))-
length(pulse)),repmat(pulse_3*amp_3,1,pulsenum_3)];
end
%% CH2
if CH2==1
   %% generating basic pulse w/o pause behind
pulse_CH2 = ones(1,phasedur_CH2);          %Monophasic
(+) pulse shape
if phasemode_CH2==1
    pulse_CH2=pulse_CH2*-1;                 %Monophasic
(-) pulse shape
elseif phasemode_CH2==2
    pulse_CH2=[pulse_CH2,pulse_CH2*-1];     %Biphasic
(+/-) pulse shape
elseif phasemode_CH2==3
    pulse_CH2=[pulse_CH2*-1,pulse_CH2];     %Biphasic (-
/+) pulse shape
end
pulse_CH2=[pulse_CH2,zeros(1,(round(fs/freq_CH2))-
length(pulse_CH2))];
    if ramp_CH2==1
        ramp_delta_CH2=round(amp_CH2/freq_CH2,3);
        amp_CH2r=ramp_delta_CH2:ramp_delta_CH2:amp_CH2;
            for n = 1:length(amp_CH2r)
```

```matlab
            output_CH2 = [output_CH2, amp_CH2r(n) .*
pulse_CH2];
            end
    end
output_CH2=[zeros(1,offset_CH2),output_CH2,repmat(pulse_
CH2*amp_CH2,1,pulsenum_CH2)];
end
output=[output,0];
output_CH2=[output_CH2,0];
output(2,1:numel(output_CH2)) = output_CH2;
```